

4 FINAL REPORT 6

TO

SPACE NUCLEAR PROPULSION OFFICE

(CLEVELAND EXTENSION)

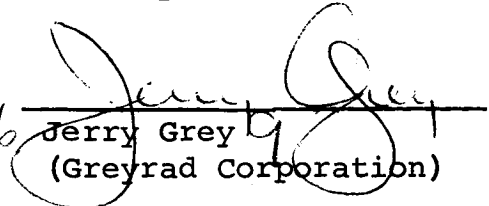
NATIONAL AERONAUTICS AND SPACE ADMINISTRATION

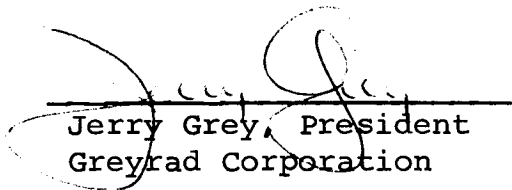
CONTRACT SNPC-55

3) ANALYTICAL INVESTIGATION OF KEY PROBLEMS IN THE
WATER-INJECTION-COOLED DIFFUSER FOR
NUCLEAR ROCKET ENGINE/STAGE TEST STANDS 2 - 3 4

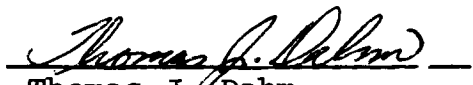
Prepared by:

Approved by:

6 
Jerry Grey
(Greyrad Corporation)


Jerry Grey, President
Greyrad Corporation

September 15, 1967


Thomas J. Dahm
(Aerotherm Corporation)

REPORT NO. SNP-3

GREYRAD CORPORATION
SIXTY-ONE ADAMS DRIVE
PRINCETON, N. J. 08540

609 921-2939

TABLE OF CONTENTS

	<u>Page No.</u>
TITLE PAGE	i
TABLE OF CONTENTS	ii
LIST OF ILLUSTRATIONS	iv
I. SUMMARY	1
II. INTRODUCTION	3
A. Purpose	3
B. History	4
III. ANALYSIS	7
A. General Approach	7
B. Inlet Duct Conditions	7
C. Water-Jet Penetration	10
D. Conditions at Origin of Mixing	15
E. Condition at End of Mixing for an Infinitely Long Duct	18
F. Mixing Analysis	21
1. General	21
2. Reichardt's Inductive Theory of Turbulent Mixing	25
3. Application of Reichardt's Theory to the Wet-Duct Diffuser	27
G. Calculation of State Parameters	43
H. Limitations and Special Properties of the Solution	49

TABLE OF CONTENTS--continued

	<u>Page No.</u>
IV. COMPUTER PROGRAM	51
V. EFFECTS OF CERTAIN INPUT PARAMETERS	52
A. Coolant Jet Azimuth	52
B. Mixing Coefficient	52
C. Evaporation Characteristics	54
VI. COMPARISON WITH EXPERIMENTAL DATA	59
A. Westinghouse Astronuclear Laboratory	59
B. Aerojet-General Corporation	63
VII. FULL-SCALE E/STS-2 & 3 PERFORMANCE PREDICTION	70
A. Input Data (Reference Case)	70
B. Reference Case Results	73
C. Effect of Adjusting Coolant Distribution	73
VIII. CONCLUSIONS	78
IX. RECOMMENDATIONS	81
REFERENCES	82
APPENDICES	
Appendix A - Notation	A-1
Appendix B - Analysis of Nonuniform Inlet-Duct Flow	B-1
Appendix C - Water Jet Penetration Across a Variable Gas Flow Field	C-1

TABLE OF CONTENTS--continued

	<u>Page No.</u>
Appendix D - Sudden-Expansion Analysis (Gas Only)	D-1
Appendix E - Auxiliary Computer Program Listing: Inlet Condition Subroutines (PEN)	E-1
Appendix F - Main Mixing Computer Program Listing	F-1
Appendix G - Computed Results for "Reference Case" of Full-Scale E/STS 2-3 Performance Prediction Analysis	G-1
Appendix H - Computed Results for "Modified Design" Case of Full-Scale E/STS 2-3 Performance Prediction Analysis	H-1

LIST OF ILLUSTRATIONS

<u>Figure No.</u>	<u>Title</u>	<u>Page No.</u>
1	Diagram of Mixing Duct and Inlet, Showing Notation	8
2	Inlet Mach Number Profiles	11
3	Water Jet Penetration Trajectories in Variable-Velocity Gas Flow	12
4	Sensitivity of Maximum Jet Penetration to Trajectory Cutoff Angle	14
5	Streamline Locations in the Inlet and Mixing Ducts	16
6	Sample Calculations of Conditions After Complete Mixing, Showing Effect of Water Flow Rate	22

LIST OF ILLUSTRATIONS--continued

<u>Figure No.</u>	<u>Title</u>	<u>Page No.</u>
7	Distribution of Momentum Flux According to Reichardt's Theory for a Single Jet Discharging into a Quiescent Atmosphere	28
8	Influence of Constant-Pressure Assumption on Hydrogen Continuity in the Mixing Duct	32
9	Apparent Loss of Coolant Jet Mass due to Mixing in a Confined Duct for a Single Jet on the Centerline	38
10	Typical Computed Hydrogen Concentration Distributions for Two Flux Correction Schemes (No Reflections & Doublet Reflection)	39
11	Typical Axial Pressure Distribution for Two Flux Correction Schemes (Doublet and Sextant Reflection)	40
12	Comparisons of Hydrogen Concentrations for Doublet & Sextant Reflections	41
13	Effect of Azimuthal Location on Mixed Temperature Profile	53
14	Effect on Mixed Temperature Profiles of Changing Mixing Coefficients c_m and c_k , Keeping $c_m = c_k$	55
15	Effect on Mixed Temperature Profiles of Changing Mixing Coefficients c_m and c_k Independently	56
16	Effect of Coolant Evaporation Rate on Mixed Temperature Profiles	57
17	Comparison of Analytical Predictions With Westinghouse Data: Axial Location $x = 7.5$ " (\sim One Duct Diameter)	60

LIST OF ILLUSTRATIONS--continued

<u>Figure No.</u>	<u>Title</u>	<u>Page No.</u>
18	Comparison of Analytical Predictions With Westinghouse Data (Continued): Axial Location $x = 17.5''$ (~ 3 Duct Diameters)	61
19	Comparison of Analytical Predictions With Westinghouse Data (Continued): Axial Location $x = 35''$ (~ 6 Duct Diameters)	62
20	Comparison of Analytical Predictions With Aerojet-General Experiments Case 1 - Coolant Flow = 0.2 lb/sec.	65
21	Comparison of Analytical Predictions With Aerojet-General Experiments Case 2 - Coolant Flow = 1.5 lb/sec.	66
22	Comparison of Analytical Predictions With Aerojet-General Experiments Case 3 - Coolant Flow = 3.0 lb/sec.	67
23	Comparison of Analytical Predictions With Aerojet-General Experiments Case 4 - Coolant Flow = 4.7 lb/sec.	68
24	Predicted Full-Scale Mixing-Duct Temperature Profiles for "Reference Case" (see Tables III and VI for Conditions)	74
25	Parametric Plot of Coolant Injection Design Variables for Full-Scale E/STS 2-3 Configuration	75
26	Predicted Full-Scale Mixing-Duct Temperature Profiles for "Modified Design" Case (see Tables III and VII for Conditions)	77
C-1	Empirical Penetration Correlation Used in the Analysis (from Reference 15)	C-4

I. SUMMARY

The axisymmetric wet-duct mixing analysis and computer program of Reference 1 have been successfully revised to remove many of the restrictive assumptions required. The improved program allows duct pressure to vary, thereby automatically satisfying the conservation equations everywhere; permits any axisymmetric inlet velocity profile; provides four different sets of coolant injection characteristics simultaneously; and permits variation of momentum and mass mixing rates and coolant evaporation rate.

It was determined by a series of "computer experiments" that the assumed mixing coefficients, especially the mass mixing coefficient c_k , dominate the mixing-duct temperature profiles, whereas evaporation rate of the coolant is unimportant. That is, the presence of coolant at a given point in the flow field is significant; whether it appears there in liquid or vapor form is of essentially no importance.

Correlations of the improved analytical program with early scale-model Westinghouse test data and recent Aerojet-General experiments revealed that the computer program was always over-conservative. Correlations with Westinghouse experiments, which employed axial liquid injection, were considerably better than those with Aerojet-General tests, which used radial liquid injection. It appeared likely that the differences between experiment and analysis were caused principally by (a) differences between assumed and actual mass mixing coefficient c_k , and (b) differences (in the AGC tests) between degree of initial coolant-jet dispersion. Both these effects can be readily incorporated into the analysis, and it is recommended that the AGC experiments be used in this way to establish proper analytical values for c_k and the effective coolant injection location.

A full-scale E/STS-2, 3 performance prediction was made for the current set of input conditions and configuration. Predicted temperature profiles indicated non-ideal distribution of coolant, so the coolant-injection distribution was revised (rather arbitrarily) and used to analyze a "modified design" case. This modified design, although certainly not optimum,

revealed much better performance; i.e., the hydrogen gas was almost fully cooled between 1 and $1\frac{1}{2}$ mixing duct diameters downstream, and was completely cooled at 2 diameters. Clearly, however, the results of these analyses depend critically on the values selected for the mixing coefficient c_k and, perhaps, several other key inputs.

It was therefore concluded that a parameter study of the exhaust duct should be performed, incorporating proper values (estimated from AGC experiments as described earlier) for c_k and effective coolant injection location, in order to optimize the coolant injection pattern for E/STS-2 and 3 preliminary design purposes. The present analysis and computer program are believed to be entirely suitable for such a study without further modification.

II. INTRODUCTION

A. Purpose

The program described in this report was undertaken in order to improve upon the feasibility analysis^{1*} performed in a prior contract² (SNPC-49) and to predict flow parameters in a single geometrical configuration of the E/STS-2 and E/STS-3 water-injection-cooled subsonic diffuser. The pertinent portion of the work statement for the present contract³ (SNPC-55) is as follows:

"Conduct an analysis of the 'water injection' concept as applied to the AGC conceptual E/STS 2/3 exhaust duct configuration utilizing the basic analysis and computer program developed under Contract SNPC-49, 'Analytical Feasibility Study of a Water-Injection-Cooled Diffuser for Nuclear Rocket Engine/Stage Test Stands E/STS 2 and 3,' and modified as follows:

1. The primary mixing analysis shall retain the constant pressure assumption, since the present large-plenum duct configuration with an average Mach No. of approximately 0.3 at the entrance does not violate the constant pressure process assumption. However, the analysis shall be modified to provide Mach No. profiles and verify that the continuity equation is satisfied at all downstream points.
2. The analysis shall be restricted to one fixed geometry duct. As in the previous study developed under Contract SNPC-49, no turning of the stream shall be considered.
3. The penetration distances of individual jets shall be different; that is, solutions to the analysis made under Contract SNPC-49 shall be superimposed for different water orifice mass flow rates simultaneously (3 or more).

* Superscript numbers indicate references listed on pages 82 and 83.

4. The jet penetration analysis of R. Ingebo of the Lewis Research Center shall be incorporated and the large-jet data developed in the tests in the Lewis Icing Tunnel shall be utilized.
5. The importance of vaporization characteristics of the injected water shall be evaluated by considering different cases varying from full equilibrium to zero evaporation.
6. A single non-flat inlet Mach No. profile shall be provided to replace the flat profile considered in the analysis made under Contract SNPC-49.

"Approximate geometry: The water is injected radially into the gas stream at the exit of the diffuser which is 140" in diameter. The diffuser discharges into a large diameter (32' circular) plenum-type 90° turn.

"Approximate Test Condition: The gas conditions at the water injection station are 300#/sec. of hydrogen at 5000°R. The Mach No. profile varies from 0 at the diffuser wall to about 0.7 at the center. The water flow rates and available injection pressures will be specified by the Government.

"The Ingebo correlation, the large-jet data, the exact duct geometry, and the exact test conditions will be supplied by the Government upon request after start of work."

B. History

The analysis described in Reference 1 was performed in order to determine the general feasibility of the water-injection-cooled subsonic diffuser concept, and therefore included a number of rather restrictive assumptions. It was specifically recommended in Reference 1 that the generality and applicability of the analysis could be considerably improved by removal of the following restrictions:

1. Constant pressure in the mixing duct.
2. A single radial penetration distance for all injected coolant.
3. Flat inlet gas velocity profile.
4. Equilibrium coolant vaporization.
5. Prandtl and Schmidt numbers of unity for the mixing process.

The current contract (Reference 3) was therefore undertaken by Greyrad in order to remove these restrictions from the original analysis contracted in Reference 2.

Note that in the above work statement, taken from Reference 3, the restrictive constant-pressure assumption was reinstated in order to decrease program cost, since it was stated by NASA that maximum Mach numbers would not exceed 0.3. However, since the inlet Mach number profile was not flat, the peak centerline Mach numbers (see later text) were nearly unity, and the analysis as undertaken in this contract had to be generalized by again removing the constant-pressure assumption as was originally recommended.

A further restriction was imposed on the present analysis in order to reduce cost and time: only a single duct geometry and set of inlet conditions were to be considered. The final geometry selected varied somewhat from that stipulated in the above work statement, as will be detailed later in the report.

The present report therefore:

1. Describes the modifications made in the original program.
2. Presents the revised computer program in its entirety.
3. Demonstrates several important effects of the modifications, particularly in the area of mixing and evaporation assumptions.

4. Re-compares the revised program output with old Westinghouse Astronuclear Laboratory (WANL) scale-model test data and new Aerojet-General Corporation (AGC) scale-model test data.
5. Presents predicted flow parameter distributions for the selected geometry and inlet flow conditions.

III. ANALYSIS

A. General Approach

The overall approach to the analysis is the same as that described in detail in Reference 1, and much of the introductory and explanatory material appearing in that reference need not be repeated here. The major modifications are those which needed to be introduced in order to remove the previously-assumed restrictions listed in the previous section. This section describes the revised program in some detail, with the principal emphasis placed on the modifications made to the original analysis presented in Reference 1.

Note that, as indicated in the work statement given earlier, the analysis still pertains to a basically one-dimensional flow configuration with no bends, and therefore does not exactly simulate the actual geometry of the E/STS 2 - 3 ducts as described in a later section. Important features of the geometrical model used in the analysis are shown in Figure 1. A complete list of all notations used in this report appears in Appendix A.

B. Inlet Duct Conditions

In removing the restriction to "flat" inlet hydrogen velocity profiles used in Reference 1, it was necessary to establish a sufficiently general Mach number profile to use in the subsequent analysis. Since there was some doubt as to the actual profile, four different profiles were established, and were later used to determine the sensitivity of the analysis to variations in the inlet profile. The four profiles used, taken from References 4 and 5, are shown in Figure 2.

These profile data were used to establish values for mean Mach number \bar{M}_1 and "flow coefficient" c_{w1} (see Table I) by the methods illustrated in Appendix B.

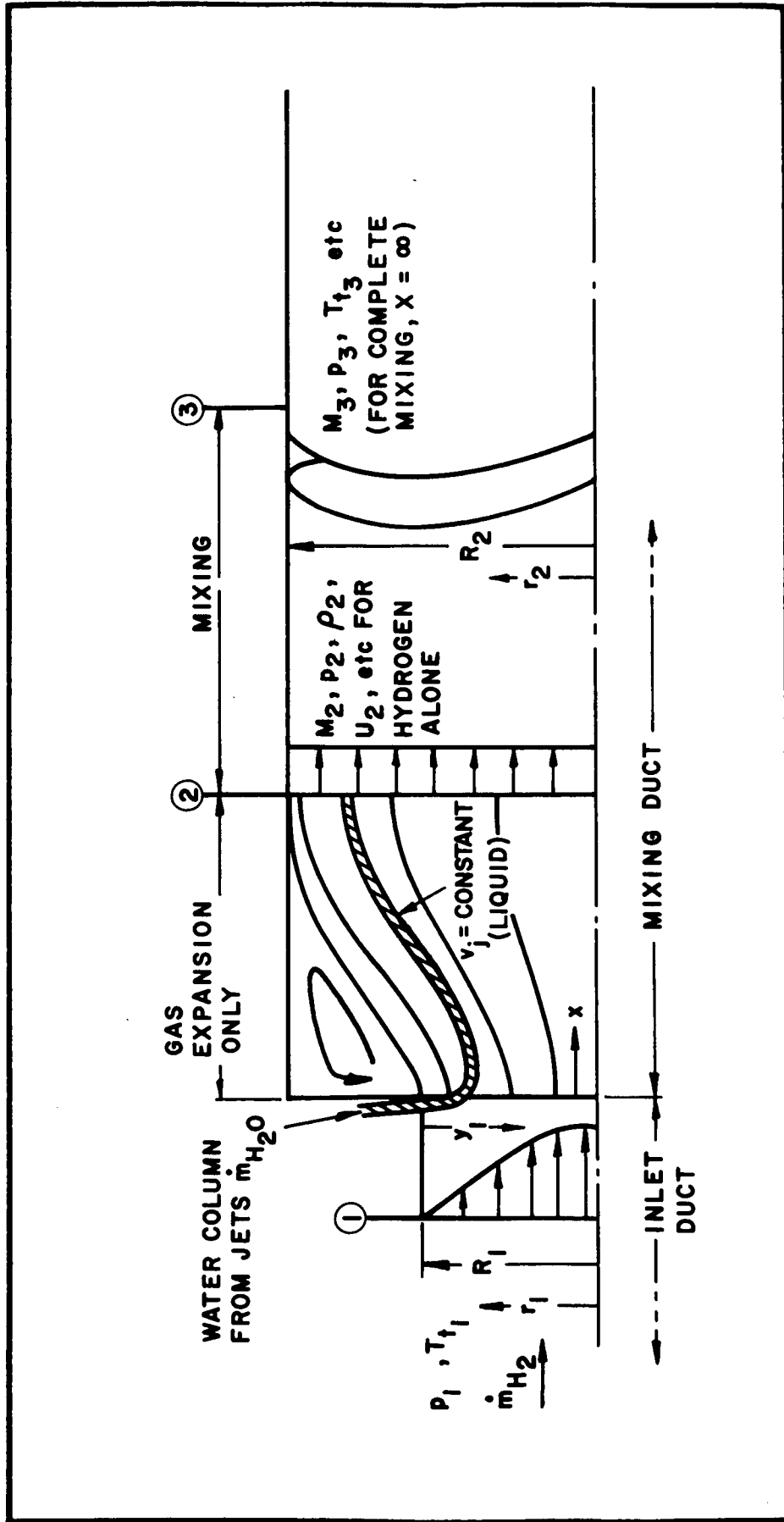


FIGURE I

DIAGRAM OF MIXING DUCT AND INLET, SHOWING NOTATION

TABLE I

Inlet Gas Profile Data (see Figure 2)

<u>Profile</u>	<u>Reference</u>	<u>\bar{M}_1</u>	<u>c_{w1}</u>
1	4	0.595	0.388
2	4	0.583	0.511
3	(Avg)	0.580	0.456
4	5	0.681	0.649

Values of c_w and \bar{M}_1 then provide the duct static pressure p_1 (assumed uniform across the subsonic inlet duct exit plane):

$$p_1 = \frac{\dot{m} c^*}{c_{w1} A_1} \frac{\Gamma}{\gamma^{\frac{1}{2}} \bar{M}_1 \left(1 + \frac{\gamma - 1}{2} \bar{M}_1^2\right)^{\frac{1}{2}}} \quad (1)$$

The effective inlet stagnation pressure is then:

$$p_{t1} = p_1 \left(1 + \frac{\gamma - 1}{2} \bar{M}_1^2\right)^{\frac{\gamma}{\gamma - 1}} \quad (2)$$

and the average inlet-gas dynamic pressure is:

$$q_g = \frac{\gamma p_1 \bar{M}_1^2}{2} \quad (3)$$

C. Water-Jet Penetration

To keep the analysis flexible, the computer program still provides the option of injecting the water axially at preselected radial locations, in a manner similar to that used by Westinghouse, or radially, in which case the penetration analysis of Appendix C can be employed.

For the more interesting case of radial injection, the non-flat inlet profile introduces a substantial change in the penetration calculation as compared with that of Reference 1. As shown in Appendix C, the dimensionless penetration coordinates, X and η' , are related by:

$$X = \left(\frac{q_j}{g_g} \right)^2 \left(\frac{D_j}{D_1} \right)^3 \left(\frac{x}{D_1} \right) = \frac{1}{64} \int_0^{\eta'} \left[\int_0^{\eta'} \frac{M^{4/3}}{\bar{M}} d\eta' \right] d\eta' \quad (4)$$

where $\eta' = \frac{y_1}{R_1} = 1 - \frac{r_1}{R_1}$

and $q_j = \frac{\rho_j^v v_j^2}{2}$ (calculated from input numbers of water jets and diameters, and either input water mass flow rate or total pressure)

Values of η' and X for the Mach number profiles of Figure 2 are presented in Figure 3. For convenience, the liquid-jet trajectory in a uniform gas flow field is also presented.

All calculations germane to the nonuniform inlet profile are conducted with a separate computer program called PEN which is presented in Appendix E. Required inputs are tabular $M - \eta$ data, number of values of η considered, and isentropic exponent ($\gamma = 1.4$ for the calculations here). Output results are \bar{M} , c_w , η_1 , η_2 , η' , and X , along with certain other data. The results of these calculations are used in the mixing program in the form of tabular data assembled in a data subroutine called KEMD.

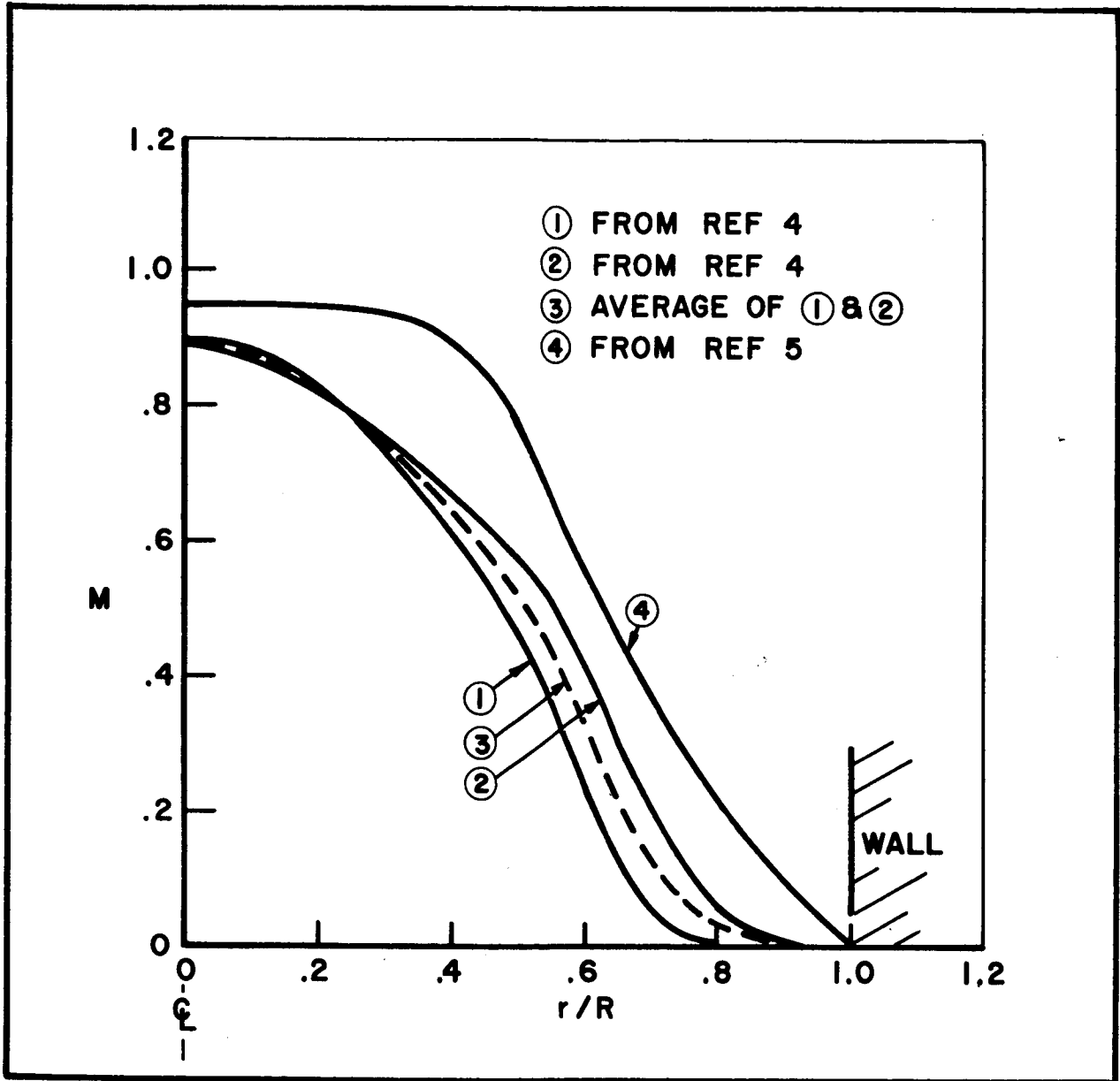


FIGURE 2
INLET MACH NUMBER PROFILES

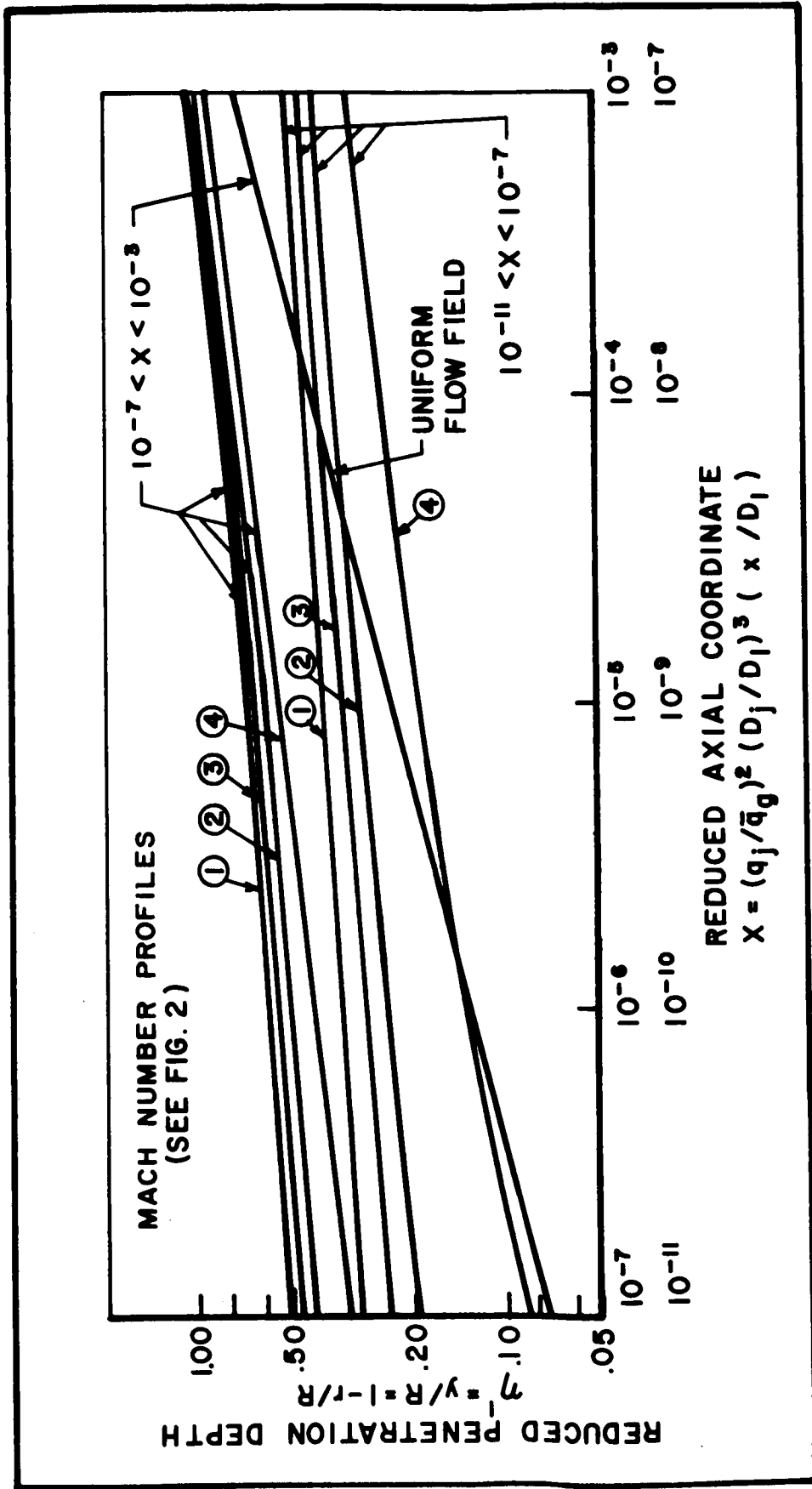


FIGURE 3

WATER JET PENETRATION TRAJECTORIES IN VARIABLE-VELOCITY GAS FLOW

The penetration trajectory results are approximated (within $\Delta\eta' \approx \pm 0.02$) by an equation of the form:

$$\eta' = aX^n \quad (5)$$

where a and n are constants whose magnitudes depend upon the range of X . Inasmuch as η' is asymptotic in X , it has been found convenient to truncate the penetration at some arbitrarily defined maximum trajectory inclination α_{\max} . This is done by using the following relation, obtained through appropriate manipulation of Equation (5):

$$\eta_{j_1} = 1 - 2 \left(\frac{a}{2} \right)^{\frac{1}{1-n}} \left[n \left(\frac{q_j}{q_g} \right)^2 \left(\frac{D_j}{D_1} \right)^3 \tan \alpha_{\max} \right]^{\frac{n}{1-n}} \quad (6)$$

If η_{j_1} is less than D_{jc}/D_1 (where D_{jc} is the diameter of the jet input which reaches the centerline, if any), an indication of centerline penetration is printed out. The effect of truncation at α_{\max} on penetration is shown in Figure 4 by examining the dependence on α_{\max} of the parameter:

$$\left(n \tan \alpha_{\max} \right)^{\frac{n}{1-n}} \quad (\sim y_{\max} \text{ for fixed conditions})$$

for a representative value of $n = 1/11$. It may be noted that y_{\max} varies only about plus or minus 10 percent for cutoff angles varying between 76 and 88 degrees. Accordingly, a cutoff value of $\alpha_{\max} = 85$ degrees is believed to be a reasonable criterion, and has been so employed.

In the computational procedure, all water jets are assumed to have the same total pressure, and thence the same dynamic pressure, mass flux, and velocity. Jet diameters may vary between jet rows and the jet rows are allowed limited freedom on their azimuthal orientation. One to four rows, each of different diameter jets, may be employed.

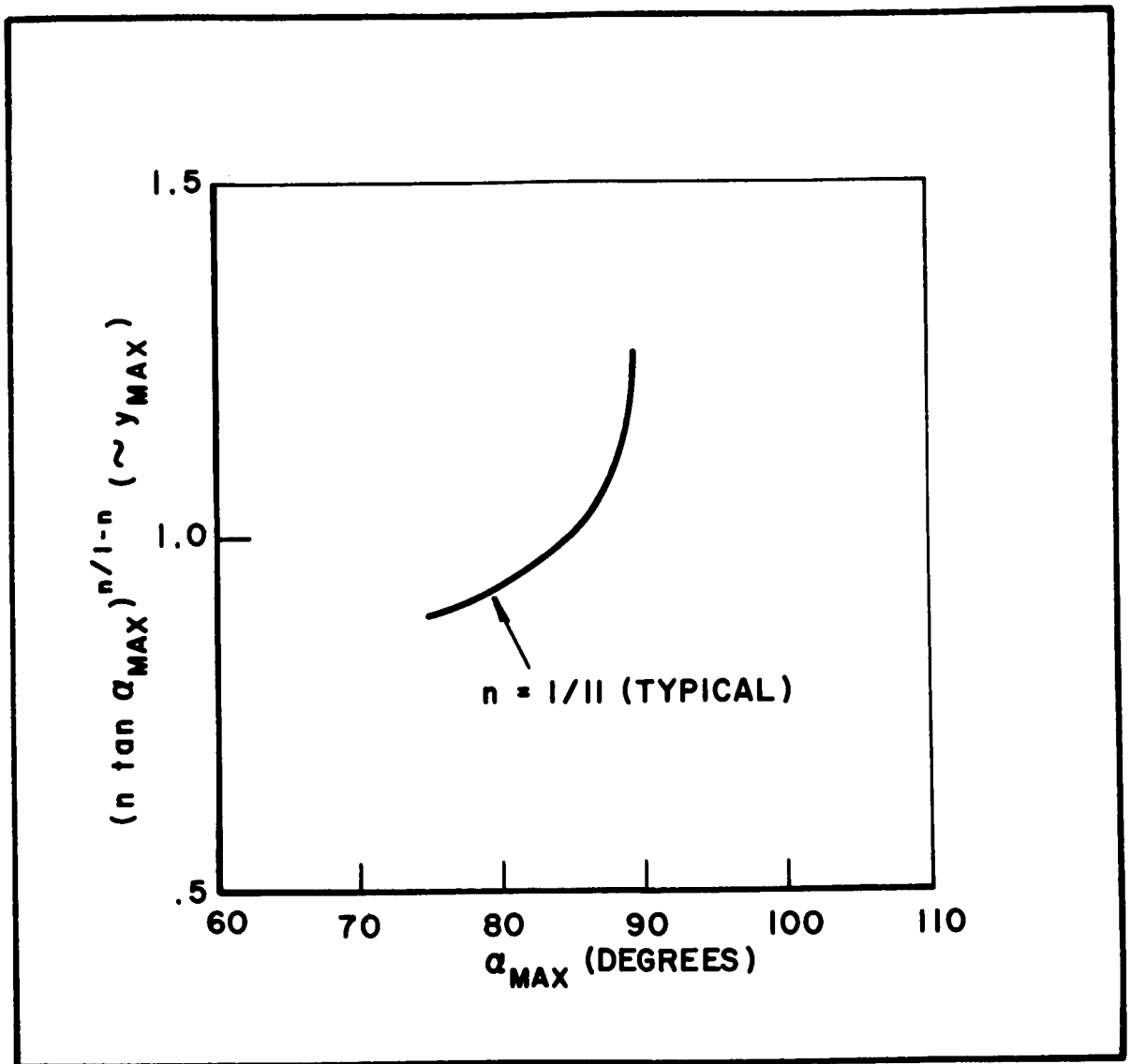


FIGURE 4
 SENSITIVITY OF MAXIMUM JET PENETRATION
 TO TRAJECTORY CUTOFF ANGLE

D. Conditions at Origin of Mixing

Mixing originates at Station 2 in Figure 1. Conditions to be defined at Station 2 include:

1. Jet column diameters D_j
2. Jet momentum, velocity, temperature, etc.
3. Radial and azimuthal locations of jets.
4. Hydrogen stream properties such as Mach number, pressure, velocity, etc.

Items 1 and 2 are simply defined by the values of the jet parameters at their point of injection, with the possible exception of a centerline jet defined by contributions from jets which penetrate the centerline:

$$D_{jc} = \sqrt{\frac{4}{\pi} \sum A_{jc}}$$

Definition of Items 3 and 4 is discussed in the following paragraphs.

For jets located in the inlet, it is assumed here, as was done in Reference 1, that mixing between the water and hydrogen in the transition region between Stations 1 and 2 will be essentially the same as would occur over the same distance if the hydrogen flow were abruptly diffused to a uniform condition within the mixing duct at its upstream end. It is further assumed that when the water jets have achieved their maximum penetration (defined in the previous section), the water columns will follow the gas streamlines in the transition between Stations 1 and 2. With the further assumption that the gas conditions are uniform at Station 2, Item 3 above can now be defined.

The method for location of the inlet duct gas streamlines within the mixing duct is presented in Appendix B. Results from the method, using the inlet profile information of Figure 2 and Table I, are presented in Figure 5. It can be seen that water jets which penetrate to a given dimensionless radius η_{j_1} in the inlet will in general appear at a much

NOTE: INLET DUCT PROFILES
 AT STATION ① DEFINED
 BY FIGURE 2.
 CONDITIONS AT STATION
 ② ARE ONE-DIMENSIONAL

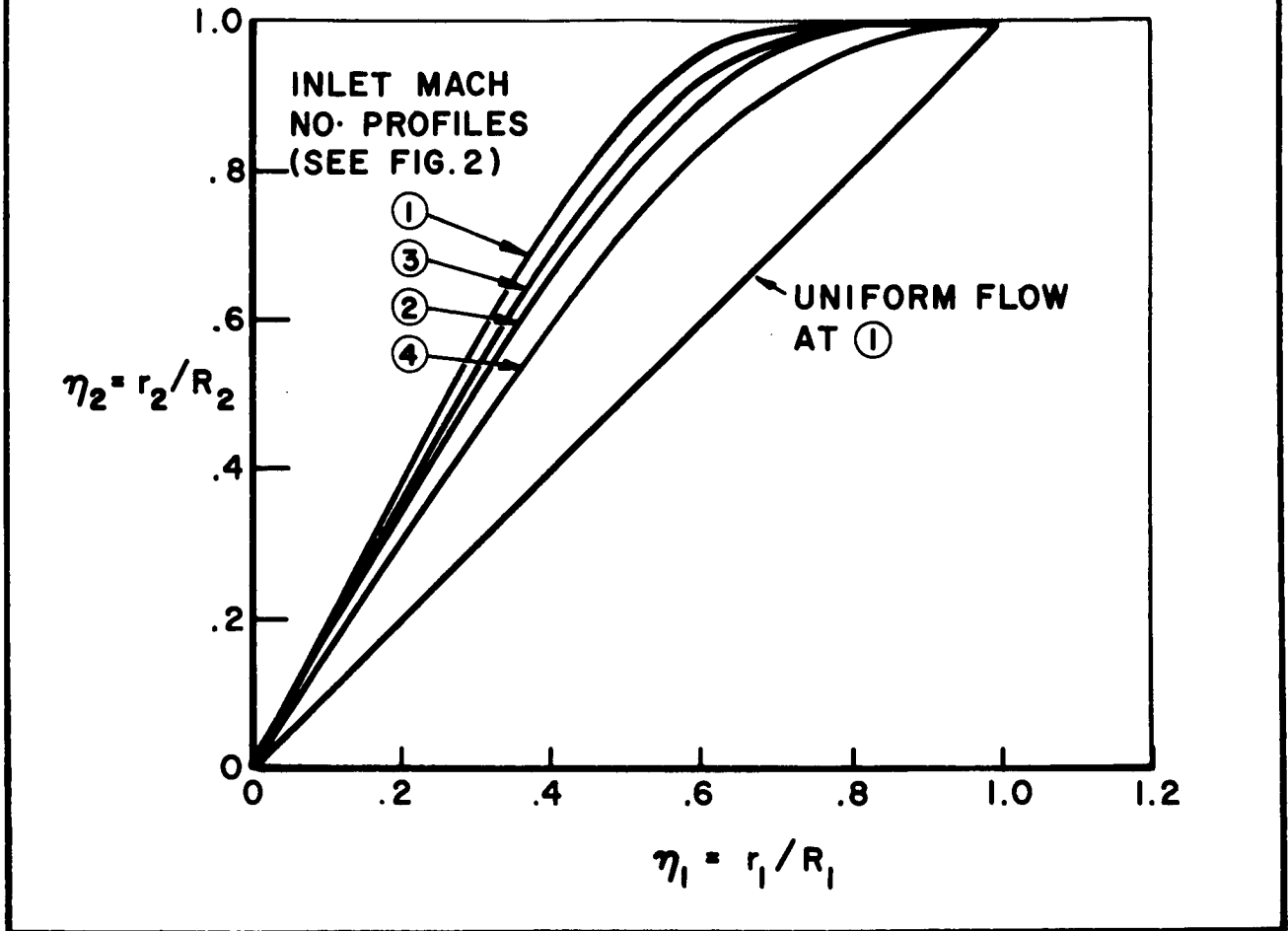


FIGURE 5

STREAMLINE LOCATIONS IN THE
 INLET AND MIXING DUCTS

greater dimensionless radius η_{j_2} in the mixing duct.

For example, if a jet is injected so that it penetrates up to about 30 percent of the distance to the inlet duct centerline, it will be virtually adjacent to the wall when it reaches the mixing duct for the first three profiles considered. On the other hand, from the penetration results of Figure 3, it can be argued that even very small jets at low dynamic pressure will penetrate the flow very easily, because the gas velocity is so low near the walls. Accordingly, these two compensating effects suggest that the radial location of the jets in the mixing duct will tend to be relatively insensitive to the inlet profile assumed, according to the present analysis.

In subsequent analyses, it is again assumed, as was done in Reference 1, that the jet radial locations in the mixing duct are independent of axial position. This is in accordance with the above-stated assumptions that the mixing-duct flow is one-dimensional and that mixing in the transition region is virtually the same as in the mixing duct. Also, the assumption that the flow is axisymmetric in the inlet implies that the aximuthal orientations of the water jets will be the same in both ducts.

Hydrogen stream properties (Item 4 above) are determined by the simple analysis of Appendix D, exactly as was done in reference 1. Here it is assumed that the mixing region is adiabatic, with negligible wall shear, and that the "base" region where D_1 expands to D_2 is at the duct inlet pressure p_1 . Performing a force balance on the system between Stations 1 and 2:

$$p_1 A_2 + \sum \dot{m}_{H_2O} u_{j_1} + \dot{m}_{H_2} \bar{u}_{H_2_1} = p_3 A_2 + (\dot{m}_{H_2O} + \dot{m}_{H_2}) u_3 \quad (7)$$

As shown in Appendix C,

$$p_1 A_2 + \dot{m}_{H_2} \bar{u}_{H_2 O} = p_2 A_2 + \dot{m}_{H_2} u_{H_2 2} \quad (8)$$

where all the parameters on the right side can be evaluated analytically (see Appendix C).

Thus, the complete flow field at the inception of mixing is defined, and may be used as input to the mixing analysis to be discussed later.

E. Condition at End of Mixing for an Infinitely Long Duct

Before proceeding to the detailed mixing analysis between Stations 2 and 3 of Figure 1, it is of interest to determine the final conditions which would exist after complete mixing. This calculation is useful for the following reasons:

1. It is desirable to know what the final conditions will be in order to properly weigh results for partial mixing.
2. Certain geometries and inlet conditions may cause choking in the mixing duct. It is desirable to be able to recognize this condition in order to evaluate the possibility of changing the assumed inlet conditions.
3. It was not certain whether accuracy requirements would necessitate consideration of pressure gradients in the mixing duct for the geometries that were to be analyzed. Accordingly, it was desirable to establish the potential magnitudes of the pressure differences in the mixing duct.
4. Assuming that pressure gradients would need to be considered, it was felt that a computational procedure for considering these pressure gradients could be established in part through development of a final condition computation procedure.

Proceeding now to the calculation of conditions after complete mixing (e.g., in an infinitely long adiabatic duct with no wall shear), we require, in addition to the previously-stated momentum relation, the constraints provided by continuity and energy considerations:

Conservation of energy requires

$$\sum \dot{m}_{H_2O} h_{t_{H_2O}} + \dot{m}_{H_2} h_{t_{H_2}} = (\sum \dot{m}_{H_2O} + \dot{m}_{H_2}) h_{t_3} \quad (9)$$

and continuity requires

$$\sum \dot{m}_{H_2O_1} + \dot{m}_{H_2_1} = (\sum \dot{m}_{H_2O_3} + \dot{m}_{H_2_3}) = \sum \dot{m}_3 \quad (10)$$

or, alternatively,

$$k_3 + (1 - k_3) = 1 \quad \text{where} \quad k \equiv \frac{\sum \dot{m}_{H_2O}}{\sum \dot{m}} \quad (11)$$

$$\text{Thus, } k_3 = \frac{h_{t_3} - h_{t_{H_2}}}{h_{t_j} - h_{t_{H_2}}} \quad (12)$$

Note that this overall conservation requirement is identical to what would be obtained from the Crocco relations for Lewis number unity. In later sections, it is assumed that

$$k = \frac{h_t - h_{t_{H_2}}}{h_{t_j} - h_{t_{H_2}}}$$

which is certainly at least always true in the water stream, the hydrogen stream, and the completely mixed stream.

Employing now the further condition that

$$(\rho u)_3 = \frac{\dot{m}_{H_2O} + \dot{m}_{H_2}}{A_2} \quad (13)$$

enough basic information is available to proceed with the solution for the conditions after complete mixing:

$$(\rho u^2)_3 = p_2 - p_3 + \frac{\sum \dot{m}_{H_2O} u_{j1} + \dot{m}_{H_2} u_{H_2 2}}{A_2} \quad (14)$$

$$(\rho uk)_3 = \frac{\sum \dot{m}_{H_2O}}{A_2} \quad (15)$$

$$\begin{aligned} [\rho u(h_t - h_{t_{H_2}})]_3 &= (\rho uk)_3 (h_{t_j} - h_{t_{H_2}}) \\ &= \frac{\sum \dot{m}_{H_2O}}{A_2} (h_{t_3} - h_{t_{H_2}}) \end{aligned}$$

It can be recognized that for an assumed value of p_3 , the numerical magnitudes of the momentum, mass, and enthalpy fluxes can be evaluated and a solution obtained for all mixed-state properties at the assumed pressure. This is accomplished in a computer subroutine called STATE, which is described in Reference 1 and, for convenience, later in the present report.

A fourth condition which permits the final determination of p_3 , and thence the final solution for all state properties, is hydrogen continuity:

$$2\pi \int_0^R \rho u(1-k)rdr = \left[\rho u(1-k)A_2 \right]_3 = \dot{m}_{H_2} \quad (17)$$

The method employed in the analysis is to evaluate the individual values of ρ , u , and k in the STATE subroutine for the assumed pressure, compare their combination on the left side of hydrogen continuity Equation (17) with the known (input) value on the right side, and modify p_3 until Equation (17) is satisfied. The same technique developed here for the determination of the final complete mixed conditions was employed for solution of state properties in the partially mixed flow field, as is discussed later.

As an example of the use of this procedure, data were computed as a function of water flow rate at fixed geometry and hydrogen conditions. These results are presented in Figure 6, which shows that for the particular geometry and conditions considered, the final pressure varies only about 0.5 percent over the entire range of water flows considered. However, by following the intermediate results during the iteration on the final pressure, it was determined that the magnitude of the left side of the hydrogen continuity Equation (17) was extremely sensitive to very small changes in pressure. This result, along with the results from studies to be described later, confirmed the need for consideration of pressure gradients in the mixing duct.

If during the iteration on final pressure it is found that the left side of Equation (17) maximizes at a value less than the magnitude of the input hydrogen mass flow rate, it is because complete mixing conditions are not physically possible for the assumed inlet conditions; that is, the flow would choke in the mixing duct before complete mixing is obtained. When the computer program encounters this situation, a message to this effect is printed out.

F. Mixing Analysis

1. General

The analysis presented in Reference 1, which is based on the assumption of constant pressure throughout the mixing duct, is incorporated into the present variable-pressure study. In the mixing region between Stations 2 and 3 in Figure 1, the conventional relations describing the diffusion of mass, momentum, enthalpy, and species in an axisymmetric constant pressure flow field are:

Mass

$$\frac{\partial \rho u}{\partial x} + \frac{1}{r} \frac{\partial \rho v r}{\partial r} = 0 \quad (18)$$

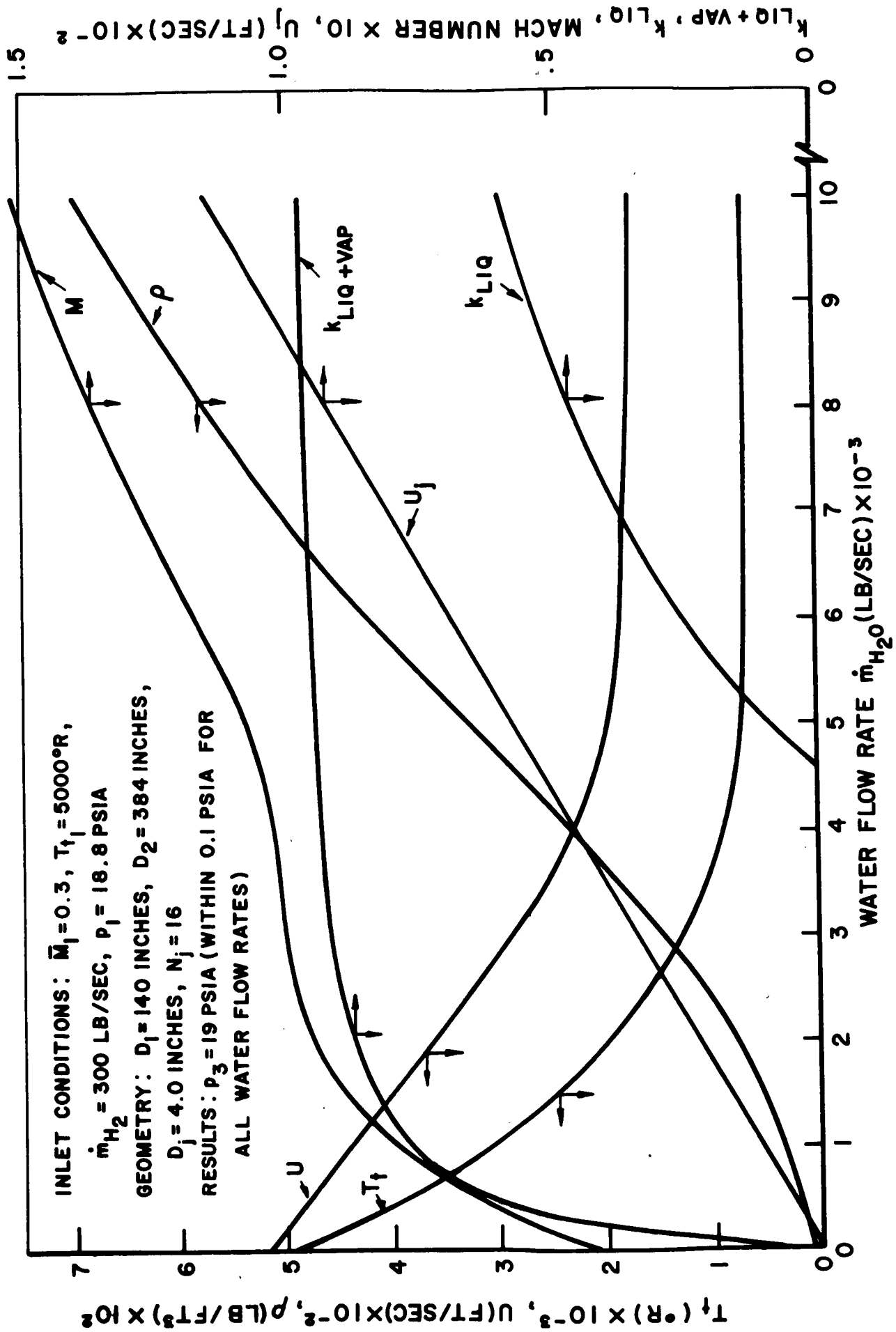


FIGURE 6
 SAMPLE CALCULATIONS OF CONDITIONS AFTER COMPLETE MIXING,
 SHOWING EFFECT OF WATER FLOW RATE

Momentum

$$\rho^u \frac{\partial u}{\partial x} + \rho^v \frac{\partial u}{\partial r} = \frac{1}{r} \frac{\partial}{\partial r} \left(\tilde{\mu}_r \frac{\partial u}{\partial r} \right) \quad (19)$$

Enthalpy

$$\rho^u \frac{\partial h}{\partial x} + \rho^v \frac{\partial h}{\partial r} = \frac{1}{r} \frac{\partial}{\partial r} \left(\frac{\tilde{k}}{c_p} r \frac{\partial h}{\partial r} \right) + (\tilde{\mu}) \left(\frac{\partial u}{\partial r} \right)^2 \quad (20)$$

Specie i

$$\rho^u \frac{\partial k_i}{\partial x} + \rho^v \frac{\partial k_i}{\partial r} = \frac{1}{r} \frac{\partial}{\partial r} \left(\rho^r (\tilde{D}) \frac{\partial k_i}{\partial r} \right) \quad (21)$$

where

$$\begin{aligned} \tilde{\mu} &= \text{effective viscosity} = \mu + \rho \mathcal{E}_m \\ \tilde{k} &= \text{effective conductivity} = k + \mathcal{E}_h \\ \tilde{D} &= \text{effective mass diffusivity} = D + \mathcal{E}_D \\ \mathcal{E} &= \text{time-mean value of turbulent diffusion} \\ &\quad \text{coefficients (eddy coefficients)} \end{aligned}$$

These four relations are general for the case of either laminar or turbulent flow (depending upon the relative magnitudes of eddy and molecular transport "properties") within the limitation that axial conduction terms can be ignored.

Equations (19), (20), and (21) may be rewritten in terms of the turbulent Prandtl and Schmidt numbers Pr' and Sc' , respectively:

$$\rho^u \frac{\partial u}{\partial x} + \rho^v \frac{\partial u}{\partial r} = \frac{1}{r} \frac{\partial}{\partial r} \left(\rho \mathcal{E}_m \frac{\partial u}{\partial r} \right) \quad (22)$$

$$\rho^u \frac{\partial \left(h + \frac{u^2}{2} \right)}{\partial x} + \rho^v \frac{\partial \left(h + \frac{u^2}{2} \right)}{\partial r} = \frac{1}{r} \frac{\partial}{\partial r} \left[\rho \mathcal{E}_{m,r} \frac{\partial}{\partial r} \left(\frac{h}{Pr'} + \frac{u^2}{2} \right) \right] \quad (23)$$

$$\rho^u \frac{\partial k_i}{\partial x} + \rho^v \frac{\partial k_i}{\partial r} = \frac{1}{r} \frac{\partial}{\partial r} \left[\frac{\rho \mathcal{E}_{m,r}}{Sc'} \frac{\partial k_i}{\partial r} \right] \quad (24)$$

It is apparent that these equations are identical in u , h_t ($=$ total enthalpy $= h + \frac{u^2}{2}$), and k_i when the turbulent Prandtl and Schmidt numbers are unity. Since these numbers generally vary from about 0.5 to 1.5 and rarely exceed 1.0 for most gases, the enormous simplification achieved by the assumption $Pr' = Sc' = 1.0$ is not only useful, but also, in general, quite accurate. Consequently, approximately similar solutions for u , h_t , and k_i will be achieved if similar boundary conditions can be established. Since arbitrary base values of enthalpy and concentration are available, any system with but two boundary values of these terms is solvable, providing there exists a solution to any of the above three equations.

2. Reichardt's Inductive Theory of Turbulent Mixing

The classical theory of Reichardt (Reference 6), as developed in some detail for the case of interest here in References 7 and 8, provides an accurate yet relatively simple approach to the highly complex mixing process to be considered.

Writing the inviscid momentum equation for the time average of velocity, using the continuity (mass) equation with $\tilde{\mu} = 0$,

$$\frac{\partial \overline{\rho u^2}}{\partial r} + \frac{1}{r} \frac{\partial}{\partial r} (r \overline{\rho uv}) = 0 \quad (25)$$

From consideration of his experimental data on free turbulent jets, Reichardt found the data to be correlated by a relation of the form:

$$\overline{\rho u^2} = \frac{k}{b^2} e^{-(r/b)^2} \quad (26)$$

where k is a constant depending on the strength of the jet, and b is a parameter dependent solely on $(x - x_j)$.

In order that Equation (26) be a solution to Equation (25), certain conditions must be satisfied. If the two equations are to be compatible, it can be shown that:

$$\overline{\rho uv} = -\frac{b}{2} \frac{db}{dx} \frac{\partial \overline{\rho u^2}}{\partial r} \quad (27)$$

Substituting this into Equation (25),

$$\frac{\partial \overline{\rho u^2}}{\partial x} = \frac{b}{2r} \frac{db}{dx} \frac{\partial}{\partial r} \left(r \frac{\partial \overline{\rho u^2}}{\partial r} \right) \quad (28)$$

Equation (28) is linear in $\overline{\rho u^2}$, and it is, therefore, possible to determine the profile of $\overline{\rho u^2}$ in a field resulting from any number of source jets by a linear superposition of the solutions for the individual jets. Equation (28) is thus the key to the mixing solution utilized here.

In addition to the differential Equation (25) stating the conservation of axially-directed momentum, there also exists the integral relation:

$$(\overline{\rho u^2})_j A_j = \int_0^{\infty} \overline{\rho u^2} 2\pi r dr \quad (29)$$

Insertion of Equation (26) yields:

$$k = (\overline{\rho u^2})_j \frac{A_j}{\pi} \quad (30)$$

which in turn yields the result for a single free jet:

$$\overline{\rho u^2} = (\overline{\rho u^2})_j \frac{A_j}{\pi b^2} e^{-\left(\frac{r}{b}\right)^2} \quad (31)$$

Equation (31) can only be used at axial distances sufficiently far downstream that the jet may be considered a point source, a stipulation which will be shown to be consistent with the wet diffuser problem herein. However, if we assume that the parameter b can be simply expressed in terms of x (where x now may replace $x - x_j$), then results can be obtained for all x by linear superposition of an infinite number of source jets of equal strength, and subsequent integration across the exit plane of the actual flow.

The parameter b has been found experimentally to vary linearly with x (see Reference 9, for example, which contains some excellent basic data for single as well as multiple jets). This dependence may be expressed

$$b = c_m x \quad (32)$$

where c_m is nearly constant and equal to 0.075 (Reference 9).

Results obtained from Reference 10 (using a computer program presented in Reference 8) for the variations of momentum flux for all values of x are plotted in Figure 7. It can be shown from the results of Figure 7 that Equation (31) is approximately correct for values of x/D_j greater than about 10, a condition quite appropriate to the wet-duct diffuser geometry.

3. Application of Reichardt's Theory to the Wet-Duct Diffuser

Consider a single axial water source jet issuing into an infinite hydrogen stream flowing parallel to the jet. Performing a linear superposition of source (hydrogen and water) momenta, the local momentum fluxes downstream of the origin of mixing are as follows, according to Reichardt's theory (Equation (31)):

$$\rho u^2 = (\rho u^2)_H + \left[(\rho u^2)_j - (\rho u^2)_H \right] \left(\frac{D_j}{2c_m x} \right)^2 e^{-\left(\frac{r}{c_m x} \right)^2} \quad (33)$$

where r is the radial distance from the centerline of the jet to an arbitrary point in the flow field.

For turbulent Schmidt number unity, it follows from the similarity arguments of the previous subsection that the species flux is:

$$\rho u k_i = (\rho u k_i)_H + \left[(\rho u k_i)_j - (\rho u k_i)_H \right] \left(\frac{D_j}{2c_m x} \right)^2 e^{-\left(\frac{r}{c_m x} \right)^2} \quad (34)$$

and for turbulent Prandtl number unity, the total enthalpy flux is:

$$\rho u (h_t - h_t^\circ) = \left[\rho u (h_t - h_t^\circ) \right]_H + \left\{ \left[\rho u (h_t - h_t^\circ) \right]_j - \left[\rho u (h_t - h_t^\circ) \right]_H \right\} \left(\frac{D_j}{2c_m x} \right)^2 e^{-\left(\frac{r}{c_m x} \right)^2} \quad (35)$$

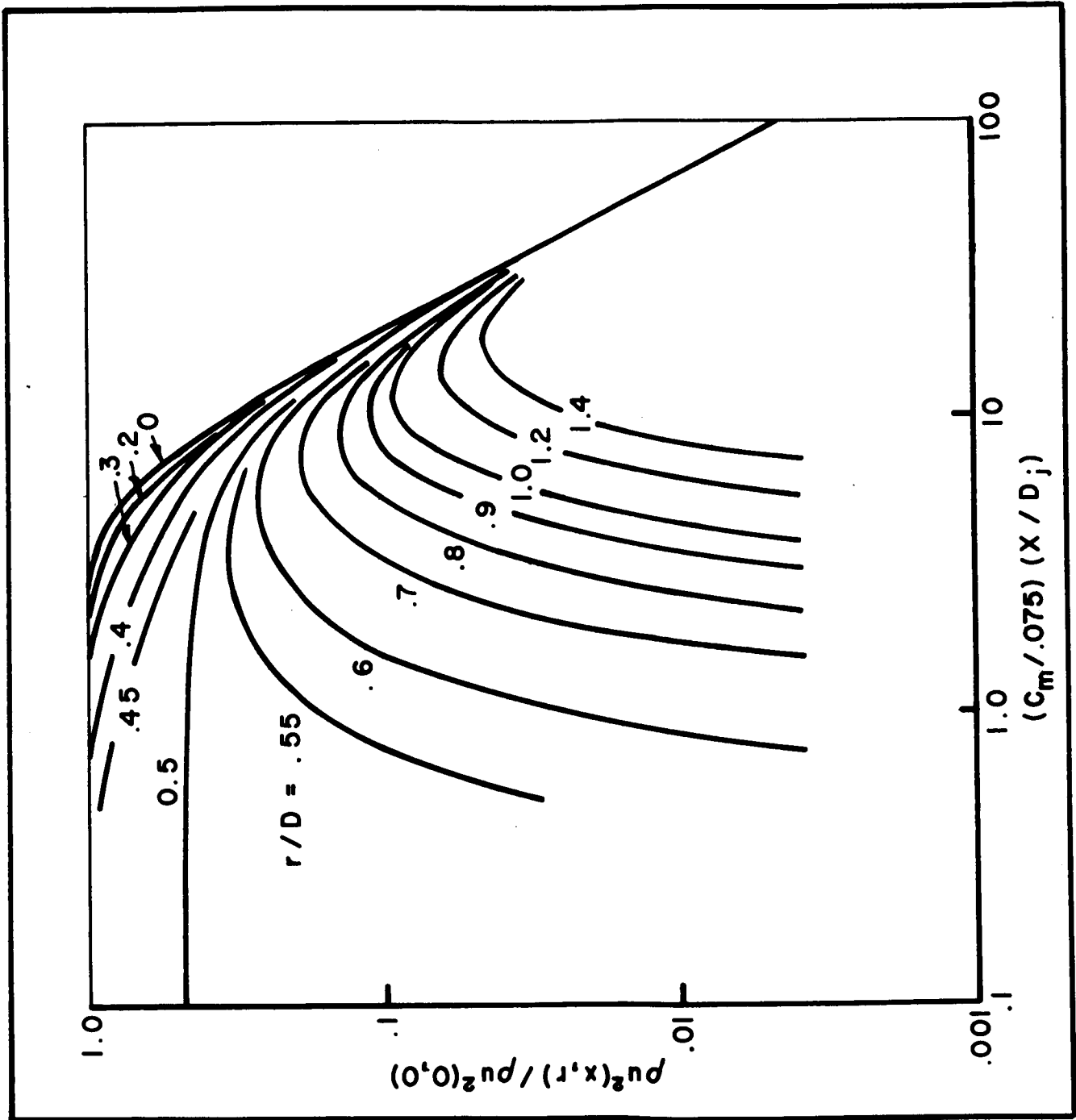


FIGURE 7

DISTRIBUTION OF MOMENTUM FLUX ACCORDING TO REICHARDT'S THEORY FOR A SINGLE JET DISCHARGING INTO A QUIESCENT ATMOSPHERE

As discussed earlier, it is necessary to establish similar boundary conditions on u , k_i , and h_t in order to obtain similar solutions for the various fluxes. Similar boundary conditions can be established for k_i and h_t by defining the following conditions for the infinite hydrogen stream:

$$\left. \begin{aligned} k_{iH} &= 0 \\ (h_t - h_t^\circ)_H &= 0 \end{aligned} \right\} \text{ at infinity} \quad (36)$$

Inasmuch as the base state for enthalpy is arbitrary, Equation (36) is satisfied by assigning to the reference enthalpy, h_t° , the value of the total enthalpy in the hydrogen stream, h_{tH} . For the two-component system considered here (water and hydrogen), Equation (36) is automatically satisfied (for the infinite free stream) by choosing the species i to be water ($k_{iH} = 0$ since there is no water at $r = \infty$).

Letting $i = 1$ and rewriting Equations (34) and (35):

$$\rho u k_1 = (\rho u)_j \left(\frac{D_j}{2c_m x} \right)^2 e^{-\left(\frac{r}{c_m x} \right)^2} \quad (37)$$

since $k_1 = 1.0$ in the jet, and

$$\rho u (h_t - h_{tH}) = \left[\rho u (h_t - h_{tH}) \right]_j \left(\frac{D_j}{2c_m x} \right)^2 e^{-\left(\frac{r}{c_m x} \right)^2} \quad (38)$$

In order to establish similar boundary conditions on velocity, it is necessary to rewrite Equation (33) in terms of velocity differences; that is:

$$\text{similar momentum flux} = \rho u (u - u^\circ) \quad (39)$$

where u° is a reference velocity. Further, for the boundary conditions on u to be similar to those established on k and h_t , u° must equal u_H which in turn must be equal

to zero. It would then appear that the present formulation is rigorously correct only when the hydrogen velocity is zero. It was, however, established through comparisons made with solutions obtained through use of the Crocco relations that the present solutions are also valid when the jet velocity is small compared to the hydrogen velocity, which will ordinarily be the case. Consequently, Equations (33), (37), and (38) have been used, despite the fact that they introduce several rather severe approximations.

Considering now the case of multiple jets in an infinite free stream, various fluxes can be linearly superimposed by simply changing the exponential function:

$$\left(\frac{D_j}{2c_m x}\right)^2 e^{-\left(\frac{r}{c_m x}\right)^2}$$

for the single jet to:

$$\sum_{i=1}^{N_j} \left(\frac{D_j}{2c_m x}\right)^2 e^{-\left(\frac{s_i}{c_m x}\right)^2}$$

where N_j is the number of jets in the infinite free stream, and s_i is the radial distance from a jet centerline to the point of interest in the flow field. Up to this point, there has been no restriction on the number of jets or their arrangement; however, they have been constrained to the same axial location and momenta.

The wet diffuser problem differs from that described above, for which a solution is available, in at least two important ways:

- (a) Axial pressure gradients will generally exist in the mixing duct as required to satisfy momentum (see previous section).
- (b) The integration limits on the right-hand side of Equation (29) are (1) zero and (2) the duct radius; as compared with (1) zero and (2) infinity for the free-jet case. This suggests that if Reichardt's

theory is employed, the mass, momentum, and enthalpy fluxes within the duct must somehow be modified to assure conservation within the system.

It will be shown later that for mixing ducts shorter than:

$$\frac{c_m x}{D_2} \approx 0.3,$$

Item (b) above is satisfied simply by allowing for each source jet two mirror images which reflect quantities of mass, momentum, or energy back into the duct in an approximately correct way. For $c_m = 0.075$, this means that Item (b) above is not critical for regions in the mixing duct upstream of four duct diameters. This technique was employed in Reference 1. In order to correct Item (a), however, a major modification to the analysis of Reference 1 is necessary.

The general approach to the inclusion of axial pressure gradients was to obtain constant-pressure solutions as in Reference 1. An integration was then performed across the flow field to check on hydrogen continuity, with results characterized by those shown in Figure 8. The results clearly demonstrate that axial pressure gradients must be considered, almost regardless of their magnitude, to assure that the hydrogen flow is conserved. If it is not conserved, it is clear that neither momentum nor energy are conserved in the system, and any resulting flow field temperature predictions will be in error.

It has been suggested that the general form of Equation (31) for mixing of a jet with stagnant fluid in a confined duct is:

$$\frac{(p - p^\circ) + \rho u^2}{(p_i - p^\circ) + \rho_i u_i^2} = \left(\frac{D_j}{2c_m x}\right)^2 e^{-\left(\frac{r}{c_m x}\right)^2} + \phi_m \left(\frac{c_m x}{D}\right) \quad (40)$$

where $\phi_m \left(\frac{c_m x}{D}\right)$ will be defined later, and is a flux correction due to the confined duct flow, and the subscript i denotes initial conditions. For the case of a free jet, p° is taken as the ambient pressure so that

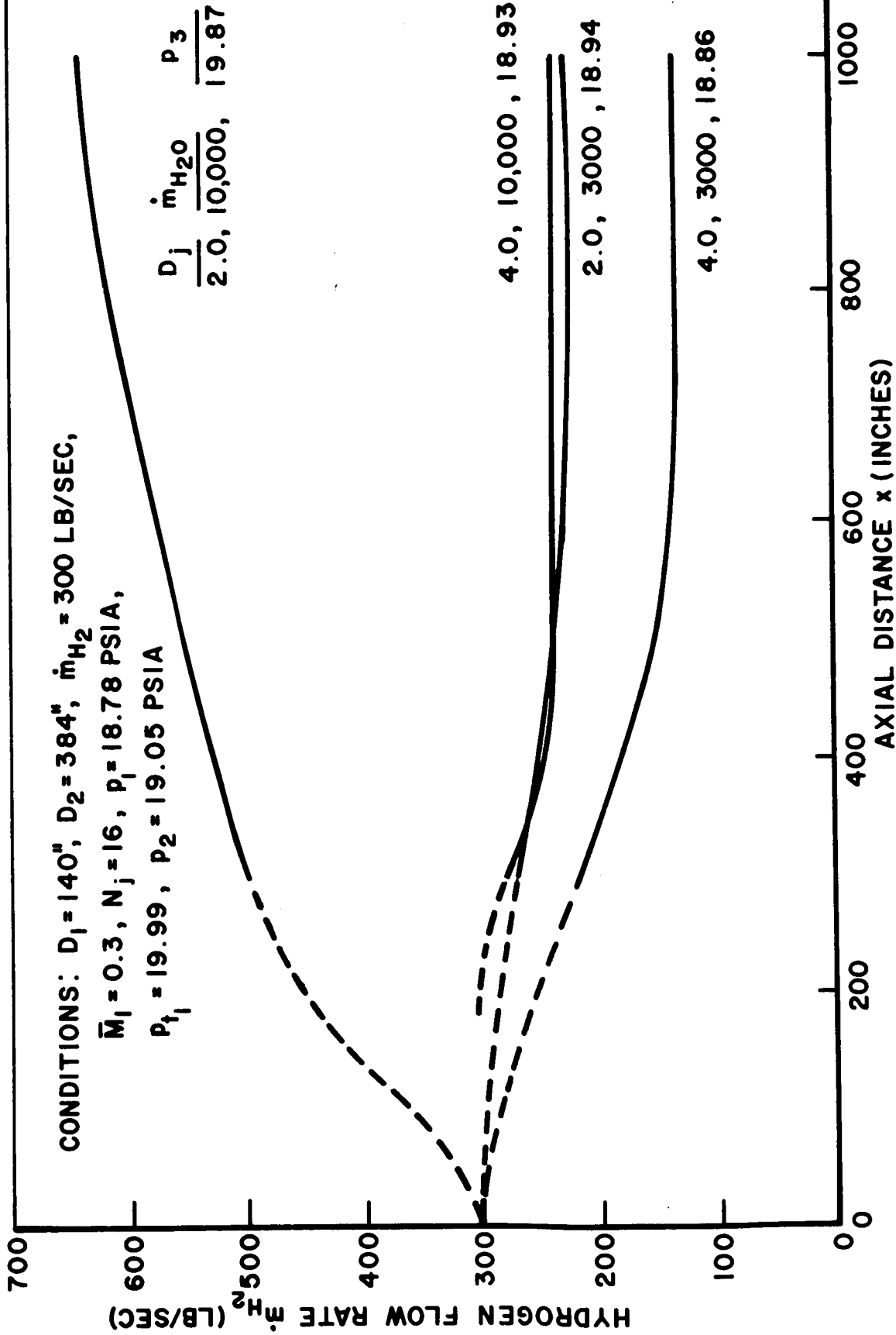


FIGURE 8
 INFLUENCE OF CONSTANT-PRESSURE ASSUMPTION ON
 HYDROGEN CONTINUITY IN THE MIXING DUCT

$(p - p^\circ)$ is always zero, and $\phi_m \left(\frac{c}{D}\right)$ is identically zero.

When fluxes due to jets are superimposed on fluxes due to the hydrogen, the local momentum flux for the wet diffuser analysis, according to Equation (40), is:

$$\begin{aligned} \rho u^2 = & (p_2 - p) + \rho_H u_H^2 \\ & + \left(\rho_j u_j^2 - \rho_H u_H^2 \right) \left[\sum_{i=1}^{3N_j} \left(\frac{D_j}{2c_m x} \right)^2 e^{-\left(\frac{s_i}{c_m x}\right)^2} \right. \\ & \left. + \sum_{j=1}^{N_j} \phi_{m_j} \left(\frac{c}{D_2} \right) \right] \end{aligned} \quad (41)$$

and p° need not be specified. The upper limit on the first summation, $3N_j$, reflects the one incident distance and two reflected distances considered in the final computer formulation for each jet.

It has been demonstrated that although mass and energy transport are in general different than momentum transport (see Reference 9, for example), experimental mass and energy fluxes can nevertheless be satisfactorily predicted by employing mixing constants appropriate to the flux considered (c_m for momentum, c_k for mass, and c_h for energy). However, consideration was given to the likelihood that, for the wet diffuser problem, condensed species may diffuse differently than do gas particles. This possibility for different mixing was included in the present computer program where the local water mass flux is:

$$\rho u k_1 = \rho_j u_j \left[\sum_{i=1}^{3N_j} \left(\frac{D_j}{2c_k x} \right)^2 e^{-\left(\frac{s_i}{c_k x}\right)^2} + \sum_{j=1}^{N_j} \phi_{k_j} \left(\frac{c}{D_2} \right) \right] \quad (42)$$

and the enthalpy flux is:

$$\rho^u (h_t - h_{t_H}) = \left[\rho_j^u (h_{t_j} - h_{t_H}) \right] \left[\sum_{i=1}^{3N_j} \left(\frac{D_j}{2c_h x} \right)^2 e^{-\left(\frac{s_i}{c_h x} \right)^2} + \sum_{j=1}^{N_j} \phi_{h_j} \left(\frac{c_h x}{D_2} \right) \right] \quad (43)$$

Consistent with the argument presented just subsequent to Equation (12), it is assumed here that:

$$c_k = c_h \quad \text{and, as will be seen later,} \quad (44)$$

$$\phi_k \left(\frac{c_k x}{D_2} \right) = \phi_h \left(\frac{c_h x}{D_2} \right) \quad (45)$$

Now, as noted previously, jet mass, momentum, and energy will not be conserved in a confined duct if the free-jet theory of Reichardt is employed without modification. Consideration must therefore be given to suitable methods for the modification of Reichardt's theory for the present problem. This is done through study of the simple case of a single jet located on the centerline of the entrance of the mixing duct, and evaluation of the mass flow rate from the water mass flux relation.

Consider the mass flux relation given by Equation (42). The mass flow rate of water in the mixing duct at any axial location can be obtained by evaluation of the following double integral, which can be performed before the solution for state properties.

$$\dot{m}_{H_2O} = \int_0^{2\pi} \int_0^R (\rho u k_1) r dr d\theta \quad (46)$$

If all is well, the water flow rate from Equation (42) will be the input water flow rate. The function:

$$\phi_k \left(\frac{c_k x}{D_2} \right)$$

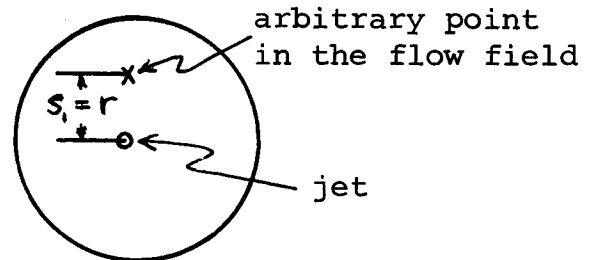
is so defined as to always satisfy this requirement. Nevertheless, its definition depends upon the degree of rigor applied to the physics of the problem. Several approaches were considered:

- (a) Consideration of fluxes due to an incident distance from a jet to a point in the flow field according to the theory of Reichardt, with a uniform mass flux added across the flow field by an amount sufficient to yield a water flow rate equal to the input flow rate.
- (b) Same as above, except for additional consideration of two mirror images of the source jet (the reflection method used in Reference 1).
- (c) Arrangements of six source jets outside the duct for each actual jet within the duct, so as to artificially confine the water flow to the duct.

Note that the upper limits on the first summations of Equations (41) through (43) are N_j , $3N_j$, and $7N_j$ for approaches (a), (b), and (c), respectively. These approaches for a single jet on the centerline appear physically as shown below:

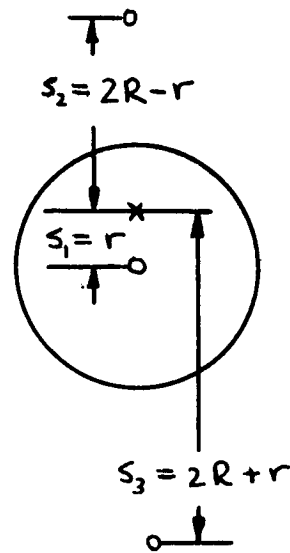
- (a) No reflecting jets

for $\xi \equiv \frac{D_2}{2c_k x}$,



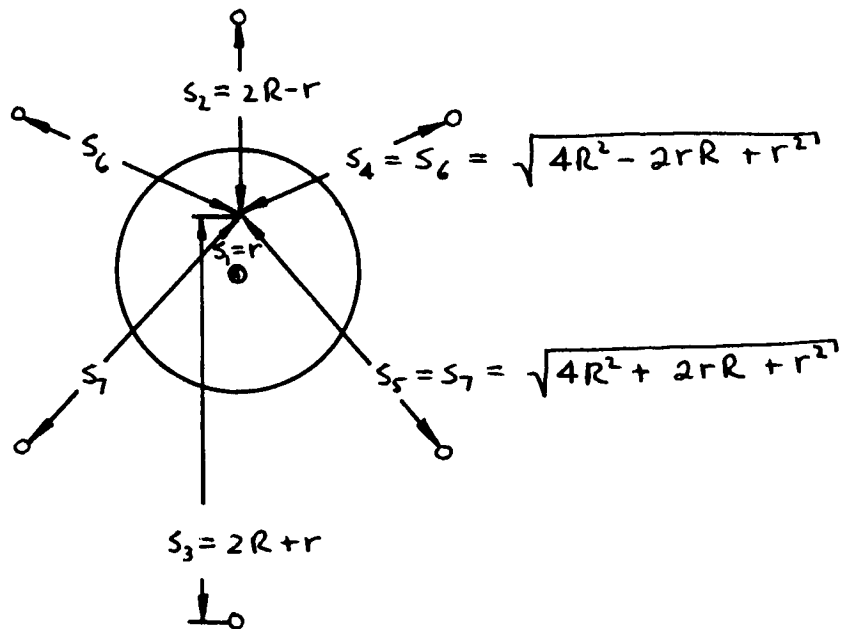
$$\phi_k \left(\frac{c_k x}{D_2} \right) = \left(\frac{D_j}{D_2} \right)^2 e^{-\xi^2} \quad (47)$$

(b) Two reflecting jets
(doublet reflection)



$$\Phi_k \left(\frac{c_k x}{D_2} \right) = \left(\frac{D_j}{D_2} \right)^2 \left\{ e^{-(3\xi)^2} + 2e^{-\xi^2} - 2e^{-(2\xi)^2} + 4\xi \left[\operatorname{erf}(\xi) + \operatorname{erf}(3\xi) - 2\operatorname{erf}(2\xi) \right] \right\} \quad (48)$$

(c) Six "reflecting" jets
(sextant reflection)



$$\Phi_k \left(\frac{c_k x}{D_2} \right) = \left(\frac{D_j}{D_2} \right)^2 - 2 \int_0^1 \left[\sum_{i=1}^7 \left(\frac{D_j}{2c_k x} \right)^2 e^{-\left(\frac{s_i}{c_k x} \right)^2} \right] \eta d\eta \quad (49)$$

The flux correction function can be evaluated from the jet geometry, c_k , and the axial location, without consideration of thermodynamic or fluid-dynamic variables. For the simple case of a single jet on the centerline, the functions can be evaluated analytically for the first two approaches, as indicated. More complex geometries require numerical integrations such as for the sextant system above.

Variations of water flow rate without the flux correction functions for each of the geometries considered above are presented in Figure 9. As noted earlier for the doublet reflection scheme, water mass loss is negligible for $\frac{c_k x}{D} < 0.3$.

A series of sample problems were run during the course of the computer program development to determine the relative effectiveness of the various schemes. Input conditions were chosen such as to cause large pressure gradients in the mixing duct. Certain of these results are presented in Figure 10, showing the computed hydrogen concentration distribution in the duct for the first two schemes.* The first scheme is the simplest operationally, but does not satisfy the necessary physics in the sense that concentration gradients must be zero at the wall if there is to be no mass flux across the wall. The second scheme does satisfy this physical constraint, and at the same time would appear to yield faster mixing. Note that for both cases the final hydrogen concentration is that which would be computed from the input.

Results from the doublet system with the flux correction function are compared with the sextant system without flux corrections in Figures 11 and 12. The latter scheme is perhaps the most appealing physically, but is more cumbersome operationally. Axial pressure distributions are in agreement in Figure 11 for values of x less than about 600 inches ($\frac{c_k x}{D_2} \approx 0.32$). Far downstream, the

* For these and all later runs, local mixing duct pressure is that required to satisfy hydrogen continuity, regardless of the degree to which other conservation constraints are satisfied.

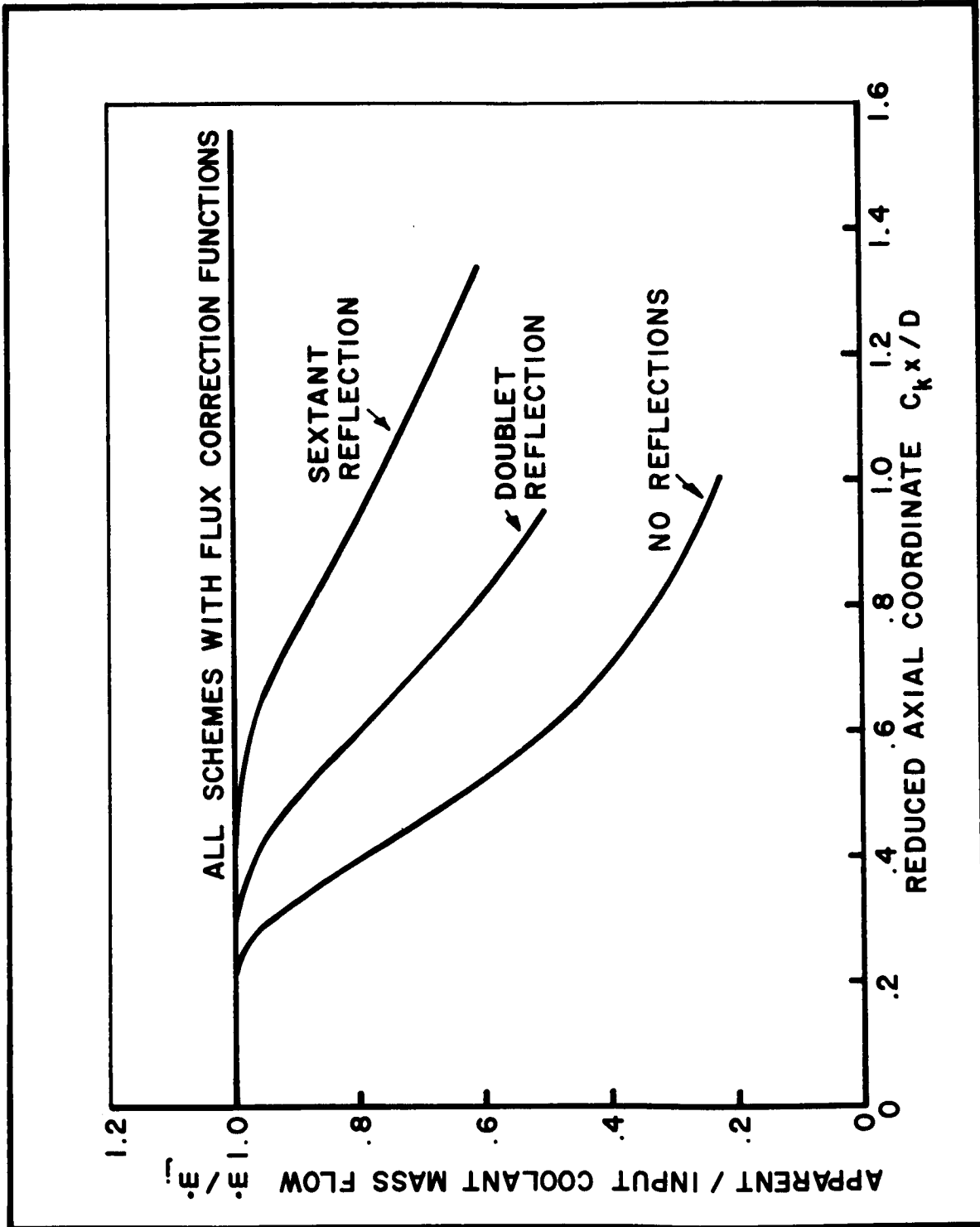


FIGURE 9

APPARENT LOSS OF COOLANT JET MASS DUE TO MIXING IN A
 CONFINED DUCT FOR A SINGLE JET ON THE CENTERLINE

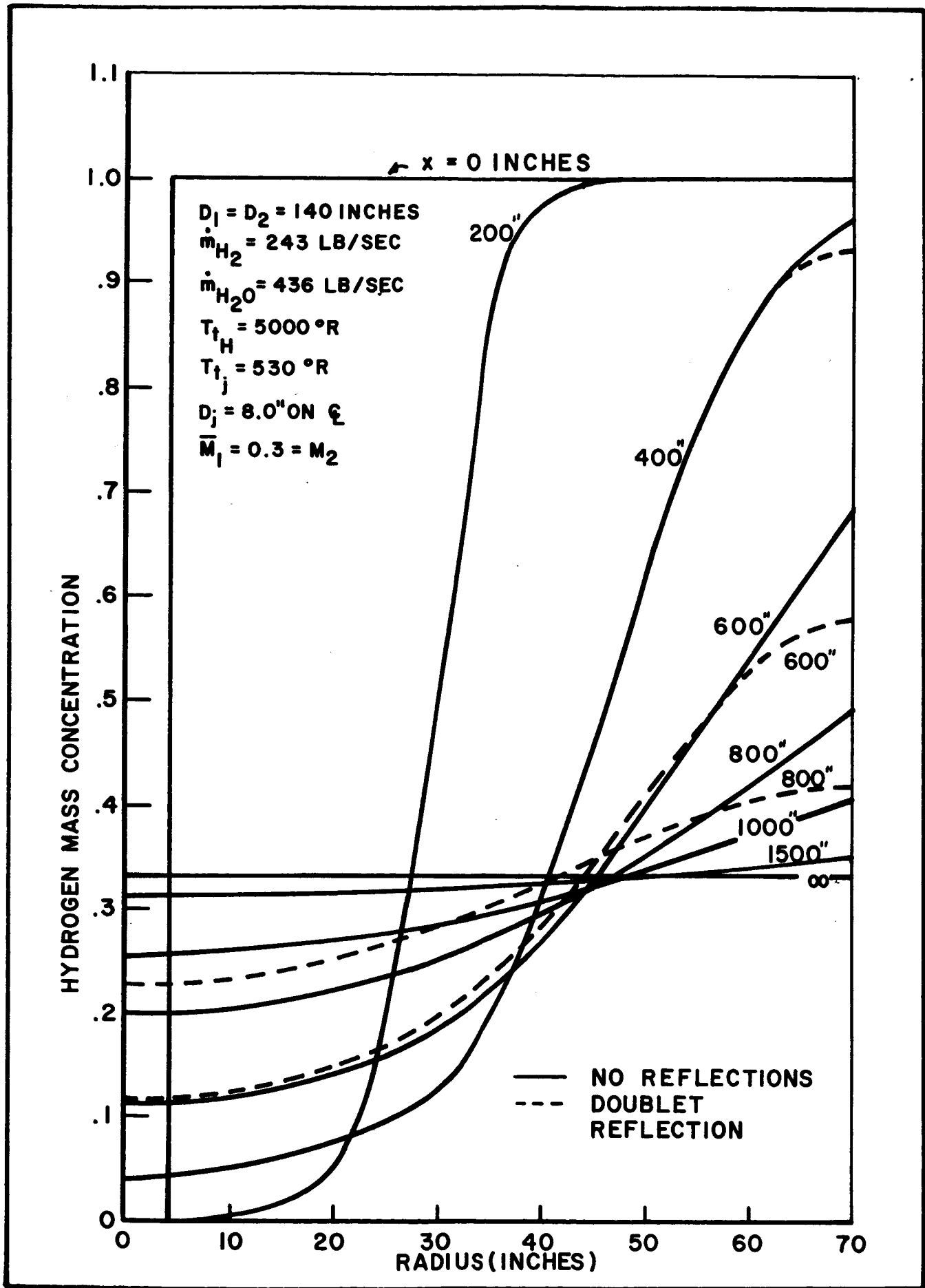


FIGURE 10

TYPICAL COMPUTED HYDROGEN CONCENTRATION DISTRIBUTIONS FOR TWO FLUX CORRECTION SCHEMES (NO REFLECTIONS & DOUBLET REFLECTION)

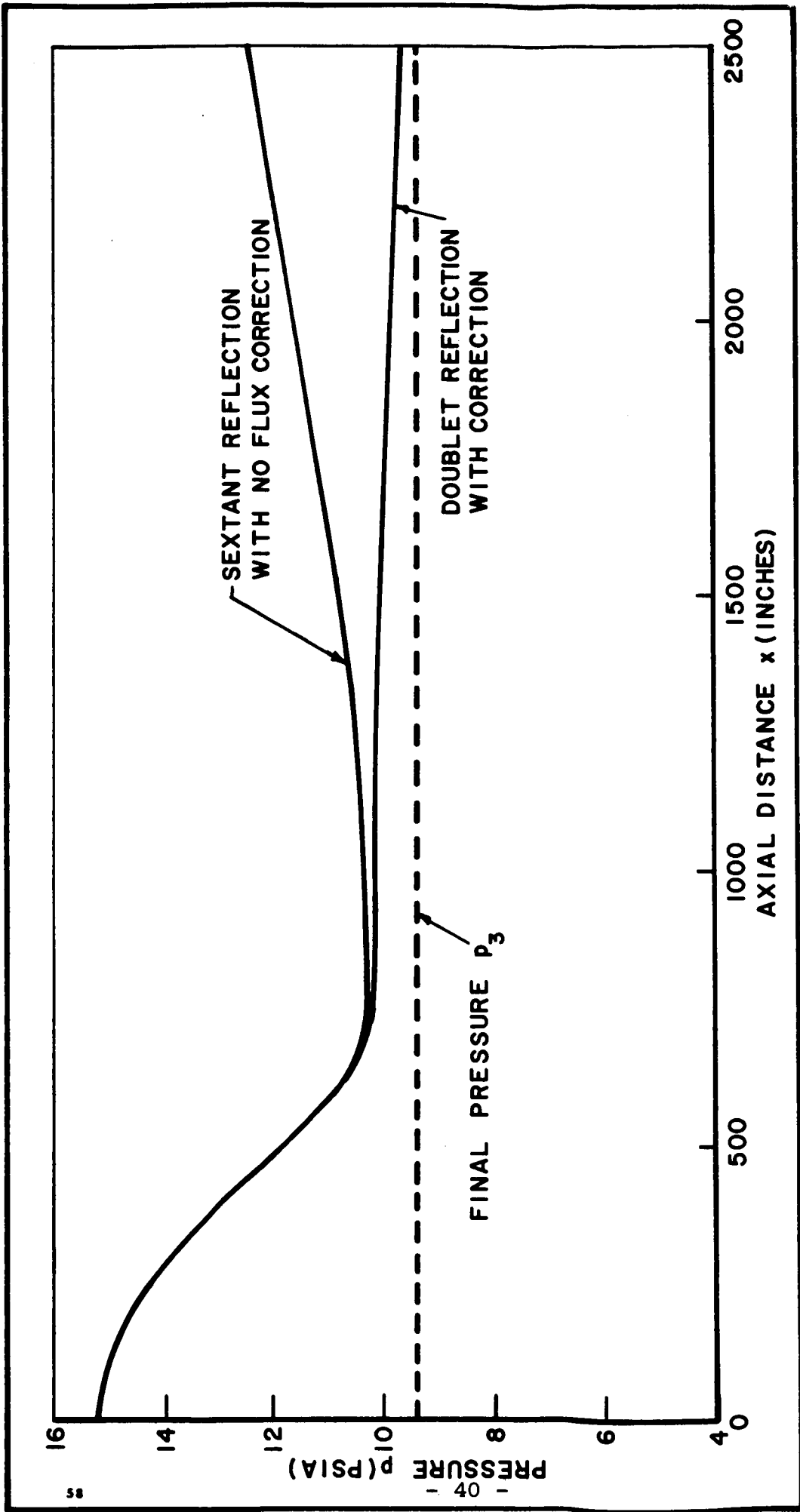


FIGURE 11

TYPICAL AXIAL PRESSURE DISTRIBUTION FOR TWO FLUX CORRECTION SCHEMES
(DOUBLET AND SEXTANT REFLECTION)

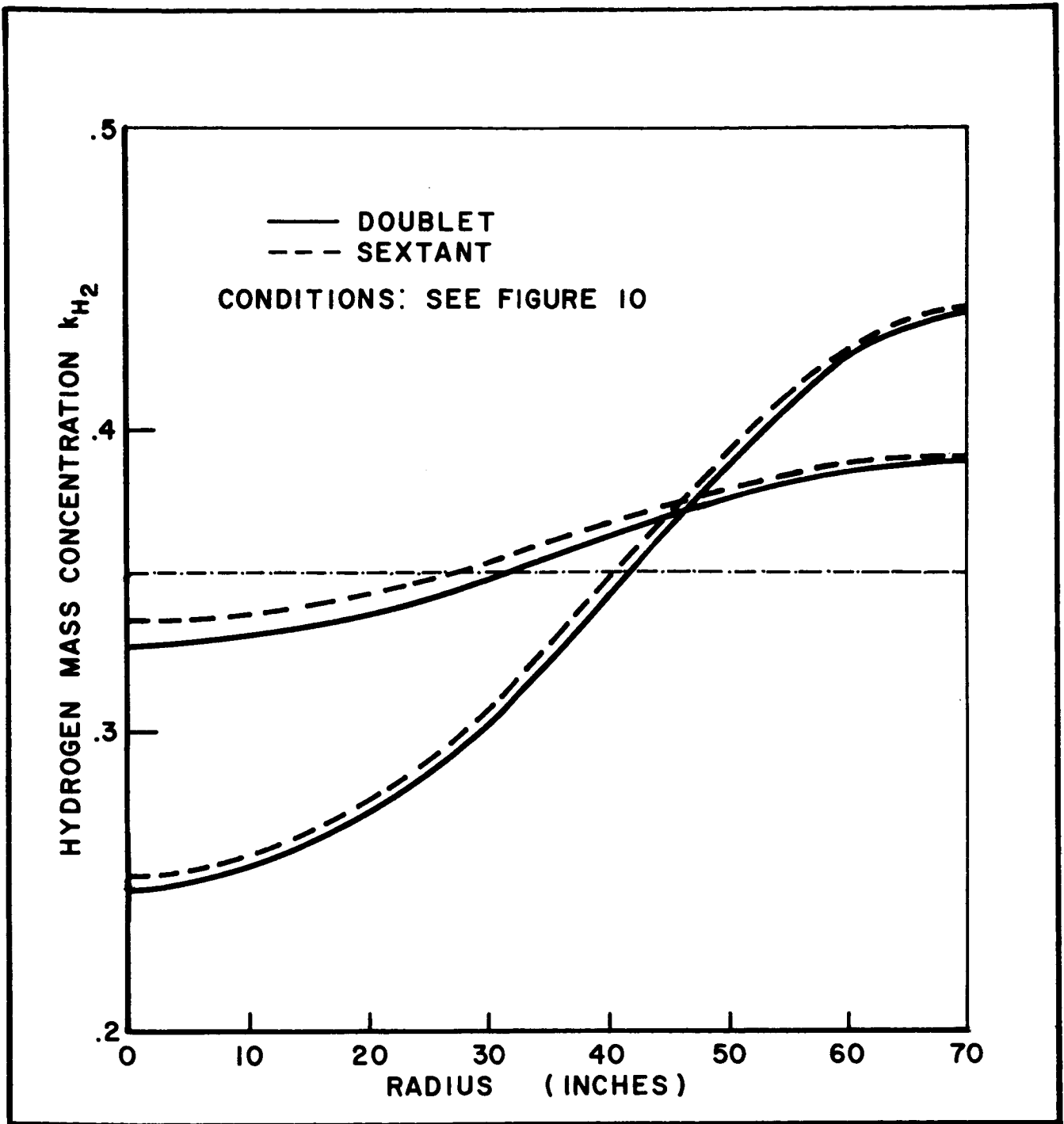


FIGURE 12

COMPARISONS OF HYDROGEN CONCENTRATIONS
FOR DOUBLET & SEXTANT REFLECTIONS

predicted pressures diverge, the pressures for the sextant system being in error due to failure to provide overall conservation. Hydrogen concentration distributions for these two schemes are presented in Figure 12, where it is seen that the results are substantially identical at $x = 800$ inches. At $x = 1000$ inches, the sextant system shows higher hydrogen concentration due to loss of water from the system.

As a result of the foregoing "computer experiments," the doublet reflection scheme has been adopted. The flux correction functions for energy and momentum have been obtained by analogy to the mass flux correction function.

The general definition of the momentum function is presented below, its value in general being obtained by numerical integration of the indicated integral. The mass and energy flux correction functions are identical in format to Equation (50), differing only in the subscripts--the "m" being replaced by "k" and "h" respectively:

$$\sum_{j=1}^{N_j} \phi_{m_j} \left(\frac{c_m x}{D_2} \right) = \frac{\sum_j A_j}{A_2} - \frac{1}{\pi} \int_0^{2\pi} \int_0^1 \left[\sum_{i=1}^{3N_j} \left(\frac{D_j}{2c_m x} \right)^2 e^{-\left(\frac{s_i}{c_m x} \right)^2} \eta \, d\eta \, d\theta \right] \quad (50)$$

Various test cases have been run to establish that conditions far downstream in the mixing duct are identical to those established previously for the completely mixed conditions, demonstrating the overall consistency of the analysis and assumptions.

G. Calculation of State Parameters

The mixing analysis discussed above provides the following information for each assumed static pressure:

$$1. \text{ momentum flux } \rho u^2 \equiv a \quad (51)$$

$$2. \text{ enthalpy flux } \rho u (h_t - h_{t_H}) = \rho u h + a \frac{u}{2} - \rho u h_{t_H} \quad (52)$$

$$3. \text{ water mass flux } \rho u k_{H_2O} \equiv c' \quad (53)$$

4. local mixing duct pressure P

5. hydrogen stagnation enthalpy h_{t_H} (from input T_{t_H})

A subroutine called STATE solves these fluxes simultaneously to obtain the desired quantities of local velocity, density, stagnation pressure, stagnation temperature, Mach number, and mass concentrations of condensed water, vaporized water, and hydrogen. The solution procedure is presented briefly in the following paragraphs.

In this subsection, the subscripts 1, 2, and 3 refer to condensed water, vapor water, and hydrogen, respectively. The parameter p is either pressure (in atmospheres), or number of moles, depending upon where it appears. The approach to the solution is to guess a static temperature, calculate all properties from the stoichiometry, evaluate an enthalpy flux for the guessed temperature, and compare it to the enthalpy flux obtained from the main mixing program. Temperature is re-estimated until convergence is obtained on the correct enthalpy flux. The iteration procedure on the assumed pressure is discussed later.

All necessary thermochemical data are stored in the form of curve-fit constants obtained from KEMD. Enthalpies and entropies at a given temperature are calculated in STATE, employing the curve-fit equations.

Details of the analysis are as follows:

The system contains P moles of gas (where P is the duct static pressure) composed of p_2 and p_3 moles of water vapor and hydrogen, respectively. It also contains p_1 moles of condensed water. The mass of water is:

$$(p_1 + p_2) m_1 = (pm)_1 + (pm)_2 \equiv pm_1 + pm_2 \quad (54)$$

the mass of hydrogen is:

$$p_3 m_3 = (pm)_3 \equiv pm_3 \quad (55)$$

and the total mass is:

$$(pm)_1 + (pm)_2 + (pm)_3 = Pm \quad (56)$$

where m is the molecular weight of the mixture (system mass divided by total number of moles of gas). In volume units, there are $R^\circ T$ volume units of gas and $p_1 m_1 / \rho_l$ volume units of liquid.

Based on the above system:

$$k_{H_2O} = \frac{(p_1 + p_2) m_1}{Pm} = \text{mass concentration of total water} \quad (57)$$

$$\rho = \frac{Pm}{R^\circ T + \frac{(pm)_1}{\rho_l}} \quad \text{where } \rho_l = \text{liquid density}$$

$$= 62.4 \text{ lb/ft}^3 \quad (58)$$

$$p_2 + p_3 = p \quad (59)$$

If liquid water is present in the system, equilibrium between the water and its vapor requires that:

$$p_2^e = k_p = e^{-\frac{\Delta F}{R^\circ T}} = e^{-\left(\frac{\Delta h}{R^\circ T} + \frac{\Delta s}{R}\right)} \quad (60)$$

where superscript ()^e signifies p_2 with liquid present.

From the momentum and water mass flux outputs of the mixing program, Equations (51) and (53),

$$\rho^{\frac{1}{2}} k_{H_2O} = \frac{c'}{\sqrt{a'}} \equiv c \quad (61)$$

Squaring Equation (61), and introducing Equations (57 and (58),

$$c^2 = \frac{(pm_1 + pm_2)^2}{Pm \left(R^\circ T + \frac{pm_1}{\rho_t} \right)} \quad (62)$$

which, with Equation (56), yields:

$$(pm_1 + pm_2)^2 = c^2 \left(R^\circ T + \frac{pm_1}{\rho_t} \right) (pm_1 + pm_2 + pm_3) \quad (63)$$

Two possibilities exist:

--Either liquid water is present and p_2 is obtained from Equation (60), and Equations (63) and (59) are solved for p_1 ;

--Or liquid water is absent ($p_1 = 0$) and Equation (63) is solved for p_2 ($= p_2^a$ where "a" stands for anhydrous).

To establish whether or not liquid water is present at the assumed temperature, a comparison is made between p_2^a and p_2^e with the following result:

If $p_2^a > p_2^e$, liquid water is present and $p_2 = p_2^e$.

If $p_2^a \leq p_2^e$, liquid water is absent and $p_2 = p_2^a$.

The final equations for p_2^a and p_1 (if liquid water is found to be present at the assumed temperature) are:

$$p_2^a = \left(1 - \frac{m_3}{m_1}\right) \frac{c^2 R^\circ T}{2} + \sqrt{\left[\left(1 - \frac{m_3}{m_1}\right) \frac{c^2 R^\circ T}{2}\right]^2 + c^2 R^\circ T p m_3} \quad (64)$$

$$p_1 = \frac{\underbrace{-\left[2 p m_2 \frac{c^2}{\rho} (p m_2 + p m_3) - c^2 R^\circ T\right]}_b + \sqrt{b^2 - 4 \left(1 - \frac{c^2}{\rho}\right) \left[(p m_2)^2 - c^2 R^\circ T (p m_2 + p m_3) \right]}}{2 m_1 \left(1 - \frac{c^2}{\rho}\right)} \quad (65)$$

In either case, p_3 is calculated from Equation (59). The above equations and the thermochemical data are sufficient to calculate all required properties. The procedure necessary to complete one iteration is as follows:

1. p_m is calculated from Equation (56) using the results of Equations (64) or (65) with p_2^e .

2. ρ is calculated from Equation (58).

3. $u = \sqrt{\frac{a}{\rho}}$ (66)

4. Static enthalpy $h = \frac{p_1 h_1 + p_2 h_2 + p_3 h_3}{p_m}$ $\left(\frac{\text{cal}}{\text{gm}}\right)$ (67)

where the h 's are molar enthalpies at the assumed temperature.

5. Total enthalpy $h_t = h + \frac{u^2}{2}$ (68)

6. Enthalpy flux = $\rho u (h_t - h_{t_H})$ (69)

7. The magnitude of Equation (69) is compared with the magnitude of Equation (52), and the error ϵ is defined by:

$$\epsilon = (\text{Flux})_{69} - (\text{Flux})_{52} \quad (70)$$

8. An error derivative $\frac{d\epsilon}{d\ln T}$ is obtained by finite differences.

9. A new temperature for another iteration is calculated:

$$T_{\text{new}} = T_{\text{old}} e^{-\epsilon / \frac{d\epsilon}{d\ln T}} \quad (71)$$

At this point, the percentage change in temperature between iterations is tested against convergence criteria. If convergence is obtained, mass concentrations are calculated as follows:

$$k_1 = \frac{pm_1}{Pm}, \quad k_2 = \frac{pm_2}{Pm}, \quad k_3 = \frac{pm_3}{Pm} \quad (72)$$

The mixture "effective gaseous" properties are calculated at the static temperature, and stagnation temperature, pressures, and flow Mach numbers are calculated from the following relations (obtained from the two-phase flow relations of Reference 11):

$$\bar{\gamma} = \frac{\gamma_g (\beta + 1)}{\gamma_g \beta + 1} \quad (73)$$

where:

$$\gamma_g = \frac{1}{R^\circ \left(\frac{k_2}{m_2} + \frac{k_3}{m_3} \right) + \frac{\frac{k_2}{m_2} c_{p2} + \frac{k_3}{m_3} c_{p3}}{1}} \quad (74)$$

and:

$$\beta = \frac{\frac{k_1}{m_1} c_{p1}}{\frac{k_2}{m_2} c_{p2} + \frac{k_3}{m_3} c_{p3}} \quad (75)$$

$$a^2 = \bar{\gamma} R^\circ T \left(\frac{k_2}{m_2} + \frac{k_3}{m_3} \right) \quad (76)$$

$$M^2 = \frac{u^2}{a^2} \quad (77)$$

$$T_t = T \left(1 + \frac{\bar{\gamma} - 1}{2} M^2 \right) \quad (78)$$

$$p_t = p \left(\frac{T_t}{T} \right)^{\frac{\bar{\gamma}}{\bar{\gamma} - 1}} \quad (79)$$

These equations are valid for perfect-ideal gases. The results are approximate because the "gases" considered are non-ideal (c_p not constant) and imperfect for cases of high condensed water mass fraction. The equations also assume frozen composition during adiabatic stagnation. Although the relations are approximate, their only purpose is for the final printout--i.e., they are not employed anywhere in the problem solution proper.

If the calculation does not converge in thirty-one iterations, the total pressure is printed out of the computer program as zero, along with other information useful for debugging purposes, and control is returned to the main mixing program.

The above solution procedure assumes complete chemical, thermal, and kinetic equilibrium between mixture constituents. Provision for chemical nonequilibrium is provided by employing a factor (VPF) on Equation (60) which is unity for equilibrium, and can provide varying degrees of chemical nonequilibrium to the extent of no vaporization (VPF = 0)

Within the output subroutines (OUTR or OUTCL), converged state properties at a given axial location are stored until they are obtained for all output locations, after which an integration of hydrogen mass flux across the flow cross-section is obtained. If the integrated hydrogen flow is equal to its input magnitude, the state data are printed out. If it is not equal, a new pressure is assumed and the procedure reiterated until hydrogen continuity is satisfied in the manner employed for the determination of the complete mixing conditions as described earlier.

H. Limitations and Special Properties of the Solution

1. Conditions conducive to adverse pressure gradients will, in general, yield reverse flow somewhere in the mixing duct. The program will not obtain convergence for these conditions. Adverse pressure gradients may result in cases of very high jet velocity, which are not typical.
2. The present approach considers mixing in a duct of constant diameter only. The program could be modified to consider variable diameter. It could also be modified to consider "dumping" into a large plenum where three fluids would need to be considered: the water, the hydrogen, and the completely mixed fluid composed of water and hydrogen, which would serve as the atmosphere for a free-jet solution.
3. The analysis is restricted to the assumptions of thermal and kinetic equilibrium, but will allow chemical nonequilibrium to be considered in an approximate way. Although the program is presently restricted to consideration of condensed water injection into gaseous hydrogen flow, it is a simple matter to modify it to consider any other two fluids.
4. The arrangement of jets that will yield an accurate solution is quite restrictive. The arrangements must be such that accurate integrations across the flow field can be obtained when required. The present program considers radial distribution within only two azimuths (except for the axisymmetric case of a single jet on the centerline), and information along these azimuths must be representative of the extremes within the flow field. However, as mixing progresses the flow tends toward an axisymmetric distribution and the integrations become quite good almost regardless of the jet arrangement. The program does not consider an odd number of jets in any one row (except when there is a jet on the centerline as a result of either input or maximum penetration). The program is dimensioned for a maximum of four rows of cooling jets (each row having jets of a different diameter), with no more than 98 jets in any one row.

The numbers of jets between rows can vary, but their number must be a multiple of a base even number.

From an accuracy point of view, it is desirable to choose an arrangement which will maximize the base number. The base number determines the azimuth other than 0° that will be considered in the program; that is, a base number of 2 will consider 0° and 90° , 4 will consider 0° and 45° , etc. The jets may be oriented such that a jet in any given row is at zero azimuth, or such that the zero azimuth falls midway between two jets.

5. Because of the perfect-ideal gas relations employed in the calculations of sonic velocity, stagnation temperatures, and stagnation pressures, these results are neither valid nor reasonable for condensed water concentrations greater than about 99.9 percent. Computed densities, velocities and concentrations are still valid for these cases, however.

IV. COMPUTER PROGRAM

The analysis described in Section III has been programmed in FORTRAN IV. Input data have been kept flexible, so that the program can be used not only for the specific E/STS-2, 3 geometries of interest in the subject contract, but can be applied to virtually any confined or free-jet mixing process.

Details of the analysis and general features of the program have been discussed in detail in Section III. The complete mixing program itself, with all subroutines, appears in Appendix F; the subroutines for establishing variable-velocity inlet conditions and liquid-jet penetration into a variable velocity gas stream (discussed in Section III and in Appendices B and C) appear in Appendix E. A complete card deck of the entire program has been submitted to NASA SNPO-C under separate cover. Writing and debugging of the program and supervision of all data runs (to be discussed in subsequent sections) were performed by Aerotherm Corporation, Palo Alto, California, under the supervision of Mr. Thomas Dahm.

V. EFFECTS OF CERTAIN INPUT PARAMETERS

Problems of critical importance to E/STS -2,3 performance are the evaporation rate and mixing rate of the coolant jets, after injection into the hot gas stream. Although these characteristics must ultimately be established experimentally, it was considered worthwhile to explore their effects by a series of "computer experiments" run under typical test conditions. Results of these "experiments", as well as an evaluation of the effect of azimuthal coolant-jet location, are described in this section.

A. Coolant Jet Azimuth

A typical set of full-scale conditions was selected, using three rows of coolant jets, each with an arbitrarily-selected penetration distance. Temperature profiles one mixing-chamber-diameter downstream of the mixing-chamber entrance were then calculated on two different radial rays: one in a plane passing through the centerline of the coolant jets, and one in a plane midway between the centerlines of two adjacent jets. Results appear in Figure 13, showing that even after only one mixing-chamber diameter, and with an arbitrary, non-optimized coolant injection pattern, the maximum temperature difference between the two cases was only 850°F (650°R in line and 1500°R between jets, at the wall location). Thus it is clear that no significant azimuthal variations are to be expected in the mixing regions of interest.

B. Mixing Coefficient

The mixing coefficients c_m and c_k govern the rates at which the coolant jet momentum and mass, respectively, diffuse into the gas stream. In the analysis of Reference 1, these values were both selected at 0.075 on the basis established in Reference 9, and this is the value used in the computations described later in this report. However, it is not clear whether the unevaporated liquid particles would diffuse at the same rate as the coolant vapor, and thus the effective value of c_k may change. In fact, c_k may take different values at different points in

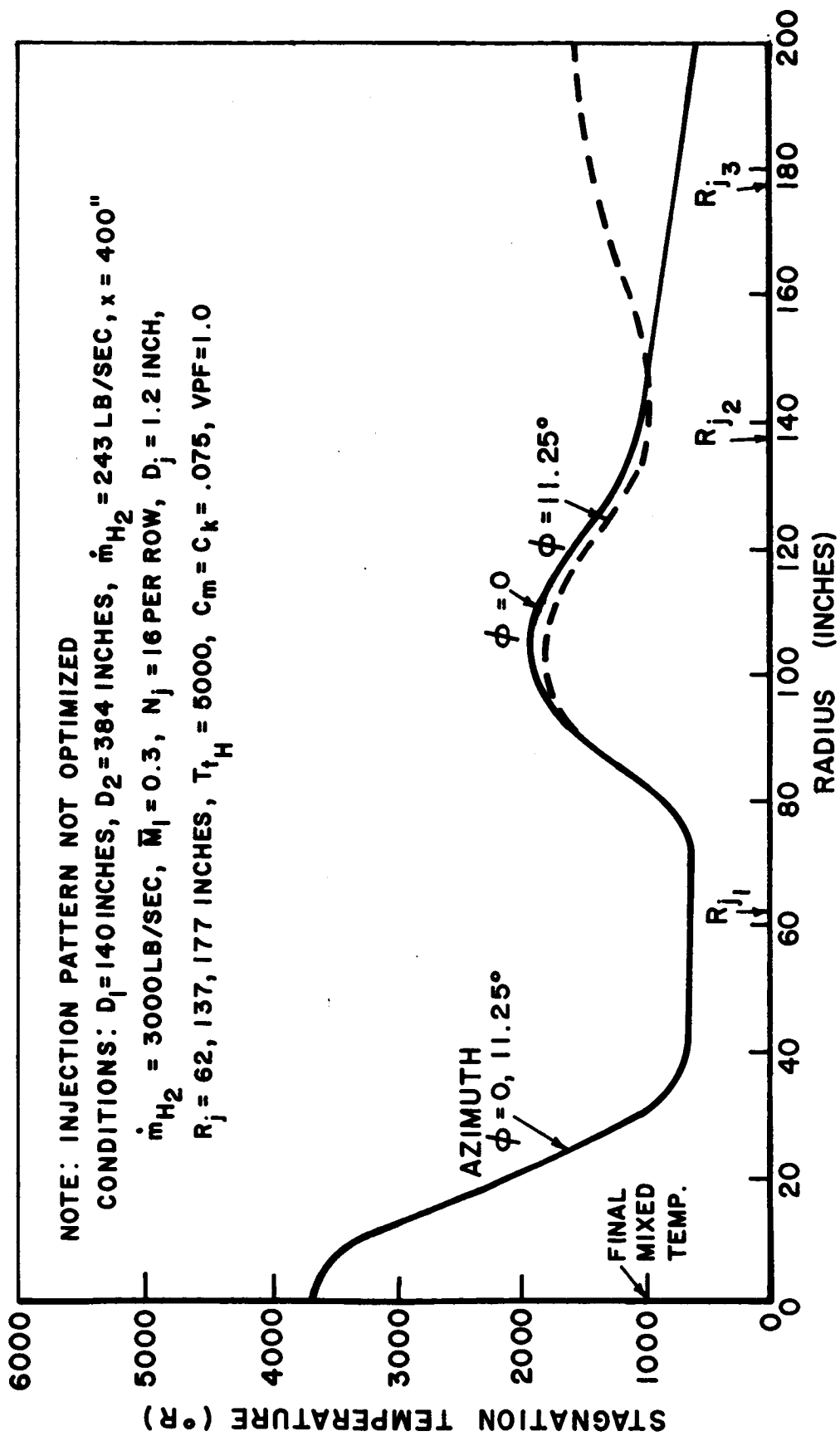


FIGURE 13

EFFECT OF AZIMUTHAL LOCATION ON MIXED TEMPERATURE PROFILE

the flow field, depending on the relative component concentrations. It was therefore decided to run several "experiments" with different values of c_m and c_k . These are shown in Figures 14 and 15, which were performed for the same typical set of full-scale conditions used for Figure 13.

In these figures, mixed temperature profiles are shown at a location one mixing-duct diameter downstream of the inlet, with an arbitrary (non-optimized) selection of coolant-jet penetration distances and different combinations of c_m and c_k . Figure 14 shows the effect of simultaneously changing both coefficients, and illustrates the serious effect of a decrease in mixing effectiveness (i.e., the lower values of c_m and c_k result in sharply reduced mixing). The relative effectiveness of the two coefficients may be seen in Figure 15, where doubling of c_k without changing c_m was quite effective in improving mixing, whereas then doubling c_m had little further effect.

It therefore appears that the mass mixing coefficient c_k can have an important effect on the overall performance of the water-injection-cooled duct system, as was postulated in Reference 1. It is clear that experimental measurements of the effective c_k for various water vapor-liquid concentrations in hot hydrogen would be extremely helpful in establishing the confidence level of any analysis utilizing this mixing coefficient.

C. Evaporation Characteristics

The effect of evaporation rate in the mixed temperature profiles can be evaluated by simply introducing a multiplying coefficient VPF into the equilibrium coolant vapor pressure formulation of Equation (60) such that when VPF=1, vapor-liquid equilibrium exists (as was used in Reference 1), and when VPF=0, no evaporation occurs; i.e., the injected water mixes with the hydrogen as specified by the mixing analysis and the selected values of c_m and c_k , but it is present in the liquid particle form only.

Results of this evaluation are shown in Figure 16 for the same typical set of conditions used in Figures 13, 14, and 15 to establish the effect of the mixing coefficients. The conclusions to be drawn from Figure 16 are extremely significant: when only 50% of the equilibrium value of water vapor is allowed to appear (VPF=0.5), there is virtually no difference in the

NOTE: COOLANT INJECTION PATTERN NOT OPTIMIZED
 CONDITIONS: SEE FIGURE 13; ALSO $\phi = 11.25^\circ$

CASE	C_m	C_k
20	.075	.075
22	.0325	.0325
25	.15	.15

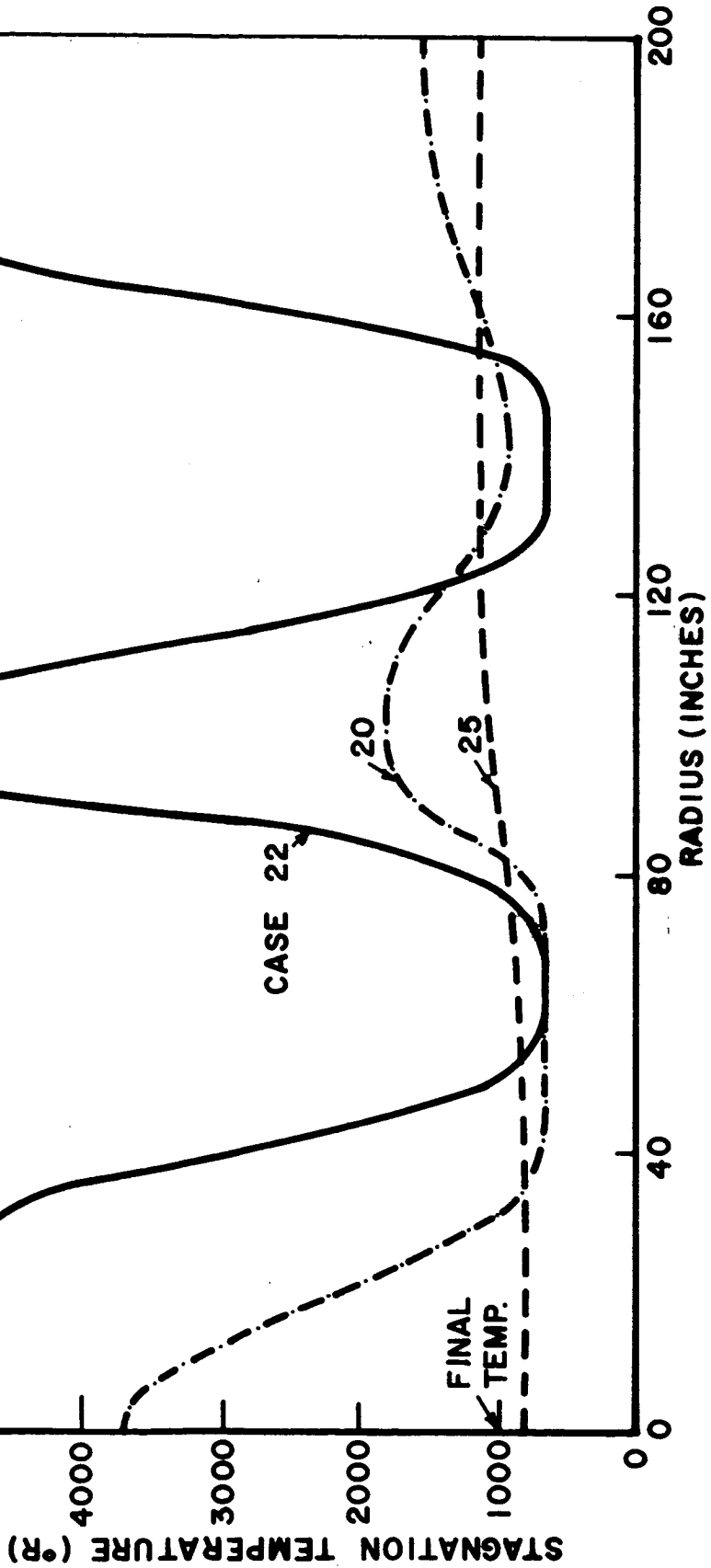


FIGURE 14
 EFFECT ON MIXED TEMPERATURE PROFILES OF CHANGING
 MIXING COEFFICIENTS C_m AND C_k , KEEPING $C_m = C_k$

NOTE: COOLANT INJECTION PATTERN NOT OPTIMIZED
 CONDITIONS; SEE FIGURE 13; ALSO $\phi = 11.25^\circ$

CASE	C_m	C_k
20	.075	.075
21	.075	.15
25	.15	.15

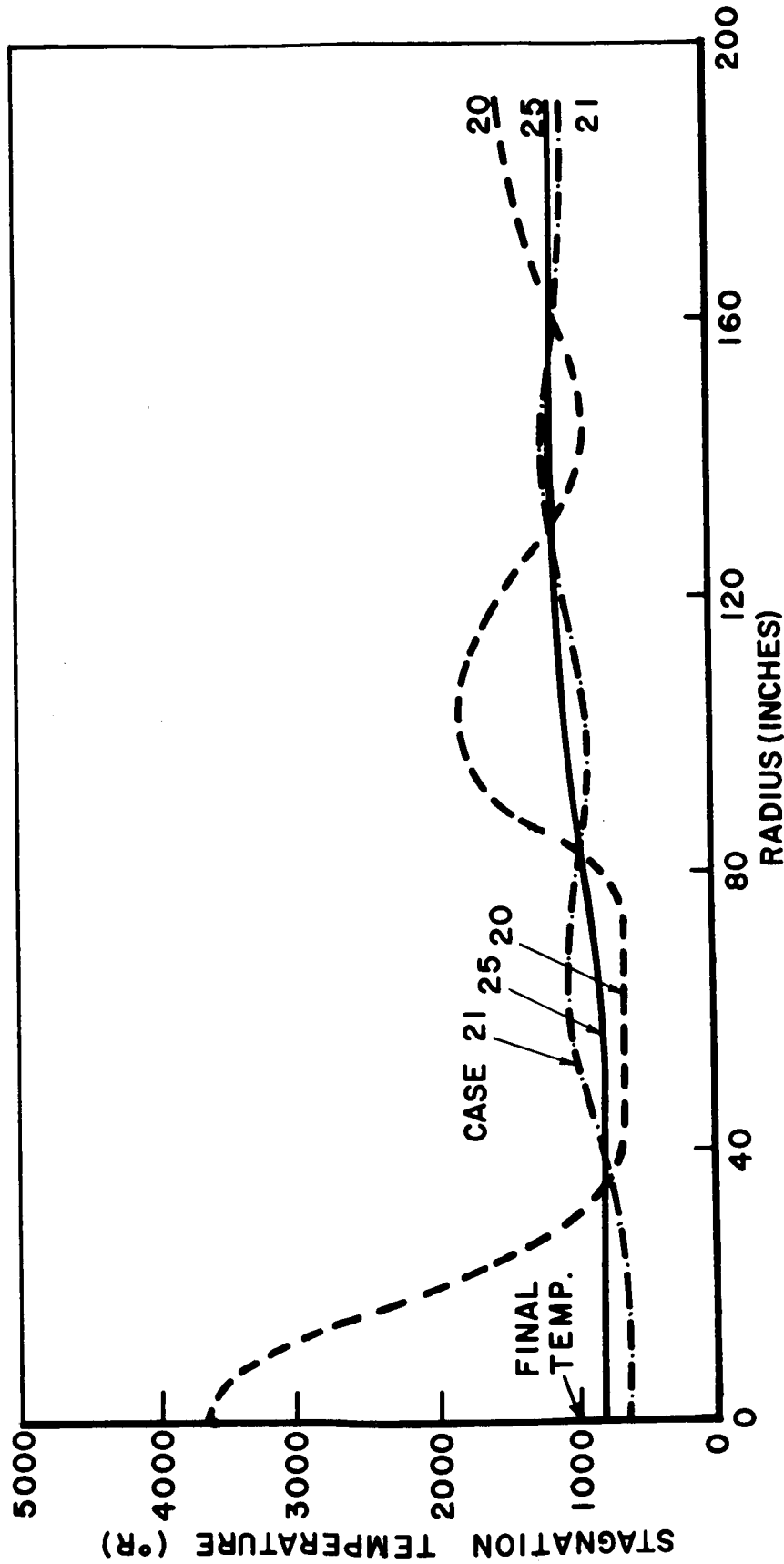


FIGURE 15

EFFECT ON MIXED TEMPERATURE PROFILES OF CHANGING
 MIXING COEFFICIENT C_m AND C_k INDEPENDENTLY

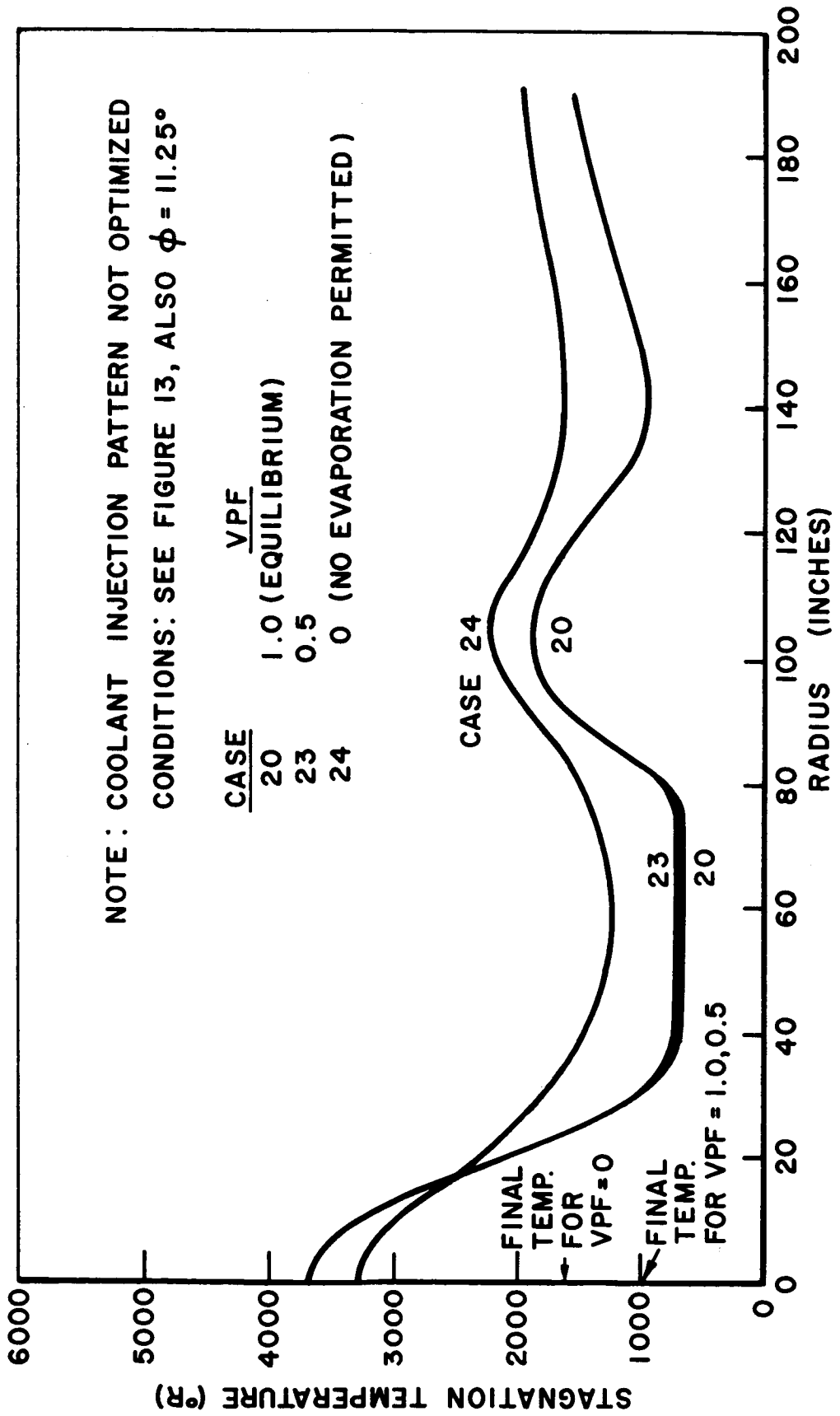


FIGURE 16
 EFFECT OF COOLANT EVAPORATION RATE ON MIXED TEMPERATURE PROFILES

mixed temperature profile, and even when no evaporation is permitted (VPF=0) the maximum difference in mixed temperatures is only about 500° F higher than in the equilibrium case. Further, note that the maximum temperature (at the duct centerline for this one-mixing-duct-diameter downstream location) is lower when no water evaporates than when equilibrium vaporization is permitted. This, of course, results from the fact that the mixing characteristics depend on local temperatures, densities, and other properties affected by the relative liquid-vapor concentration.

Note also that the conditions for this case include a total water flow rate (3,000 lb/sec) only just sufficient to reduce the infinite-duct final mixed temperature to 1000°R if it all were to evaporate; thus it is clearly established that the presence of water at any location is far more important than whether or not it evaporates. The general conclusions to be drawn from the "computer experiment" results of Figures 14, 15, and 16, therefore, is that the mixing characteristics of the injected coolant are far more important than the vaporization characteristics; in general, an increase in mixing effectiveness (characterized by c_k and, to a lesser extent, c_m) is far more desirable than an increase in the vaporization rate constant k_p .

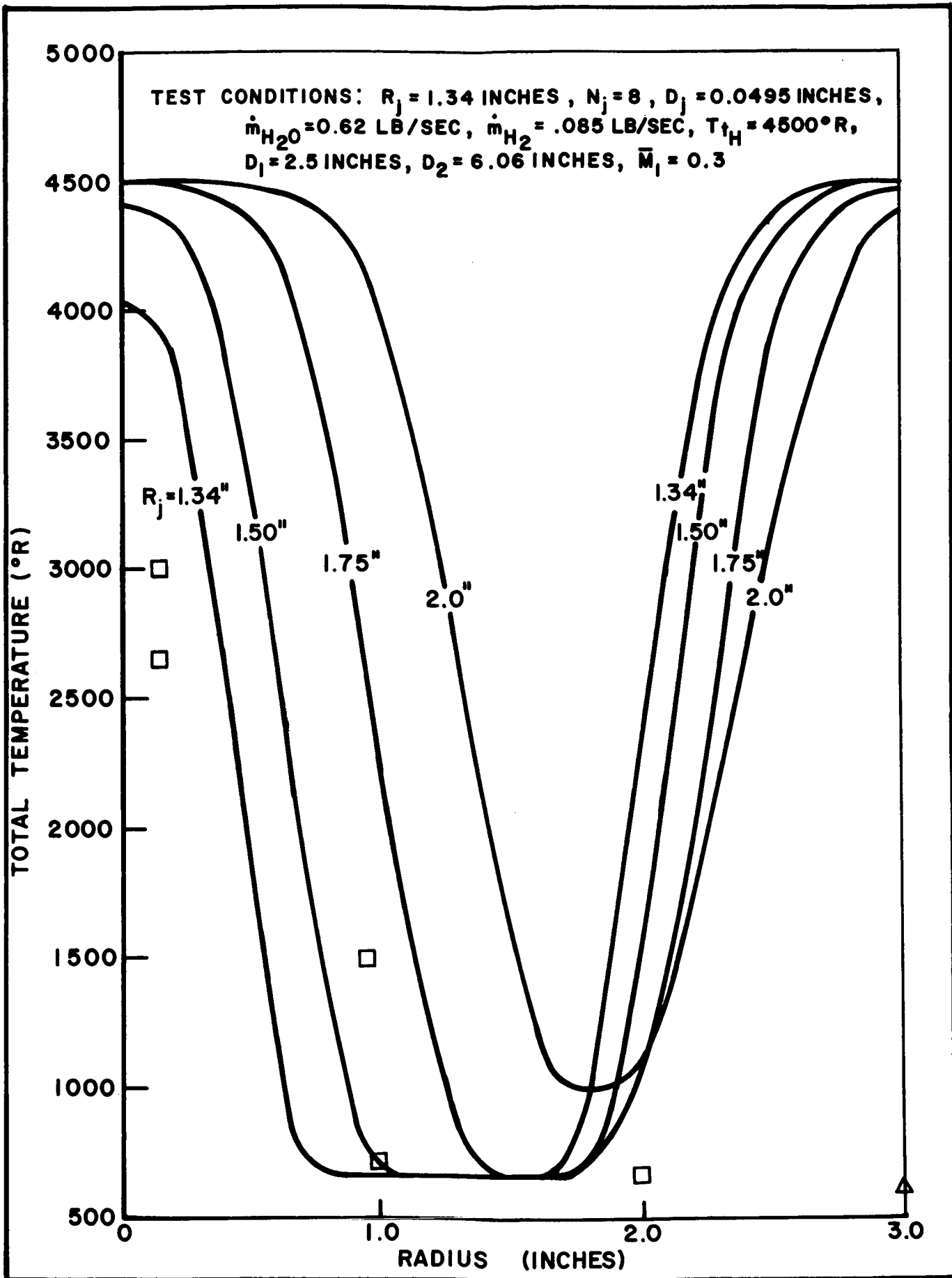
VI. COMPARISON WITH EXPERIMENTAL DATA

In order to establish the validity of the analytical simulation technique described in this report, the available experimental temperature data were compared with computed predictions of the mixed temperature profiles. There were two relatively complete sets of data available: the Westinghouse Astronuclear Laboratory tests described in Reference 12 (also used in Reference 1 for analytical-experimental comparisons), and a new series of scale model tests run at Aerojet-General Corporation, as described in Reference 13. In each case, the computer program input data (e.g., inlet conditions, inlet profile, geometry, readout instrument locations, etc.) were set to correspond as closely as possible with the conditions of the experiment.

A. Westinghouse Astronuclear Laboratory

The geometry, inlet conditions, water flow rates, and readout locations indicated in Reference 12 were used as input data to the computer program of Appendix F, and predicted temperature profiles were calculated for comparison with the expected results of Reference 12. Since the coolant injection in these experiments was axial, no penetration subroutine was necessary. However, because the inlet Mach number profile for these tests was not measured, it was not possible to calculate the outward shift of the coolant due to this inlet-flow nonuniformity. Consequently the computer prediction was run for four different effective jet locations ranging from $R_j = 1.34"$ to $R_j = 2.0"$, as shown in Figures 17, 18, and 19. It was estimated that $R_j = 1.75"$ probably represented the most likely effective jet location, and the $R_j = 1.75"$ curve in these figures should be used in any comparisons, especially at the downstream locations (Fig. 18 and 19) where the analytical assumptions are more nearly correct.

Correlations between analytically predicted temperatures and measured temperatures are quite good for all radii out to the effective jet radius R_j at the two downstream instrumentation locations (17.5" and 35", or roughly 3 and 6 mixing-duct diameters downstream). The theory is overconservative at the 7.5" axial location (about 1 mixing-duct diameter), probably



64
FIGURE 17
COMPARISON OF ANALYTICAL PREDICTIONS WITH WESTINGHOUSE
DATA: AXIAL LOCATION $x = 7.5''$ (~ 1 DUCT DIAMETER)

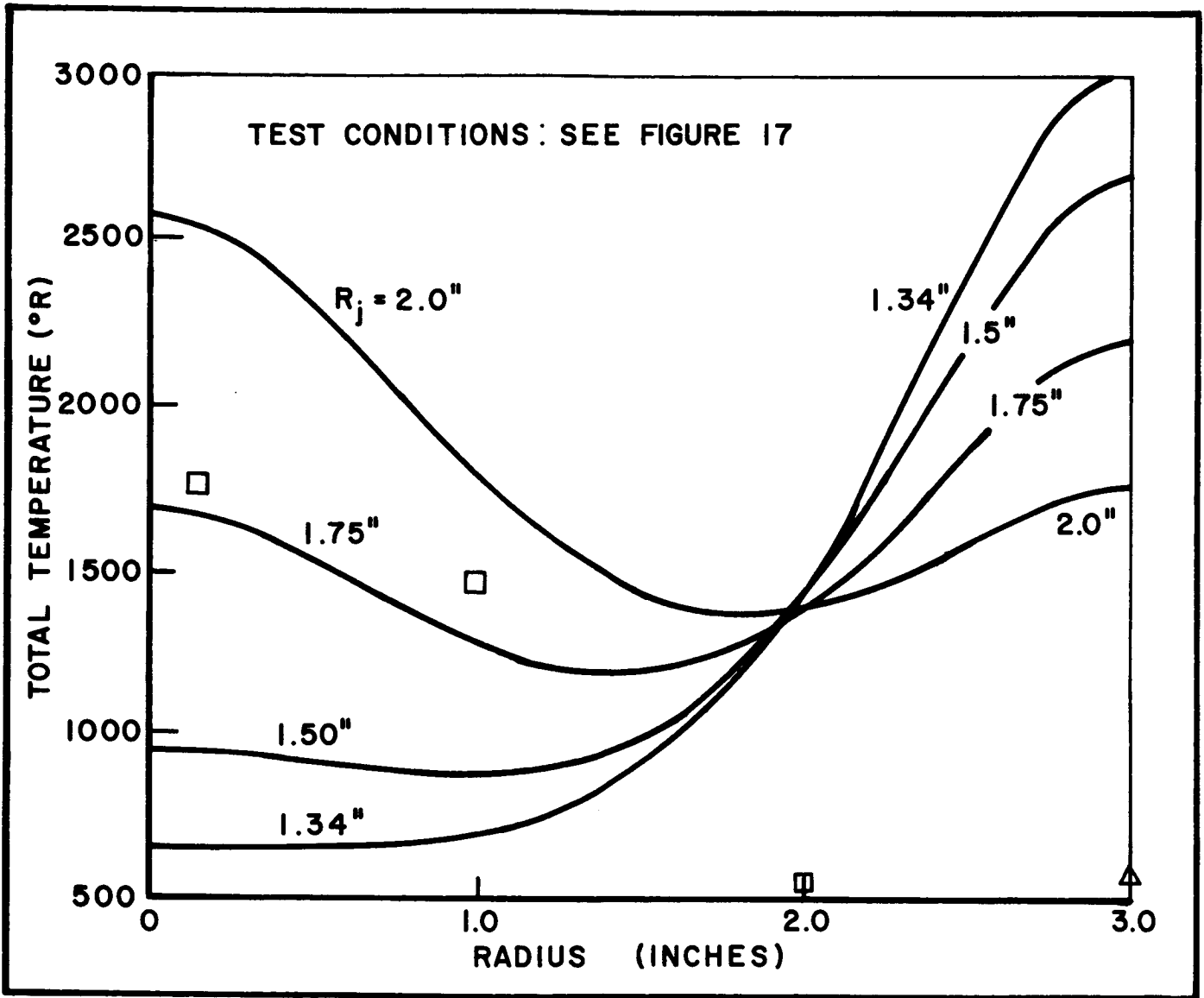


FIGURE 18

COMPARISON OF ANALYTICAL PREDICTIONS WITH WESTINGHOUSE DATA (CONTINUED): AXIAL LOCATION $X=17.5"$ (~ 3 DUCT DIAMETERS)

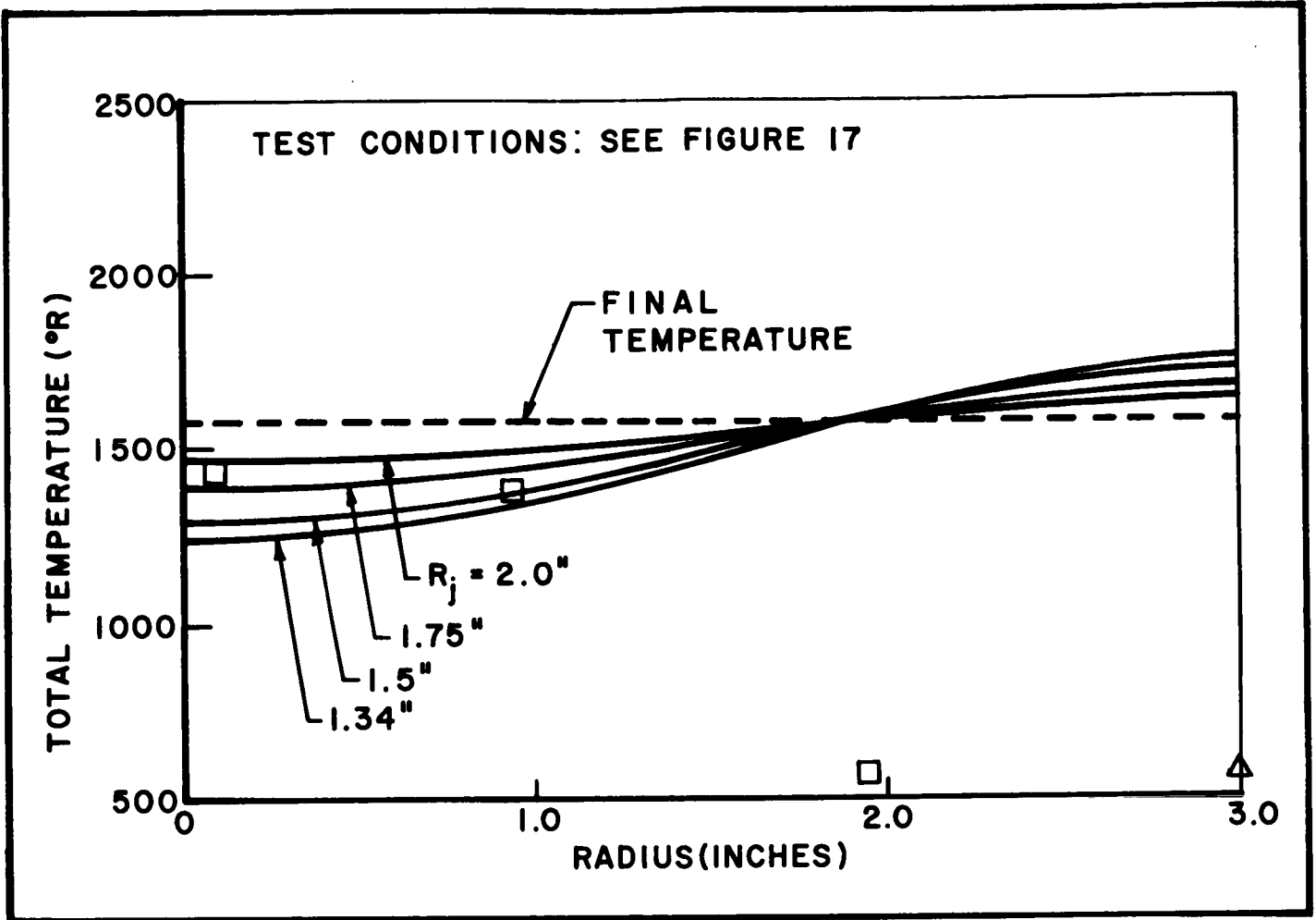


FIGURE 19

COMPARISON OF ANALYTICAL PREDICTIONS WITH WESTINGHOUSE DATA (CONTINUED): AXIAL LOCATION $X = 35''$ (~ 6 DUCT DIAMETERS)

due to the analytical assumption that the sudden-expansion flow regime is small compared with the overall mixing length.

For radial locations greater than the effective jet radius R_j , the experiments indicated much lower temperatures than the analysis in all cases (i.e., the analytical predictions are overconservative). There appears to be no reasonable justification for the low temperatures that were measured at these outer radii. In fact, it can be argued that since the water appears to have diffused toward the centerline approximately in the amounts predicted at $x = 35$ inches, it is physically improbable that there was sufficient water at the outer radial locations to yield local saturation temperatures or lower. Accordingly, the experimental data for the outer radii are suspect. From the data of Reference 12 it does not appear that these outer temperature measurements were significantly influenced by any of the experimental parameter variations.

Note that the correlation in Figures 18 and 19 is much better than was observed in Reference 1, using the same experimental data. This improvement is a direct result of properly satisfying the conservation constraints in the present analysis.

A point of interest is the node which appears in the analytical results of Figures 17, 18, and 19, at a radius of about 1.9 inches. This node represents the point at which the temperature is independent of the radial location of the coolant jets. Note that it lies only just slightly outside the $9/32 D_2$ criterion developed in Reference 1 for simultaneous equivalent cooling at the duct wall and centerline.

B. Aerojet-General Corporation

The geometry, inlet conditions, water flow rates, and readout locations indicated in Reference 13 were used as input data to the computer program of Appendix F, and, as in the case of the Westinghouse data, predicted temperature profiles were calculated for comparison with the experimental results of Reference 13.

The Aerojet-General scale-model tests provided the capability for evaluating the multiple-injection-ring concept, and also the radial penetration results. The experimental conditions

duplicated consisted of four cases, corresponding to four different coolant injection flows, as listed in Table II below. All other input data appear in Figures 20, 21, 22, and 23, which illustrate results of the correlation.

TABLE II

COOLANT FLOW CHARACTERISTICS FOR AEROJET-GENERAL
EXPERIMENTS

CASE	FIGURE NO.	\dot{m}_{H_2O} (LB/SEC)	ACTUAL D _j (IN)	ACTUAL N _j	COMPUTER D _j (IN)	COMPUTER N _j
1-203	20	0.2	0.050	3	0.0397	4
2-202	21	1.5	0.125	3	0.1081	4
3-204	22	3.0	0.032	90	0.03225	90
4-201	23	4.7	(As above - all jets simultaneously)			

Note that because of the computer program limitation to even numbers of coolant jets in each row, the actual AGC 3-jet rows were simulated by 4-jet rows having the same total coolant flow and the same penetration characteristics. Also, the zero azimuth was assumed to intersect a coolant jet in each row, and no distinction was made as to the azimuthal locations of the readout instrumentation, since these data were not available. These small modifications almost certainly could not seriously affect the correlations.

The correlations in Figures 20, 21, 22, and 23 are strikingly consistent in their indications that the analysis is highly conservative in all cases. In fact, the experimental data show that mixing is virtually complete as close as one-third of a mixing duct diameter from the entrance, and demonstrate virtually no dependence on either axial or radial location.

Although good correlation would not be expected for the axial locations at 7" and 20" (roughly 1/3 and 1 mixing duct diameter downstream of the entrance), because of the analytical assumptions discussed earlier, the theory should be adequate to predict the 40", 60", and 120" data (roughly 2, 3, and 7

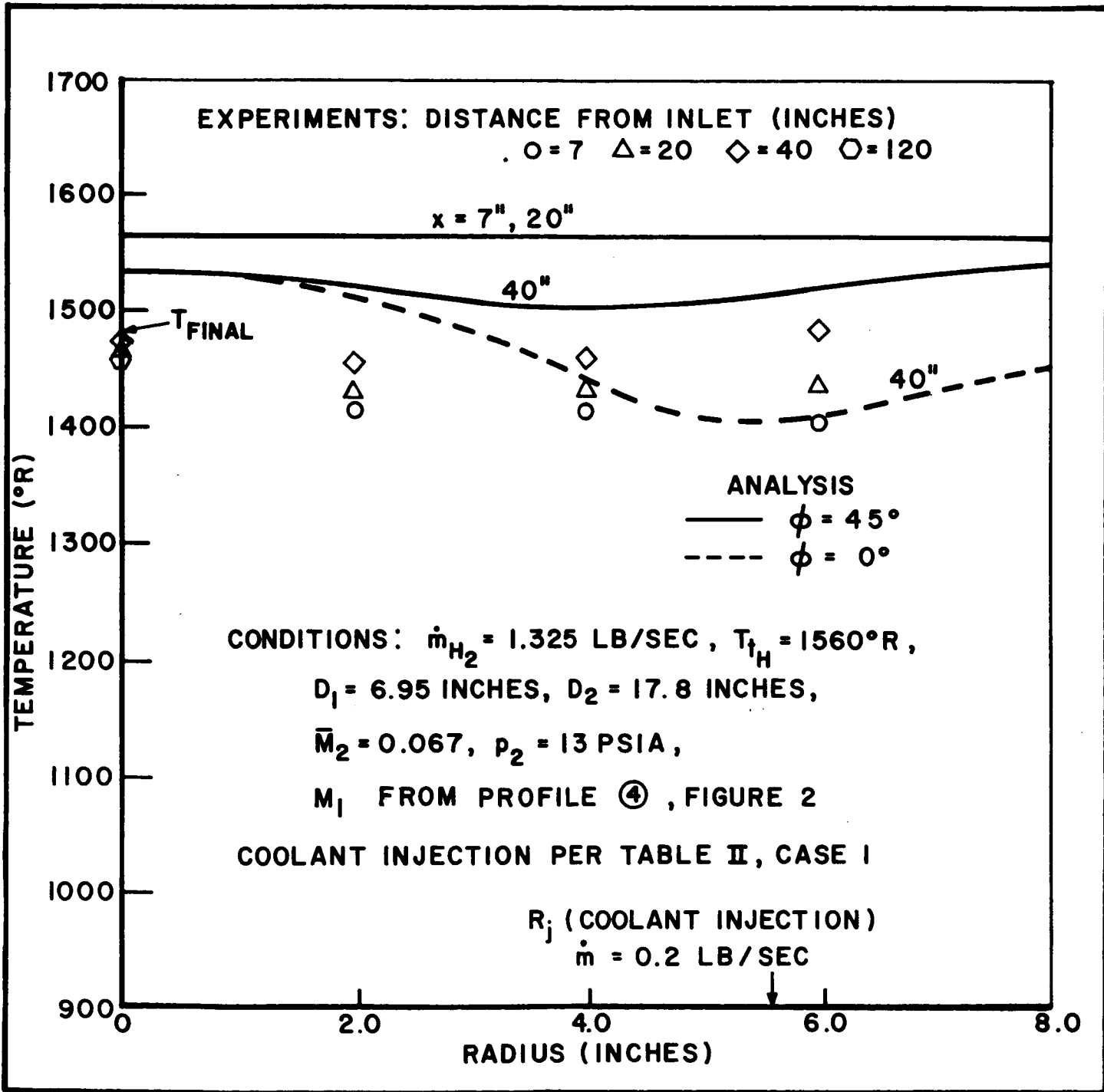


FIGURE 20

COMPARISON OF ANALYTICAL PREDICTIONS WITH
 AEROJET-GENERAL EXPERIMENTS
 CASE I - COOLANT FLOW = 0.2 LB/SEC

EXPERIMENTS - DISTANCE FROM INLET (INCHES)

○ = 7 Δ = 20 ◇ = 40 ⊗ = 60 ⊙ = 120

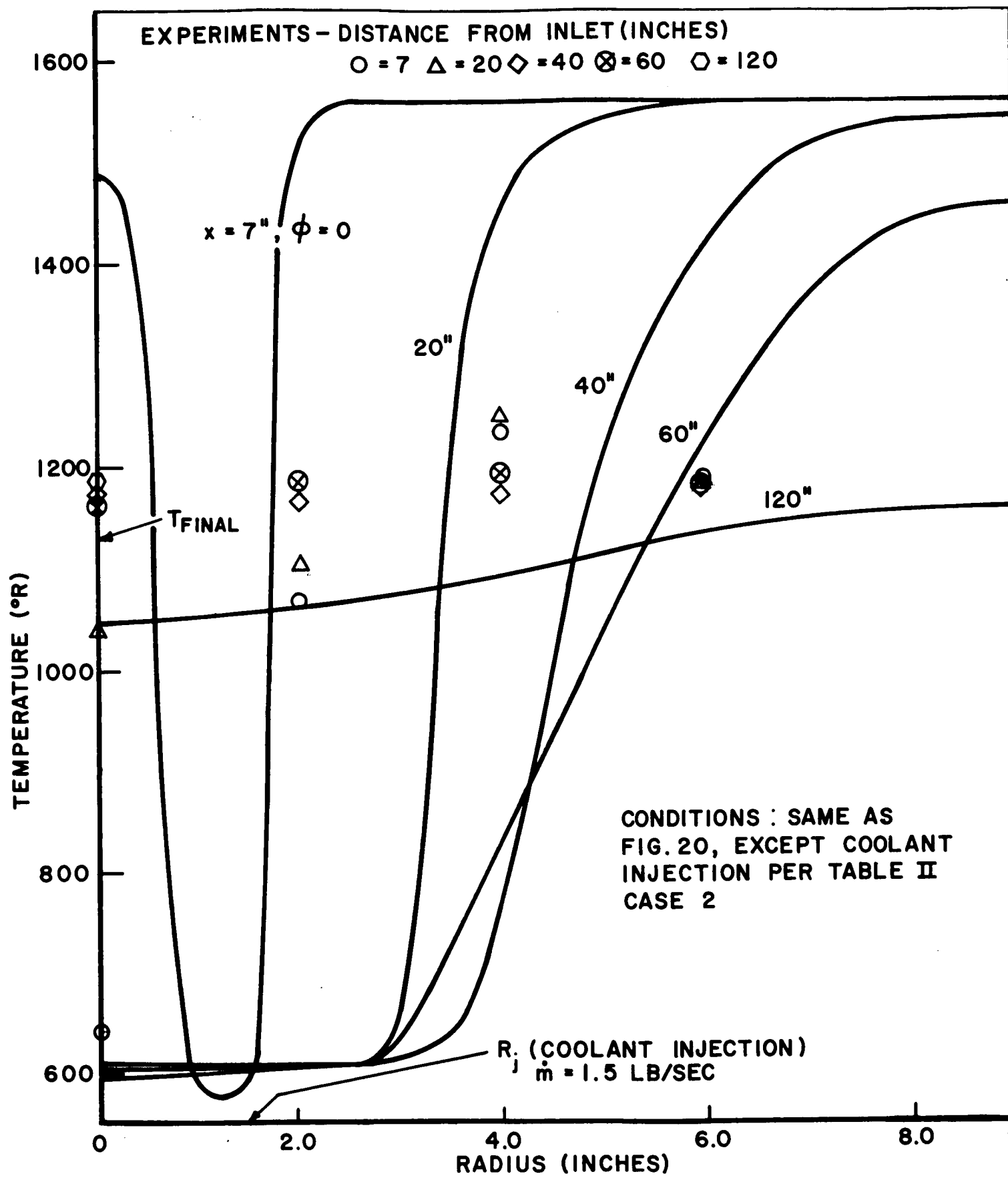


FIGURE 21

COMPARISON OF ANALYTICAL PREDICTIONS WITH
AEROJET-GENERAL EXPERIMENTS
CASE 2 - COOLANT FLOW = 1.5 LB/SEC

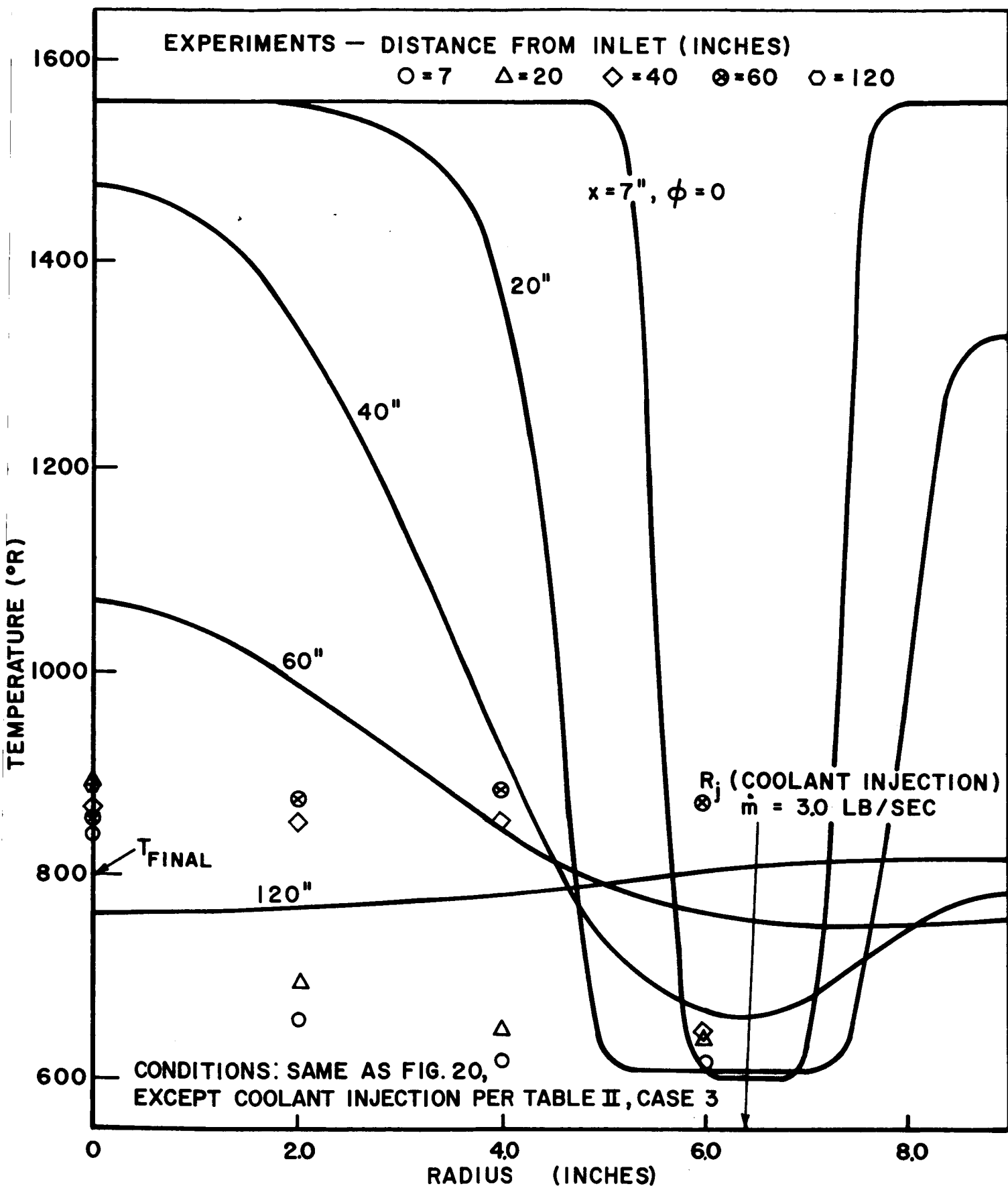


FIGURE 22

COMPARISON OF ANALYTICAL PREDICTIONS WITH
AEROJET-GENERAL EXPERIMENTS
CASE 3-COOLANT FLOW = 3.0 LB/SEC

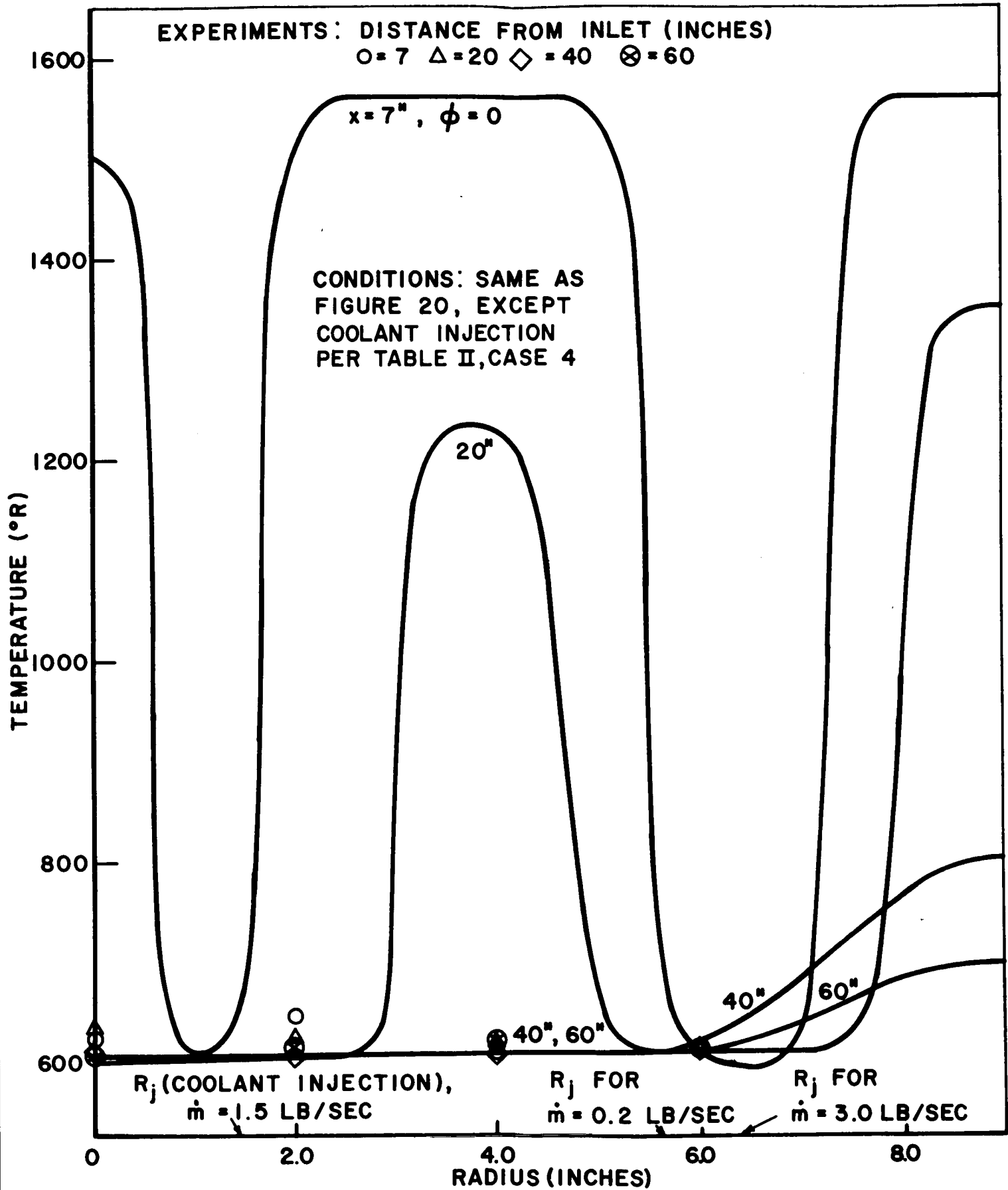


FIGURE 23
 COMPARISON OF ANALYTICAL PREDICTIONS WITH
 AEROJET-GENERAL EXPERIMENTS
 CASE 4 - COOLANT FLOW = 4.7 LB/SEC

mixing-duct diameters downstream, respectively). This is borne out by the somewhat trivial conditions of Figures 20 and 23 (for very little coolant flow and maximum coolant flow, respectively). In the other two cases, correlation is somewhat sporadic, but is still conservative, with actual mixing taking place much more rapidly than predicted.

There are two effects which appear to explain the very high mixing rates indicated by the experiments. First, the actual coolant jets will have diffused somewhat during their penetration phase, whereas the analysis assumes that they are still point sources at the penetration depth (radius R_j), and only begin to diffuse at that point. Second, the droplet mixing coefficient c_k may be higher than the analytical value of 0.075 indicated in Reference 9 for gases and vapor. This could have a very strong effect on the predicted mixing rate; e.g., see the previously-discussed "computer experiments" illustrated in Figures 14 and 15.

Other secondary effects which may have led to differences between analysis and experiments are the possible ambiguity in temperature probe data (i.e., what temperature do the probes read: gas, liquid, equilibrium mixture, or some non-equilibrium combination?), the nonuniformity of flow upstream of 80" in the mixing duct, as illustrated by the nitrogen Mach number profile data of Reference 13, etc.

Note that the most significant effect, namely the possible change in c_k for the droplets, can easily be included in the computer program as soon as its proper value can be established. It is also possible to simulate the initial diffuse nature of the jet at its penetrated radius R_j by injecting it (numerically, of course) an appropriate distance $-x_j$ upstream of the mixing duct entrance. It is believed that these two changes can be used to correlate any desired set of experimental data, depending on the choices of c_k and $-x_j$.

VII. FULL-SCALE E/STS 2-3 PERFORMANCE PREDICTION

A. Input Data (Reference Case)

Parameters for the "reference case" were selected to match the most probable full-scale design configuration and inlet conditions as closely as possible. These conditions are somewhat different from those originally specified in the subject contract (Ref. 3), as listed earlier in this report, due to design decisions made by SNPO and Task Force personnel during the course of the program. The final "Reference Case" conditions used in the performance predictions defined in References 14 and 15 are listed in Tables III and IV.

TABLE III

INPUT CONDITIONS FOR "REFERENCE CASE" OF FULL-SCALE
E/STS 2-3 PERFORMANCE PREDICTION ANALYSIS

<u>PARAMETER</u>	<u>SYMBOL</u>	<u>VALUE</u>
Hydrogen Flow	\dot{m}_{H_2}	230 lb/sec
Water Flow	\dot{m}_{H_2O}	2743 lb/sec
Inlet duct diameter	D_1	126 in.
Mixing duct diameter	D_2	384 in.
Hydrogen total temperature (Inlet)	T_{tH}	4500 R
Water temperature (Inlet)	T_{tJ}	530 R
Inlet Mach number profile	$M_1(r)$	Fig. 2, curve 4
Mixing coefficients	c_m, c_k, c_h	0.075
Vapor pressure factor	VPF	1.0
Coolant Injection Data	--	(See Table IV)

TABLE IV

COOLANT INJECTION INPUT DATA FOR "REFERENCE CASE" OF FULL-SCALE E/STS 2-3 PERFORMANCE PREDICTION ANALYSIS

ROW	ACTUAL D_j (IN)	ACTUAL N_j	COMPUTER D_j (IN)	COMPUTER N_j	\dot{m}_{H_2O} LB/SEC	COMPUTED R_j (IN)
1	0.25	96	0.25	96	279	150
2	0.5	72	0.5	72	836	118
3	1.25	3	0.884	6	218	35.1
4	2.25	6	5.51*	1*	1410	0*

* Coolant injected in the fourth row (6 holes with $D_j=2.25$ ") was found to penetrate the centerline, and therefore this row was replaced in the computer solutions with a single jet on the centerline, having the same total mass flow as the actual case.

The independent input variables of Tables III and IV yield the dependent conditions listed in Tables V and VI:

TABLE V

CALCULATED INITIAL CONDITIONS FOR "REFERENCE CASE" OF FULL-SCALE E/STS 2-3 PERFORMANCE PREDICTION ANALYSIS

<u>PARAMETER</u>	<u>SYMBOL</u>	<u>VALUE</u>
Inlet-duct flow coefficient	c_w	0.649
Inlet-duct average Mach number	M_1	0.681
Inlet-duct pressure	p_1	11.1 psia
Inlet-duct effective total pressure	\bar{p}_t	15.1 psia
Mixing-duct initial Mach number	M_2	0.0477
Mixing-duct initial pressure	p_2	11.5 psia
Mixing-duct initial total pressure	\bar{p}_{t2}	11.5 psia
Mixing-duct initial velocity	u_2	594 ft/sec

TABLE VI

CALCULATED COMPLETE-MIXING CONDITIONS FOR "REFERENCE CASE" OF FULL-SCALE E/STS 2-3 PERFORMANCE PREDICTION ANALYSIS

<u>PARAMETER</u>	<u>SYMBOL</u>	<u>VALUE</u>
Pressure	P_3	11.5 psia
Total pressure	P_{t3}	11.6 psia
Total temperature	T_{t3}	829° R
Density	ρ_3	0.0144
Mach number	M_3	0.115
Velocity	u_3	257 ft/sec
Concentrations:		
Liquid water	$k_{H_2O \text{ liq}}$	0
Water vapor	$k_{H_2O \text{ vap}}$	0.923
Hydrogen	k_{H_2}	0.0774

B. Reference Case Results

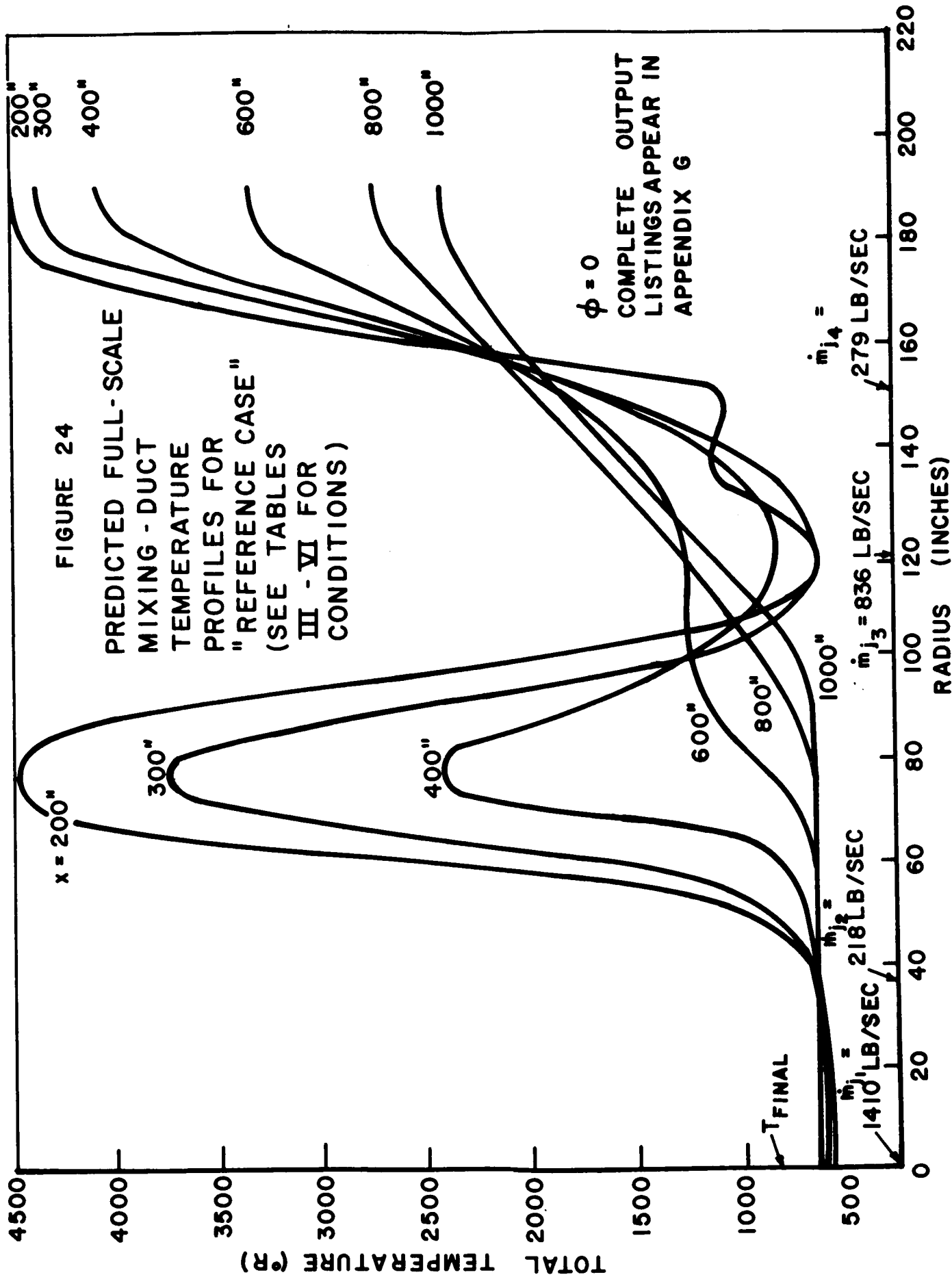
Complete parameter profiles of total temperature, total pressure, density, Mach number, velocity, and component compositions were calculated for two azimuth angles and eleven radii at each of eight axial stations downstream of the mixing-duct inlet: 50", 100", 200", 300", 400" (~ 1 duct diameter), 600", 800" (~ 2 duct diameters), and 1000". These results are tabulated in Appendix G, and are summarized (in the form of total temperature profiles) in Figure 24.

The computed results for the reference full-scale design indicate that the hydrogen is overcooled at the duct centerline and inadequately cooled at the wall of the mixing duct. For example, a water concentration of 98% appears at the centerline of the $X = 1000$ inch station, 79% of which is in the form of condensed liquid.

C. Effect of Adjusting Coolant Distribution

It is clear from the results of Appendix G and Figure 24 that some manipulation of coolant injection characteristics can be utilized to improve the predicted wet-duct performance. Although this additional computation was not included in the contract Statement of Work (Reference 3), it is considered to be of sufficient importance to the final preliminary-design conclusions of this study that one additional case was run.

In order to assist in the selection of appropriate injection conditions, Figure 25 was prepared for the "Reference Case" input conditions of Table III. This is simply a parametric plot of the mass flow rate \dot{m}_j per jet and penetration radius R_j as functions of injection-port diameter D_j and injection pressure drop ΔP_j . These data were utilized to estimate (rather arbitrarily) a set of coolant injection characteristics for a "Modified Design" case which might show some improvement in performance over the "Reference Case" illustrated in Figure 24. These new coolant injection inputs are listed in Table VII:



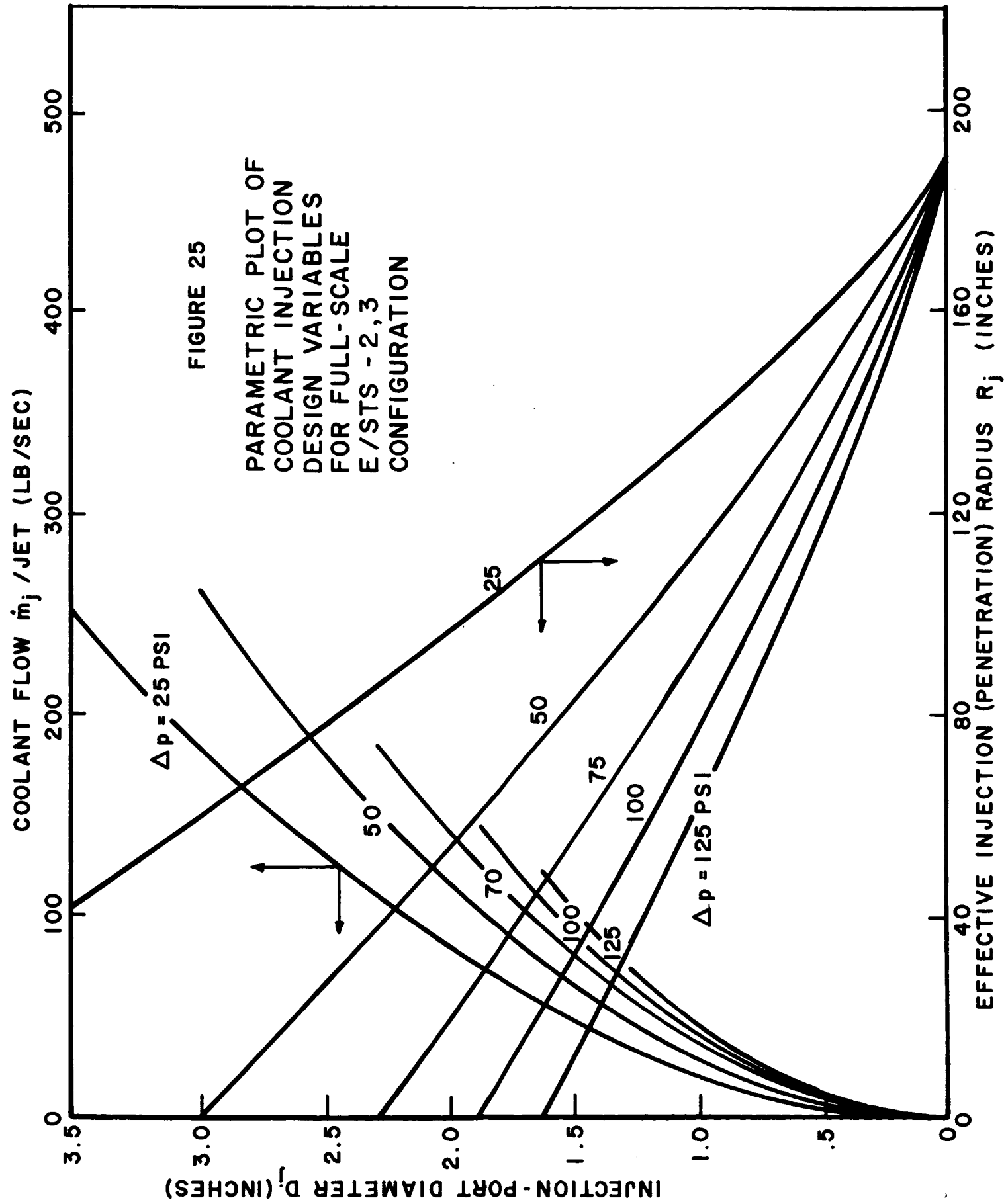


TABLE VII

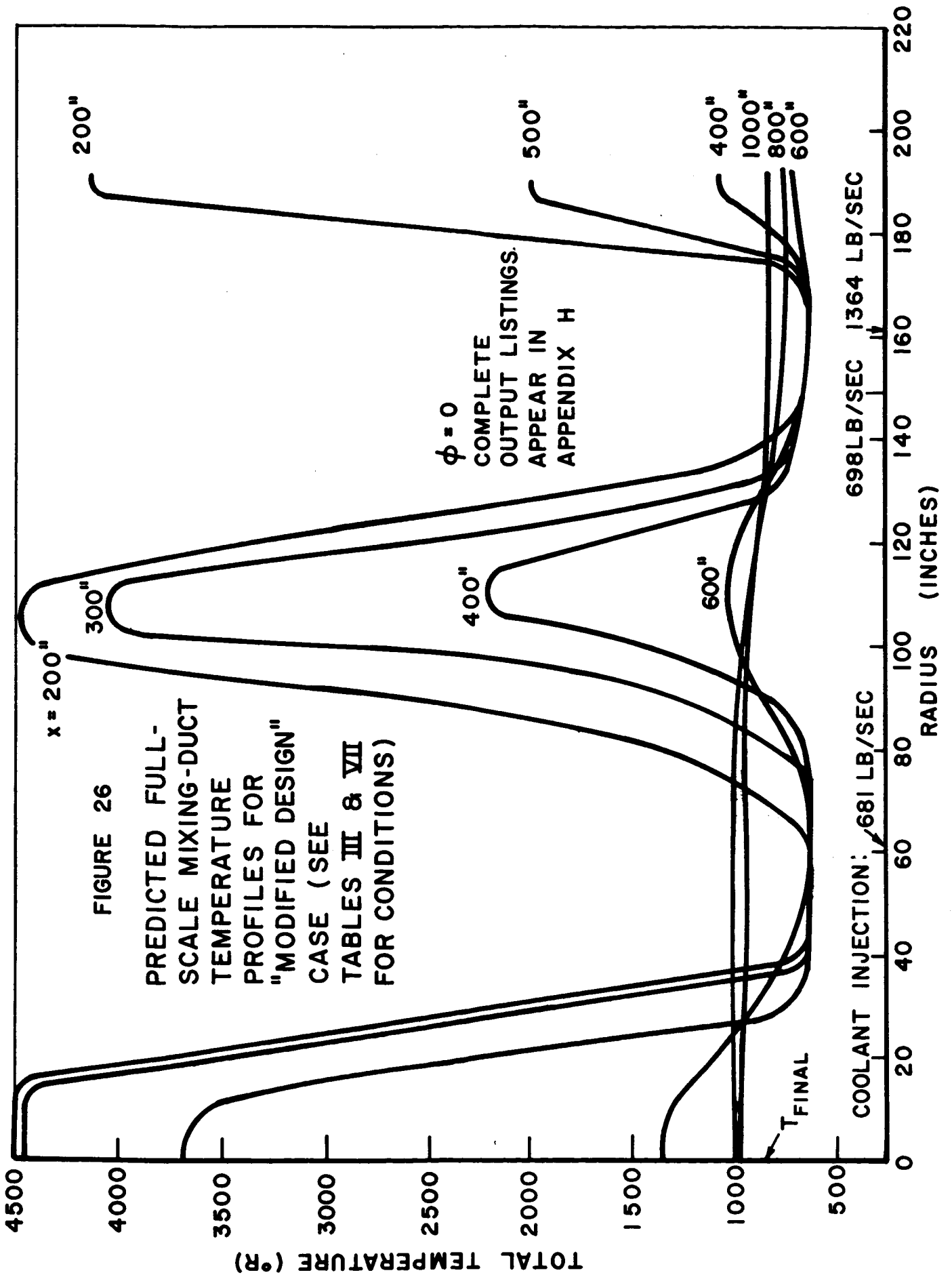
REVISED COOLANT INJECTION INPUT DATA FOR "MODIFIED DESIGN"
CASE OF FULL-SCALE E/STS 2-3 PERFORMANCE PREDICTION ANALYSIS

ROW	ACTUAL D_j (IN)	ACTUAL N_j	COMPUTER D_j (IN)	COMPUTER N_j	\dot{m} H ₂ O (LB/SEC)	COMPUTED R_j (IN)
1	0.5	264	0.829	96	1364	161
2	0.75	60	0.75	60	698	149
3	2.87	4	2.87	4	681	62

Note that the selected configuration consists of only 3 rows (the jets which penetrate all the way to the centerline appear superfluous, since a jet which does not penetrate to the centerline will diffuse there quite rapidly). The resulting pressure drop (uniform among all jets) is only 24.8 psi, with a coolant velocity of 60.8 ft/sec.

Results of these "Modified Design" calculations are listed in Appendix H, with a summarization (again in terms of total temperature profiles) appearing in Figure 26. It is clear that even with the rather arbitrary selections of coolant input conditions, a significant improvement has been obtained; i.e., the 600-inch station is almost fully cooled and the 800-inch station is completely cooled, with all water evaporated at that point.

Note that substantial improvements are still possible over even these profiles. It is clear (especially after careful perusal of the tabulated outputs of Appendix H) that much more effective distributions of coolant are possible. Further, as discussed earlier, the possibility, indicated by the AGC experiments, that the mixing coefficient c_k may be substantially larger than the value 0.075 used here, could result in vastly improved cooling performance in any case.



VIII. CONCLUSIONS

1. The axisymmetric wet-duct mixing analysis and computer program of Reference 1 have been successfully revised to include the following improvements:
 - a. The mixing-duct pressure is no longer constrained to be constant, but is permitted to vary so as to meet the requirements of the conservation equations.
 - b. The inlet-duct velocity profile is no longer constrained to be flat, but may take any desired axisymmetric form.
 - c. Conservation of mass and energy are automatically satisfied everywhere in the duct.
 - d. Up to four different sets of coolant injection characteristics (jet diameters and numbers of jets) can be used simultaneously in order to simulate more effective cooling.
 - e. Different mass and momentum mixing-rate characteristics can be simulated as well as variations in each independently of the other.
 - f. Nonequilibrium coolant evaporation rates can be simulated.
 - g. A number of minor improvements have been made; e.g., assurance of convergence under all conditions, verification of the imaging technique used to convert the basically free-jet analysis to a confined-duct case, etc.

The present program, with these improvements incorporated, is now considered fully satisfactory to simulate many mixing problems (assuming, of course, that requisite fluid properties are changed).

2. A series of "computer experiments" demonstrated that the most significant physical input parameter which still requires determination is the mass mixing coefficient c_k , which may depart considerably for the liquid-vapor coolant mixture from the generally-accepted gas-vapor value used in the numerical calculations.

An increase in this parameter improves mixing performance very rapidly; a decrease could cause serious deterioration in mixing performance. The momentum mixing coefficient c_m is also important to the mixing performance, but is neither as effective as c_k nor is it likely to vary as much from the accepted value.

3. Another "computer experiment" demonstrated that evaporation rate has virtually no effect on duct performance; that is, even if no evaporation occurs at all, mixing-duct profile temperatures are only slightly affected. The significant feature, as indicated in the preceding paragraph, seems to be the presence of water at a given point in the flow field, and whether it is in liquid or vapor form appears to be of little importance.
4. Correlation of the improved analytical program with experimental scale-model data taken at Westinghouse Astronuclear Laboratory was quite good at downstream measurement stations within the injection radius, but the analysis was highly overconservative for the outer mixing duct radii. There appears to be no theoretical justification for the extremely low measured temperatures, which are also completely independent of axial location at these outer radii.
5. The analytical simulation of Aerojet-General Corporation scale-model experiments was highly overconservative for all comparisons made. There are apparently two principal causes for this overconservation:
 - a. The mass mixing coefficient c_k for the liquid water particles appears to be higher than the generally-accepted value used in the analysis,
 - b. The injected coolant is actually quite well diffused after penetration of the gas stream, whereas the analysis assumes it to appear as a point source at the penetration radius. Both these effects can easily be accounted for in any subsequent calculations by simply selecting a proper value for the mass mixing coefficient c_k and representing the coolant injection point as being an appropriate distance upstream of the mixing-duct inlet.

6. Prediction of gas-property profiles in the full-scale E/STS 2,3 mixing duct was made for a "reference case" set of conditions supplied by SNPO-C. It was found that the coolant injection parameters used in this reference case did not provide adequate cooling near the duct periphery; i.e., coolant distribution was not optimum.
7. A rather arbitrary modification to the full-scale "reference-case" coolant injection configuration was postulated and analyzed, and considerable improvement was observed. For this "modified design" case, the gas was fully cooled two mixing-duct diameters (800") downstream, and almost fully cooled between 1 and 1½ diameters (400" - 600") downstream of the inlet.
8. It was clear from a comparison of the full-scale "reference case" and "modified-design" case that much more favorable results could be obtained by proper redistribution of the coolant. However, the extreme significance of the mass mixing coefficient c_k , discussed previously, may dominate the overall mixing-duct performance for any distribution of coolant.

IX. RECOMMENDATIONS

1. Without changing the apparently fully satisfactory improved computer program, values of mass mixing coefficient c_k and/or upstream coolant injection location $-x$ should be adjusted until the computed mixing data match those obtained in the Aerojet-General experiments. (See discussion of these parameters in Item 5 of "Conclusions").
2. The value of c_k and $-x$ thus established should then be used in a computer injection parameter study, using the existing satisfactory computer program, to determine the optimum coolant injection characteristics for use in preliminary design of the full-scale E/STS 2, 3 exhaust duct.
3. Additional scale-model testing of the actual deflected-jet diffuser should be performed in order to evaluate the validity of the axisymmetric analytical model in simulating the actual full-scale non-symmetrical configuration.
4. Additional experimental studies should be performed to establish full parametric dependence of the critical mass mixing coefficient c_k . Because of the dominant effect of this parameter on mixed temperature profiles in the duct, the highest possible confidence level should be established in selecting its proper value for use in the preliminary designs of E/STS 2 and 3.

REFERENCES

1. Grey, J., "Analytical Feasibility Study of a Water-Injection-Cooled Diffuser for Nuclear Rocket Engine/ Stage Test Stands 2 and 3," Report No. SNP-2, Greyrad Corporation, Nov. 15, 1966.
2. "Feasibility Study of a Water Injection Cooled Diffuser," NASA Contract SNPC-49 with Greyrad Corporation, Sept. 7, 1966.
3. "Investigation of Key Problems in the E/STS2-3 Water-Injection-Cooled Diffuser," NASA Contract SNPC-55 with Greyrad Corporation, April 25, 1967.
4. Margetts, M.J., "Evaluation of E/STS 2-3 Scale-Model Diffuser-Ejector (Wet-Elbow System)," Report No. RN-S-0380, Aerojet-General Corporation, Jan. 1967, Fig. 3 (p. 13).
5. Rice, C. M., Letter to R. W. Schroeder, SNPO-C, July 31, 1967, (Item 14).
6. Reichardt, H., "A New Theory of Free Turbulence," Zeit. Math. u. Mech. 21, 1941, p.257; also Journal of the Royal Aeronautical Society 47, 1943, p. 167.
7. Lee, R., Kendall, R., et al., "Research Investigation of the Generation and Suppression of Jet Noise," GE FPLD Report AD 251887, January 16, 1961.
8. Kendall, R. M., and Grose, R. D., "Research on the Generation and Suppression of Noise," Report No. 110, Vidya Division of Itek Corporation, August 30, 1963.
9. Alexander, L.G., Baron, T., and Comings, E. W., "Transport of Momentum, Mass, and Heat in Turbulent Jets," University of Illinois Bulletin, Series No. 413, May 1953.
10. R. M. Kendall, Aerotherm Corporation (Personal Communication), 1966.

11. Kriebel, A. R., "Shock Waves in Particle-Laden Gas," Vidya Technical Note 531C-TN-9, June 19, 1961.
12. Faught, H. F., WANL Letter to J. L. Dooling (AGC) dated Nov. 3, 1966, with enclosure titled "Wet Duct Evaluation Program: WANL Preliminary Test Data," dated Nov. 1, 1966.
13. Margetts, M., AGC Letter to J. Grey (Greyrad) dated August 14, 1967, with enclosures of preliminary data for the Mixing and Evaporation Test Program.
14. Grey, J., Greyrad Letter to C. Carwile (SNPO-C) dated July 14, 1967.
15. Margetts, M., (AGC) Informal communication to J. Grey (Greyrad), undated.

APPENDIX A

NOTATION

APPENDIX A

NOTATION

A	Area ft ²
a	Constant defined by Equation (5); also constant defined by Equation (51); also used as speed of sound, ft/sec.
b	mixing parameter defined by Equation (26)
c	constant defined by Equation (61)
c'	constant defined by Equation (53)
c*	characteristic velocity $(1/r) \sqrt{R^\circ T_t / m}$, ft/sec.
c _h	energy mixing coefficient
c _k	mass mixing coefficient
c _m	momentum mixing coefficient defined by Equation (32)
c _p	specific heat, Btu/lb.
c _w	flow coefficient
D	diameter, inches; also used as mass diffusivity, sec/ft ² .
F	free energy, Btu/lb.
h	enthalpy, Btu/lb.
k	component fraction; sometimes used as fraction of water; also used as thermal conductivity coefficient, Btu/ft-°F-sec; also used as a constant.
k _p	equilibrium constant
M	Mach number
m	molecular weight
ṁ	mass flow rate, lb/sec
N	number
n	constant defined by Equation (5)

P	number of moles in mixture
p	absolute pressure, lb/in ² ; also used as number of component moles
Pr	Prandtl number, $\mu c_p / k$
q	dynamic pressure, lb/in ²
R	duct radius, inches; also used as effective coolant injection radius R _j , inches.
R ⁰	universal gas constant, ft-lb/ ⁰ F-mol.
r	radial coordinate, inches
s	entropy, Btu/lb.
s _i	distance from an arbitrary point to a "reflected-jet" point (see Equation 50), inches
Sc	Schmidt number, $\mu D / \rho$
T	temperature, ⁰ R
u	axial velocity component, ft/sec.
v	radial velocity component, ft/sec.
VPF	vapor pressure factor
X	dimensionless axial distance for penetration
x	axial coordinate, inches; also used as axial distance for penetration, inches
y	penetration depth, inches
α	angle of liquid-jet trajectory, degrees
β	parameter defined by Equation (75)
Γ	$\gamma^{1/2} (2/\gamma + 1)^{(r+1)/2(r-1)}$
γ	ratio at specific heats
E	turbulent diffusion coefficients
η	dimensional radius r/R
η'	dimensionless penetration depth (1 - r ₁ /R ₁)

θ	tangential coordinate, degrees
μ	viscosity coefficient, lb/ft-sec
ξ	parameter defined by Equation (47), $D_2/c_k x$; also parameter determined by Equation (D-7)
ρ	density, lb/ft ³
ϕ	azimuthal coordinate, degrees; also used as coolant-jet azimuth, degrees; also used as a function defined by Equation (40)

SUBSCRIPTS AND SUPERSCRIPTS

() ₁	inlet-duct conditions
() ₂	conditions just prior to mixing (mixing-duct entrance)
() ₃	conditions after mixing
() _c	centerline
() _{1-D}	one-dimensional
() _g	gas
() _H	hydrogen
() _{H₂}	hydrogen
() _{H₂O}	water
() _h	energy
() _j	liquid-jet
() _k	mass
() _L	liquid
() _{liq}	liquid
() _m	momentum
() _t	total
() _{vap}	vapor
() _w	wall
($\bar{\quad}$)	average value

- (\sim) effective value for turbulent flow; also dimensionless penetration parameters (see Equation (C-1))
- ()' turbulent
- ()^a value with no liquid present
- ()^e value with liquid present
- ()^o reference condition

APPENDIX B

ANALYSIS OF NONUNIFORM INLET-DUCT FLOW

APPENDIX B

ANALYSIS OF NONUNIFORM INLET-DUCT FLOW

It is desirable to express the actual inlet conditions in terms of one-dimensional parameters. A one-dimensional velocity is defined in terms of the integral of momentum across a given plane:

$$\int_A \rho u^2 dA \equiv \dot{m} \bar{u} \quad (B1)$$

$$\text{where } \dot{m} = \int_A \rho u dA \quad (B2)$$

If it is assumed that the static pressure and stagnation temperature are constant across a given plane through which flows a perfect-ideal gas, it can be shown that

$$\bar{u} = \frac{\int \rho u^2 dA}{\int \rho u dA} = \frac{\gamma^{1/2} \Gamma c^* \int_0^1 M^2 \eta d\eta}{\int_0^1 M (1 + \frac{\gamma-1}{2} M^2)^{1/2} \eta d\eta} \quad (B3)$$

for axisymmetric flow, where $\eta \equiv \frac{r}{R}$

$$\text{For } M = \text{const } (M = \bar{M}), \quad \bar{u} = \gamma^{1/2} \Gamma c^* \frac{\bar{M}}{(1 + \frac{\gamma-1}{2} \bar{M}^2)^{1/2}} \quad (B4)$$

Equation (B4) serves as a defining relation for the average Mach number \bar{M} . For a specified Mach number distribution, a mean effective Mach number can be determined by combining equations (B3) and (B4) and performing the indicated integrations across the flow field. Subsequently, a one-dimensional mass flow coefficient can be computed by inserting the calculated mean Mach number into the following relation:

$$C_w \equiv \frac{\Gamma \dot{m} c^*}{\gamma^{1/2} p A} \left[\bar{M} (1 + \frac{\gamma-1}{2} \bar{M}^2)^{1/2} \right]^{-1} = \frac{2 \int_0^1 M (1 + \frac{\gamma-1}{2} M^2)^{1/2} \eta d\eta}{\bar{M} [1 + \frac{\gamma-1}{2} \bar{M}^2]^{1/2}} \quad (B5)$$

For the assumptions employed, c_w is equal to unity or less, and application of the mean Mach number and flow coefficient as defined above to the one-dimensional relations permits introduction of the usual conservation of mass, momentum, and energy in a simplified way. As an example, the stream impulse function employed earlier in the text becomes:

$$T \equiv \int_A p dA + \int_A \rho u^2 dA = pA (1 + \gamma c_w \bar{M}^2) \quad (B6)$$

It is useful to define the location of a given streamline $\eta = r/R$ in a nonuniform flow field in terms of its location in a uniform field η_{1-0} . This is accomplished as follows:

A streamline is defined as a line or surface across which there is no net mass flux. In an axisymmetric flow, the mass flow rate between the duct centerline and a given streamline, consistent with the above assumptions, is

$$\dot{m}_\eta = 2\pi R^2 \bar{\rho u} \int_0^\eta \frac{\rho u}{\bar{\rho u}} \eta d\eta = 2\dot{m} \int_0^\eta \frac{\rho u}{\bar{\rho u}} \eta d\eta \quad (B7)$$

$$\text{where } \frac{\rho u}{\bar{\rho u}} = \frac{M(1 + \frac{\gamma-1}{2} M^2)^{1/2}}{c_w \bar{M} (1 + \frac{\gamma-1}{2} \bar{M}^2)^{1/2}} \quad (B8)$$

In a uniform flow, $\rho u / \bar{\rho u} = 1.0$, and

$$\dot{m}_{\eta_{1-0}} = \dot{m} \eta_{1-0}^2 \quad (B9)$$

Equating (B9) and (B7), the relation of streamlines between a non-uniform flow and a corresponding uniform flow is

$$\frac{2}{c_w} \int_0^\eta \frac{M(1 + \frac{\gamma-1}{2} M^2)^{1/2}}{\bar{M} (1 + \frac{\gamma-1}{2} \bar{M}^2)^{1/2}} \eta d\eta = \eta_{1-0}^2 \quad (B10)$$

If for the mixing problem it is assumed that the flow near the entrance of the mixing duct is uniform, and the flow is non-uniform in the inlet, then the value of η in the mixing duct (η_{1-0}) can be determined through evaluation of the above integral, employing the inlet profile information:

$$\eta_2 = f(\eta_1) = \frac{a}{c_w} \int_0^{\eta_1} \frac{M_1 (1 + \frac{\gamma-1}{2} M_1^2)^{1/2}}{\bar{M}_1 (1 + \frac{\gamma-1}{2} \bar{M}_1^2)^{1/2}} \eta d\eta \quad (\text{B11})$$

APPENDIX C

WATER JET PENETRATION
ACROSS A VARIABLE GAS FLOW FIELD

APPENDIX C

WATER JET PENETRATION
ACROSS A VARIABLE GAS FLOW FIELD

Determination of a water jet trajectory across a variable gaseous flow field is based upon a reasonable physical model of the phenomena which are actually occurring as a water jet penetrates a constant property flow field, for which the following empirical relation has been obtained from tests at both Aerojet-General Corporation and Lewis Research Center (see Fig. C-1 reproduced from Ref. 15):

$$\tilde{y} = 2 (\tilde{x})^{0.27} \left[(\tilde{q})^{0.5} - 0.75 \right] \quad (C1)$$

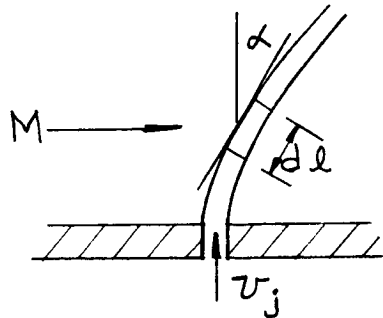
where $\tilde{y} \equiv y/D_j$; $\tilde{x} \equiv x/D_j$; $\tilde{q} \equiv q_j/\bar{q}_g$;

$$q_j \equiv \frac{\rho_j v_j^2}{2} ; \quad \bar{q}_g \equiv \frac{\gamma \rho M^2}{2} ; \quad D_j = \text{jet diameter}$$

Equation (C1) has been simplified here to the following form:

$$\tilde{y} = 2(\tilde{x})^{1/4} (\tilde{q})^{1/2} \quad (C2)$$

Consider the following sketch of a jet traversing a gaseous flow field:



From the geometry of the sketch and differentiation of Equation (C2)

$$\frac{d\tilde{y}}{d\tilde{x}} \equiv \cot \alpha = \frac{1}{2} (\tilde{x})^{-3/4} (\tilde{q})^{1/2} \quad (C3)$$

Solving Equation (C3) for \tilde{x} and inserting the result back into (C2) yields

$$\int_0^{\tilde{l}} \cos \alpha \, d\tilde{l} \equiv \tilde{y} = \frac{[2(\tilde{q})^{\frac{1}{2}}]^{\frac{4}{3}}}{4^{\frac{1}{3}}} \tan^{\frac{1}{3}} \alpha \quad (C4)$$

where $\tilde{l} \equiv l/D_j$

Differentiating Equation (C4) yields

$$\frac{d\tilde{l}}{d\alpha} = \frac{4}{3} \left[\frac{1}{2} (\tilde{q})^{\frac{1}{2}} \right]^{\frac{4}{3}} \cot^{\frac{2}{3}} \alpha \sec^3 \alpha \quad (C5)$$

It is presumed here that the change in \tilde{l} with incidence angle α depends upon the local values of \tilde{q} and α , independent of the variation of \tilde{q} across the flow field. That is, Equation (C5) applies to a constant or variable- \tilde{q} flow field. This is tantamount to a physical model in which the drag force per unit length acting normal to the water column is a function of local gas dynamic pressure, jet dynamic pressure, incidence angle, and jet diameter. Rearranging Equation (C5), remembering the geometry of the above sketch, we obtain, for injection normal to the wall,

$$\int_0^{\tilde{y}} \frac{(\tilde{q}_j / \bar{q}_g)^{\frac{2}{3}} d\tilde{y}}{\frac{4}{3} [1/2 (\tilde{q})^{\frac{1}{2}}]^{\frac{4}{3}}} = \int_0^{\alpha} \sec^2 \alpha \cot^{\frac{2}{3}} \alpha \, d\alpha = 3 \tan^{\frac{1}{3}} \alpha \quad (C6)$$

where

$$\tilde{q} \equiv \tilde{q}_j / \bar{q}_g \quad (C7)$$

\bar{q}_g = gas dynamic pressure for the average Mach number \bar{M} (see Appendix B) = $\gamma \rho \bar{M}^2 / 2$

$$\text{and} \quad \left(\frac{\tilde{q}_j}{\bar{q}_g} \right)^{\frac{2}{3}} = \left(\frac{M}{\bar{M}} \right)^{\frac{4}{3}} \quad (C8)$$

(since p = constant across the plane, by assumption)

Now,

$$\tilde{x} = \int_0^{\tilde{y}} \tan \alpha \, d\tilde{y} \quad (C9)$$

$\tan \alpha$ is obtained from Equation (C6), and \tilde{x} thus may be calculated:

$$\tilde{x} = \frac{1}{4 \bar{q}_0^{2/3}} \int_0^{\tilde{y}} \left[\int_0^{\tilde{y}} \left(\frac{M}{\bar{M}} \right)^{4/3} d\tilde{y} \right]^3 d\tilde{y} \quad (C10)$$

We now define two new variables and non-dimensionalize x and y with D and R (duct diameter and radius, respectively) instead of D_j :

$$X = \frac{1}{64} \int_0^{\eta'} \left[\int_0^{\eta'} \left(\frac{M}{\bar{M}} \right)^{4/3} d\eta' \right]^3 d\eta' \quad (C11)$$

where

$$X \equiv \left(q_j / \bar{q}_0 \right)^2 \left(D_j / D \right)^3 \left(x / D \right) \quad (C12)$$

and

$$\eta' \equiv y / R = 1 - \eta \quad (C13)$$

The right-hand side of Equation (C11) is a function of the radial coordinate in the inlet duct only, since the Mach number distribution is a function of this coordinate. Consequently, the jet trajectory can be determined for all jet dynamic pressures and jet diameters by means of a single integration across the flow field, providing the reduced trajectory coordinates η' and X indicated above are employed. It will be noted that Equation (C11) reduces to Equation (C2) for a constant Mach number distribution, as it should.

WATER PRESSURE 100 PSI

- VKC DATA: $M \geq 0.60$ (1/16 & 1/8 INCH NOZZLES)
- ◇ VKC DATA: $M \approx 0.40$ (1/16, 1/4 & 1/2 INCH NOZZLES)
- △ LRC DATA: $M \approx 0.27$ (1/4 & 1/2 INCH NOZZLES)
- LRC DATA: $M \approx 0.40$ (ALL NOZZLES)

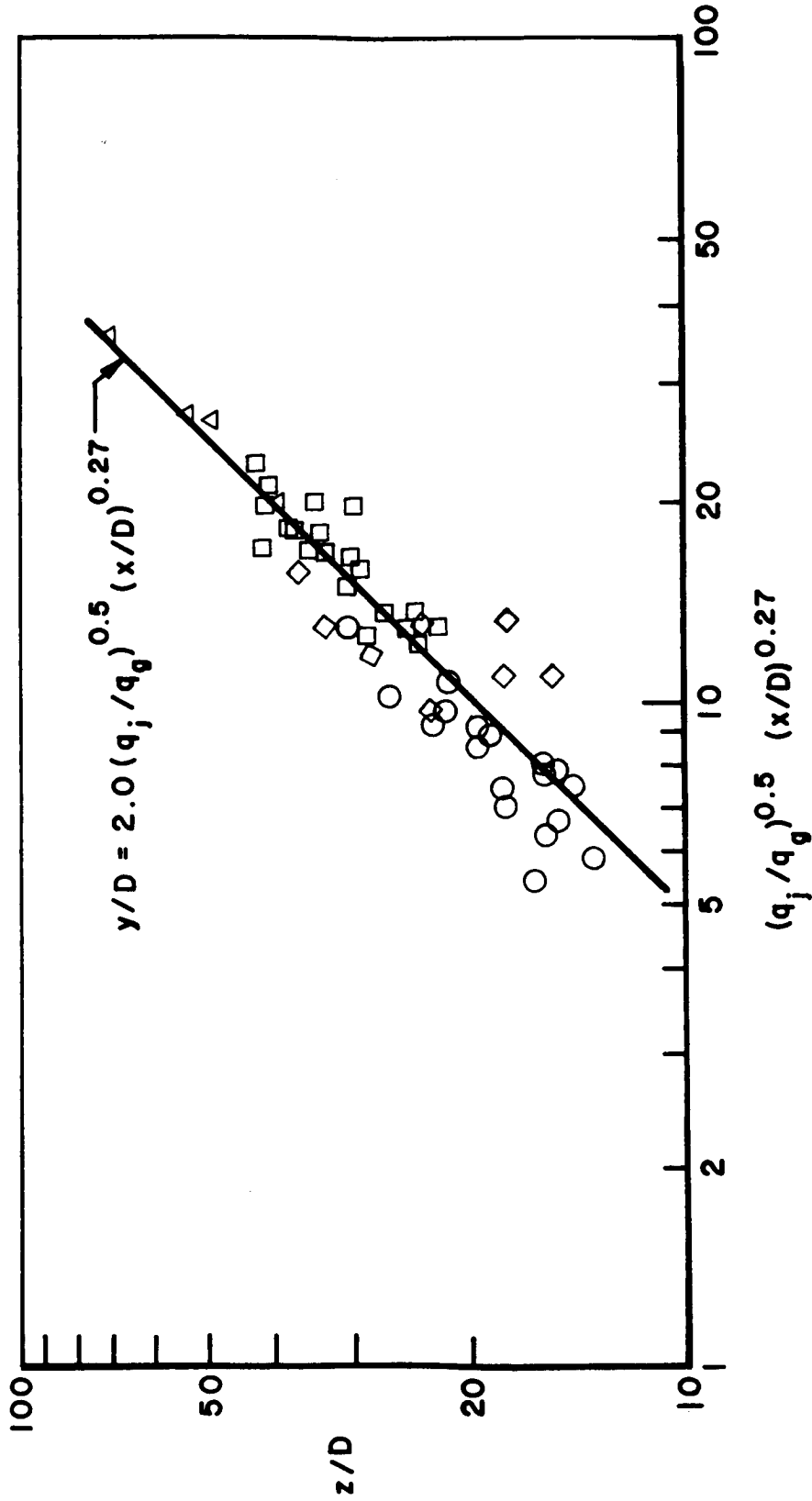


FIGURE C-1

EMPIRICAL PENETRATION CORRELATION USED IN THE ANALYSIS
(FROM REFERENCE 15)

APPENDIX D

SUDDEN-EXPANSION ANALYSIS (GAS ONLY)

APPENDIX D

SUDDEN-EXPANSION ANALYSIS (GAS ONLY)

Calculation of the gas conditions in the vicinity of the mixing duct entrance follows the general method described in Reference 1, but is here modified to account for non-one-dimensional flow.

From the momentum theorem, the single steady stream impulse function is

$$T = \int_A p dA + \int_A \rho u^2 dA \quad (D1)$$

In the absence of wall shear for cases of variable flow and cross sectional area, the change in T is given by

$$T_2 - T_1 = \int_{A_1}^{A_2} p_w dA \quad (D2)$$

where p_w is the wall pressure.

For the case of an abrupt subsonic expansion, it is classically assumed that the pressure in the base region formed by the transition between two cylindrical ducts is equal to the static pressure ahead of the expansion

$$\text{(i.e., } \int_{A_1}^{A_2} p_w dA = p_1 (A_2 - A_1)$$

From this assumption, and the impulse function developed in Appendix B for a non-uniform flow, Equation (D2) becomes

$$\frac{p_2}{p_1} = \frac{1 + c_{w_2} \left(\frac{c_{w_1}}{c_{w_2}} \frac{A_1}{A_2} \right) \gamma_1 \bar{M}_1^2}{1 + c_{w_2} \gamma_2 \bar{M}_2^2} \quad (D3)$$

If, as in Appendix B, the flow in a given cross section is assumed to be iso-energetic and isobaric, the continuity and energy equations for a perfect-ideal gas yield

$$\frac{p_2}{p_1} = \frac{c_{w_1} A_1}{c_{w_2} A_2} \frac{\bar{M}_1}{\bar{M}_2} \left(\frac{1 + \frac{\gamma-1}{2} \bar{M}_1^2}{1 + \frac{\gamma-1}{2} \bar{M}_2^2} \right)^{\frac{1}{2}} \quad (D4)$$

Combining Equations (D4) and (D3), it is seen that the average Mach number at Station 2 depends upon γ , \bar{M}_1 , c_{w_2} , and $(c_{w_1} A_1) / c_{w_2} A_2$.

For the case of uniform gaseous flow properties at Station 2, which is the assumption employed here, the solution for the Mach number at Station 2 is

$$M_2^2 = -\frac{\psi}{2} \left[1 - \left(1 - \frac{4}{\psi} \right)^{\frac{1}{2}} \right] \quad (D5)$$

where

$$\psi \equiv \frac{2\gamma - \xi}{\gamma^2 - \frac{\gamma-1}{2} \xi} \quad (D6)$$

and

$$\xi \equiv \frac{\left(\frac{A_2}{c_{w,A_1}} + \gamma \bar{M}_1^2 \right)^2}{\bar{M}_1^2 \left(1 + \frac{\gamma-1}{2} \bar{M}_1^2 \right)} \quad (D7)$$

From the solution to Equation (D5), the pressure at Station 2 is calculated here from Equation (D4) and the velocity from Equation (B4). The isentropic exponent for the hydrogen is assumed constant at $\gamma = 1.4$.

APPENDIX E

AUXILIARY COMPUTER PROGRAM LISTING:
INLET CONDITION SUBROUTINES (PEN)

*NAMEPEN

```
C PROGRAM TO CALCULATE ONE DIMENSIONAL PARAMETERS FROM MACH NUMBER
C PROFILES, AND WATER JET PENETRATION ACROSS A VARIABLE MACH
C NUMBER FLOW FIELD
  DIMENSION EM(40),ETA(40),DUM(40),ARG(40),VINT(40),ETAP(40),XT(40),
  1EXT(40),EMR(40),EJ2(40)
105 READ(2,1)KASE,NN,GAM
  1 FORMAT(2I10,E10.3)
  READ(2,2) (EM(N),ETA(N),N=1,NN)
  2 FORMAT(8E10.3)
100 DO 101 N=1,NN
  DUM(N)=EM(N)*EM(N)*ETA(N)
101 CONTINUE
  VINT(1)=EM(1)*EM(1)
  CALL MINTA(NN,ETA,DUM,VINT)
  VINT1=VINT(NN)
  GAMA=(GAM-1.)/2.
  DO 200 N=1,NN
  F=1.&GAMA*EM(N)*EM(N)
  ARG(N)=EM(N)*SQRT(F)
  DUM(N)=ARG(N)*ETA(N)
200 CONTINUE
  VINT(1)=ARG(1)
  CALL MINTA(NN,ETA,DUM,VINT)
  VINT2=VINT(NN)
  RAT=VINT1/VINT2
  VM=.5
300 VMS=VM
  F=1.&GAMA*VM*VM
  ERR =VM-RAT*SQRT(F)
  DERM=1.-GAMA*RAT*VM/SQRT(F)
  VM=-ERR/DERM&VM
  IF (ABS(ERR) -.0001) 301,301,300
301 DEN=VM*SQRT(F)
  CM=2.*VINT2/DEN
  FUNC=2./(CM*DEN)
  DO 304 N=1,NN
  EJ2SQ=VINT(N)*FUNC
  EJ2(N)=SQRT(EJ2SQ)
304 CONTINUE
  WRITE(3,3) KASE,GAM
  3 FORMAT(1X64H ONE DIMENSIONAL MACH NUMBER AND FLOW COEFFICIENT FOR C
  1ASE NUMBER,15/30X6HGAMMA=,F11.4)
  DO 302 N=1,NN
  WRITE(3,4) N,EM(N),ETA(N),EJ2(N)
  4 FORMAT(15,3E11.4)
302 CONTINUE
  WRITE(3,5) VM,CM
  5 FORMAT(1X51HMOMENTUM AVERAGED MACH NUMBER AND FLOW COEFFICIENT=,
  1F11.4,4H AND,F11.4)
  DO 401 J=1,NN
  K=NN&1-J
  ETAP(J)=1.-ETA(K)
  EMR(J)=(EM(K)/VM)**1.33333
401 CONTINUE
  VINT(1)=0.
  CALL MINTA(NN,ETAP,EMR,VINT)
  DO 402 J=1,NN
```

```

DUM(J)=VINT(J)*VINT(J)*VINT(J)
402 CONTINUE
XT(1)=0.
CALL MINTA(NN,ETAP,DUM,XT)
DO 403 J=1,NN
XT(J)=XT(J)/64.
EXT(J)=ETAP(J)*ETAP(J)
EXT(J)=EXT(J)*EXT(J)/256.
WRITE(3,6) J,ETAP(J),DUM(J),XT(J),EXT(J)
6 FORMAT(I5,4E11.4)
403 CONTINUE
GO TO 105
END

```

```

SUBROUTINE MINTA(N,X,Y,Z)
DIMENSION X(1),Y(1),S(40),Z(1)
SENSE SWITCH 5 STATEMENT NUMBER 10
S(2)=(Y(2)-Y(1))/(X(2)-X(1))
S(1)=S(2)
QC=S(2)
DO 7 I=1,N
IF(I&1-N)2,1,6
1 QB=QC
IF(I-2)7,6,5
2 XOT=X(I)-X(I&1)
XTT=X(I&1)-X(I&2)
XTO=X(I&2)-X(I)
AA=Y(I)/(XOT*XTO)
XOTT=XOT*XTT
AB=Y(I&1)/XOTT
AC=Y(I&2)/(XTT*XTO)
AAA=AA*XTT
ABB=AB*XTO
ACC=AC*XOT
QA=QC
QB=S(I)
QC=S(I&1)
S(I)=AA*(XTO-XOT)&ABB-ACC
S(I&1)=AB*(XOT-XTT)&ACC-AAA
S(I&2)=AC*(XTT-XTO)&AAA-ABB
3 IF(I-2) 9,5,4
9 S(1)=Z(1)
Z(1)=0.
GO TO 10
4 S(I)=(S(I)&QA)/2.
5 S(I)=(S(I)&QB)/2.
6 XD=X(I)-X(I-1)
YS=Y(I)&Y(I-1)
SD=S(I)-S(I-1)
Z(I)=Z(I-1)&XD/2.*(YS-XD/6.*SD)
10 CALL DATSW(5,KI)
IF(KI-2) 11,7,7
11 WRITE(3,12) I,X(I),Y(I),Z(I),S(I)
12 FORMAT(2X,I2,4(1XE10.3))

RETURN
END

```

APPENDIX F

MAIN MIXING COMPUTER PROGRAM LISTING

APPENDIX F

MAIN MIXING COMPUTER PROGRAM LISTING

NOTATION

INPUT

Card 1

KASE case number

I equals 1 if total water flow rate is input,
is greater than 1 if water total pressure is
input

INJ Base number for output azimuth determination,
equal to smallest even number of jets in a
row; numbers of jets in each row must be a
multiple of INJ

NN number of radial output stations - usually 11
which is the maximum permissible

MM number of axial output stations (maximum of 8)
that will be input on card 4

KK number of jet rows for which data are input
on card 3

Card 2

D1 inlet duct diameter (inches)

D2 mixing duct diameter (inches)

XJ axial location of jets (inches) (= 0. in the
inlet duct, greater than 0. in the mixing duct)

ALFM jet penetration truncation angle, usually 85
degrees

CW inlet duct flow coefficient (unity or less)

CM Reichardt momentum mixing constant - usually
equal to .075

CMK ratio of momentum to mass mixing constants -
usually unity

VPF factor on equilibrium vapor pressure - usually
unity

Card 3 - jet row (K) data

J(K) controls azimuthal orientation of jet row, equals 0 when 0 degree azimuth intersects a jet, = 1 when 0 degree azimuth bisects 2 jets in the row

IJ(K) equals 1 when radial location (RJ(K)) of the jet in the mixing duct is calculated; is greater than 1 when it is input

NJ(K) number of jets in the row

DJ(K) jet diameter (inches)

RJ(K) input radial location of the jet in the mixing duct (inches)

Card 4

XO(M) axial output stations (inches)

Card 5

EMHI hydrogen mass flow rate (lbm/sec)

EMJT total water flow rate (lbm/sec)

PTJ jet total pressure (psia)

TTH hydrogen stagnation temperature (°R)

TTJ water inlet temperature (°R)

EMI inlet average Mach number

OUTPUT

Line 1

D1 inlet diameter (inches)

D2 Mixing duct diameter (inches)

XJ jet axial location (inches)

ALFM Penetration truncation angle (degrees)

CW inlet duct flow coefficient

INJ jet row base number

Line 2

MDOT H (EMHI) Hydrogen flow rate (lbm/sec)
MDOT J (EMTT) Total water flow rate (lbm/sec)
PT1 average inlet stagnation pressure (psia)
PTJ jet stagnation pressure (psia)
TTH hydrogen stagnation temperature ($^{\circ}\text{R}$)
TTJ water inlet temperature ($^{\circ}\text{R}$)
M1 (EM1) average inlet Mach number
M2 (EM2) hydrogen Mach number at station 2

Line 3

P1 inlet static pressure (psia)
PT2 hydrogen stagnation pressure at 2 (psia)
P2 hydrogen static pressure at 2 (psia)
UJ jet velocity (ft/sec)
UH hydrogen velocity at 2 (ft/sec)
MIX-CM CM of input
MIX-CMK CMK of input
VAP PRES VPF of input

JET DATA (tabulated for each row)

NJ (NJ(K)) number of jets
MDOTJ EMJ(K) row water mass flow rate (lbm/sec)
JET DIAM DJ(K) in inches
JET RAD RJ(K) in inches

AZIMUTH (VJ) jet row azimuthal orientation (degrees)

COMPLETE AND PARTIAL MIXING RESULTS

P static pressure (psia)
R radius in the mixing duct (inches)
U velocity (ft/sec)
PT total pressure (psia)
T TOT stagnation temperature ($^{\circ}$ R)
RO density (lbm/ft^3)
K H2O LIQ condensed water mass fraction
K H2O VAP vapor water mass fraction
K H2 hydrogen mass fraction
MACH NO. mach number
X axial location (inches)
PHI azimuth (degrees)

WITHIN THE PROGRAM LISTINGS THE ABOVE PARAMETERS ARE (the first listed parameter is for partially mixed conditions, the last for final conditions)

P PS or PX
R RO(N)
U US (N,II) or U
PT PTS (N,II) or P
T TOT TTS (N,II) or T
RO RHOS (N,II) or RHO
K H2O LIQ CON1 (N,II) or VKK(1)
K H2O VAP CON2 (N,II) or VKK(2)
K H2 CON3 (N,II) or VKK(3)
MACH NO. VMS (N,II) or VM

X

XO(M)

PHI

PHI1

```

RC(2,1)= 7.25
RC(2,2)=1.105E&1
RC(3,1)=6.771
RC(3,2)=6.28
RG(1,1)=0.
RG(1,2)=0.
RG(2,1)=2.5E-3
RG(2,2)=8.23E-4
RG(3,1)=4.29E-4
RG(3,2)=9.2E-4
RE(1,1)=0.
RE(1,2)=0.
RE(2,1)=0.
RE(2,2)=-2.1E&6
RE(3,1)=0.
RE(3,2)=0.
RF(1,1)=5.8355E&1
RF(1,2)=5.8355E&1
RF(2,1)=6.8542E&1
RF(2,2)=6.8421E&1
RF(3,1)=4.8023E&1
RF(3,2)=4.8465E&1
DISTRIBUTION NUMBER 4
Y1(1)=0.
Y2(1)=0.
Y1(2)=.40
Y2(2)=.59
Y1(3)=.575
Y2(3)=.812
Y1(4)=.72
Y2(4)=.92
Y1(5)=.85
Y2(5)=.98
Y1(6)=1.
Y2(6)=1.
DO 12 I=1,5
EW(I)=(Y2(I&1)-Y2(I))/(Y1(I&1)-Y1(I))
EZ(I)=Y2(I)-EW(I)*Y1(I)
12 CONTINUE
YT(1)=.083
XT(1)=1.E-11
YT(2)=.16
XT(2)=3.E-10
YT(3)=.4
XT(3)=1.E-6
YT(4)=.72
XT(4)=2.E-4
YT(5)=1.
XT(5)=2.15E-3
DO 13 I=1,4
SP(I)=(ALOG(YT(I&1))-ALOG(YT(I)))/(ALOG(XT(I&1))-ALOG(XT(I)))
TP(I)=YT(I)/(XT(I)**SP(I))
13 CONTINUE
RETURN
END

```

```

SUBROUTINE PREL
C SUBROUTINE FOR AEROTHERM WET DIFFUSER MIXING PROGRAM
C THIS SUBROUTINE READS THE INPUT DATA, DOES THE HYDROGEN INLET AND
C DUMP ANALYSIS, CALCULATES JET FLOW RATES OR TOTAL PRESSURES, DOES
C PENETRATION CALCULATIONS IF REQUIRED AND PERFORMS CERTAIN PRELIM-
C INARY CALCULATIONS PRINTING OUT INTERMEDIATE RESULTS ALONG WITH A
C TABLE OF JET DATA
DIMENSION DJ(4),IJ(4),EMJ(4),DJSQ(4),AJ(4)
COMMON EMJT,EMHI,TTJ,TTH,P2,D2,D1,UJ,UH,HTJ,HTH,PX,VPF,CMK,CMKSQ,
1NN, KK, MM, INJ, ZB, BRATO, TSH, ROUH2, DROU2, DROUK, DROUH, A1,
2EMJC, DJC, RJC, DJCSQ, RD
COMMON RO(11), XO(8), DSY(11,8,2), DKSQ(11,8,2), A(8,4), BUSQ(8),
1VKK(3), RJ(4), J(4), NJ(4)
COMMON BIZ(34)
COMMON EZ(8), EW(8), Y2(8), SP(8), TP(8), YP(8)
EQUIVALENCE(CC, YM, ENN, DX, ENJ, RJC)
1 FORMAT(6I10)
2 FORMAT(8E10.3)
3 FORMAT(8E10.3)
4 FORMAT(6E10.3)
6 FORMAT(/25X,27HWATER PENETRATES CENTERLINE)
8 FORMAT(/24X,28HMIXING INPUT FOR CASE NUMBER,15/)
9 FORMAT(2X,10H D1 (IN.) ,10H D2 (IN.) , 10H XJ (IN.) ,
10HALFM (DEG),10H CW , 10H INJ )
10 FORMAT(2X,5E10.3,I6)
11 FORMAT(2X,10H MDOT H ,10H MDOT J ,10HPT1 (PSIA),10HPTJ (PSIA),
10H TTH (R) ,10H TTJ (R) ,4X,2HM1,8X,2HM2)
13 FORMAT(3X,9HP1 (PSIA),10HPT2 (PSIA),1X,9HP2 (PSIA),10HUJ(FT/SEC),
10HUH(FT/SEC),2X,6HMIX-CM,4X7HMIX-CMK3X8HVAP PRES)
14 FORMAT(2X,8E10.3/)
16 FORMAT(10X,3HXO=,F7.2,29H IS LESS THAN XJ, CASE NUMBER,15,13H NOT
1EXECUTED)
21 FORMAT(2X,9E10.3)
24 FORMAT(/20X,41HSOLUTION FOR SINGLE JET ON THE CENTERLINE/)
28 FORMAT(4(2I1,I2,2E8.2))
29 FORMAT(/34X8HJET DATA//16X2HNJ6X5HMDOTJ5X8HJET DIAM2X8HJET RAD.2X
17HAZIMUTH/23X8H(LB/SEC)4X4H(IN)6X4H(IN)5X5H(DEG))
30 FORMAT (16X,I2,4X,4E10.3)
C H2O PENETRATION AND HYDROGEN DUMP
100 READ(2,1) KASE,I,INJ,NN,MM,KK
READ(2,2)D1,D2,XJ,ALFM,CW,CM,CMK,VPF
READ(2,28)(J(K),IJ(K),NJ(K),DJ(K),RJ(K),K=1,KK)
READ(2,3)(XO(M), M=1,MM)
READ(2,4)EMHI,EMJT,PTJ,TTH,TTJ,EM1
AJT=0.
EMJC=0.
DJC=0.
C CALCULATION OF PROPERTIES AT 1
CSTAR= 7.128 *SQRT(TTH)
EM12=EM1*EM1
EMF=1.6.2*EM12
EPS=.578704*EMF*EMF*EMF/EM1
A1= .7854 *D1*D1
PT1=EMHI*CSTAR*EPS/(A1*CW)
P1=PT1/EMF**3.5
Q1=.7*P1*EM12

```

```

C      CALCULATION OF PROPERTIES AT 2
      CD=(D2/D1*D2/D1/CW&1.4*EM12)/EM1
      CC=CD*CD/EMF
      BB=2.8-CC
      AA=BB/(1.96-.2*CC)
      DD=4./(BB*AA)
      IF (DD-1.) 131,130,130
130  EM22=1.
      GO TO 132
131  EM22=-.5*AA*(1.-SQRT(1.-DD))
132  EM2F=1.8.2*EM22
      EM2=SQRT(EM22)
      P2=P1*D1/D2*D1/D2*EM1*SQRT(EMF/(EM22*EM2F))*CW
      PT2=P2*EM2F**3.5
      Q2=.7*P2*EM22
      UH= 26.07*SQRT(EM22/EM2F)*CSTAR
      ROUH=EMHI /(.7854*D2*D2)
      ROUH2=2.*Q2
      IF(XJ) 102,102,103
C      FREESTREAM DYNAMIC CONDITIONS
102  QINF=Q1
      P=P1
      GO TO 104
103  QINF=Q2
      P=P2
C      CALCULATION OF JET AREAS
104  DO 1041 K=1, KK
      ENJ=NJ(K)
      DJSQ(K)=DJ(K)*DJ(K)
      AJ(K)=ENJ*.7854*DJSQ(K)
1041 AJT=AJT&AJ(K)
      IF(I-1 ) 105,105,106
C      DETERMINATION OF WATER FLOW RATE OR STAGNATION PRESSURE
105  PTJ=P&EMJT /AJT*EMJT /AJT*.035862
      GO TO 107
106  EMJT = 5.281 *AJT*SQRT(PTJ-P)
C      CALCULATION OF WATER PROPERTIES AND PENETRATION
107  ROUJ=EMJT /AJT
      UJ=2.3077*ROUJ
      QJ=PTJ-P
      ROUJ2=2.*QJ
      RJS=RJ(1)
      DO 118 K=1, KK
      EMJ(K)=AJ(K)/AJT*EMJT
      IF(IJ(K)-1) 1071,1071,115
1071 ALFM=.017453 *ALFM
      BP=QJ/QINF*QJ/QINF
      IF(XJ) 300,300,301
300  I=1
      DDEN=D1
      AP=TP(I)
      PN=SP(I)
      GO TO 302
301  AP=4.
      PN=.25
      DDEN=D2
302  BP=BP*DJ(K)/DDEN*DJ(K)/DDEN*DJ(K)/DDEN

```

```

303 YTM=(AP/2.)**(1./(1.-PN))*(PN*BP* SIN(ALFM)/ COS(ALFM))**(PN/(1.-P
1N))
IF(XJ) 304,304,306
304 IF(YTM=.5*YP(I&1)) 306,306,305
305 I=I&1
AP=TP(I)
PN=SP(I)
IF(YP(I)-1.) 303,306,306
306 YM=YTM*DDEN
ALFM=57.296 *ALFM
IF(XJ) 108,108,109
C DETERMINATION OF JET RADII
108 I=1
ETA1=1.-YM/(.5*D1)
IF(ETA1-(DJ(K)&DJC)/D1) 114,114,400
400 ETA2=EZ(I)&EW(I)*ETA1
IF(ETA2 -Y2(I&1)) 402,402,401
401 I=I&1
IF(Y2(I)-1.) 400,403,403
402 IF(ETA2-(1.-DJ(K)/D2)) 404,404,403
403 ETA2=1.-DJ(K)/D2
404 RJ(K)=ETA2*.5*D2
GO TO 118
109 RJ(K)=.5*D2-YM
C CHECK FOR PENETRATION OF CENTERLINE
110 IF(RJ(K)-(.5*(DJ(K)&DJC))) 114,114,118
114 RJ(K)=0.
115 IF(RJ(K)) 116,116,118
C CALCULATION OF CENTERLINE FLOW PARAMETERS
116 EMJC=EMJC&EMJ(K)
AJC=EMJC/ROUJ
DJC=1.1284*SQRT(AJC)
118 CONTINUE
C CONVERSION OF INPUT TO MIXING PARAMETERS
200 TTJ=TTJ/1.8
TTH=TTH/1.8
HTJ=-4080.&TTJ
IF(TTH-1000.) 201,201,202
201 HTH=-1030.&3.365*TTH&.0001068*TTH*TTH
GO TO 203
202 HTH=-907.&3.12*TTH&.0002285*TTH*TTH
203 DROU2= ROUJ2-ROUH2
DROUK= ROUJ
DROUH=ROUJ*(HTJ-HTH)
DO 204 N=1,NN
DO 204 M=1,MM
DO 204 II=1,2
C NULL SUMMATIONS, AND DETERMINE OUTPUT RADII
DKSY(N,M,II)=0.
204 DSY(N,M,II)=0.
RD=.5*D2
RO(1)=0.
ENN=NN-1
DELRO=RD/ENN
DO 2041 N=2,NN
RO(N)=RO(N-1)&DELRO
2041 CONTINUE

```

```

C      CMKSQ=CMK*CMK
      TEST FOR IMPROPER VALUE OF XO
      DO 2044 K=1, KK
      DO 2044 M=1, MM
      DX=XO(M)-XJ
      BUSQ(M)=CM*CM*DX*DX
      A(M,K)=DJSQ(K)/BUSQ(M)*.25
      DELTX=DX
      IF (DX) 2045,2045,2048
2045  DELTX=0.
2048  IF (DELTX) 2047,2047,2044
2047  WRITE(3,16)XO(M),KASE
      GO TO 100
2044  CONTINUE
2046  WRITE(3,8) KASE
      TTJ=TTJ*1.8
      TTH=TTH*1.8
C      OUTPUT OF INPUT AND INTERMEDIATE RESULTS
      WRITE(3,9)
      WRITE(3,10)D1,D2, XJ,ALFM,CW , INJ
      WRITE(3,11)
      WRITE(3,21)EMHI ,EMJT ,PT1,PTJ,TTH,TTJ,EM1,EM2
      TTJ=TTJ/1.8
      TTH=TTH/1.8
C      PARAMETERS FOR GENERAL ESTIMATES OF STATE TEMPERATURES
      TSH=TTH/EM2F
      ZB=1.9198*.325*ALOG (ROUH/ROUJ)*.4343
      BRATO=1.42E-4
      WRITE(3,13)
      WRITE(3,14)P1,PT2,P2,UJ,UH, CM,CMK,VPF
C      DETERMINATION AND OUTPUT OF JET CONDITIONS AND GEOMETRIES
      IF(EMJC) 3005,3005,3000
3000  IF(KK-1) 3001,3001,3004
3001  IF(RJS ) 3003,3003,3002
3002  WRITE(3,6)
3003  WRITE(3,24)
      KK=1
      GO TO 3005
3004  WRITE(3,6)
      DO 3010 K=1, KK
      IF (RJ(K)) 3010,3010,3005
3010  CONTINUE
      GO TO 3003
3005  WRITE(3,29)
      DO 3007 K=1, KK
      ENJ=NJ(K)
      THETA=3.1416/ENJ*57.296
      IF(RJ(K)) 3007,3007,3006
3006  VJ=J(K)
      VJ=THETA*VJ
C      JETS WITH RADII GREATER THAN ZERO
      WRITE(3,30)NJ(K), EMJ(K),DJ(K),RJ(K),VJ
3007  CONTINUE
      IF(EMJC) 3011,3011,3008
3011  WRITE(3,32)
      32  FORMAT(/)
      GO TO 3020

```



```

C   JETS ON CENTERLINE , IF ANY
3008 RJC=0.
      WRITE(3,31) EMJC,DJC,RJC
      31  FORMAT(17X,1H1,4X,3E10.3,3X5H-----)
      WRITE(3,32)
      DJCSQ=DJC*DJC
3020 RETURN
      END

      SUBROUTINE FINAL
C   SUBROUTINE FOR AEROTHERM WET DIFFUSER MIXING PROGRAM
C   THIS SUBROUTINE CALCULATES CONDITIONS THAT WOULD EXIST IN THE
C   MIXING DUCT AFTER COMPLETE MIXING AND RECOGNIZES A CHOKED CONDIT-
C   ION IF IT WOULD EXIST
      COMMON EMJT,EMHI,TTJ,TTH,P2,D2,D1,UJ,UH,HTJ,HTH,PX,VPF,CMK,CMKSQ,
1NN,KK,MM,INJ,ZB,BRAT0,TSH,ROUH2,DROU2,DROUK,DROUH,A1,
2EMJC,DJC,RJC,DJCSQ,RD
      COMMON RO(11),XO(8),DSY(11,8,2),DKSY(11,8,2),A(8,4),BUSQ(8),
1VKK(3),RJ(4),J(4),NJ(4)
      19  FORMAT(10X,2HX=,F10.3,2X,6HINCHES10X2HP=,F10.3,2X4HPSIA)
      21  FORMAT(2X,9E10.3)
407  FORMAT(1X,I10,5E10.3)
408  FORMAT (22X32HCONDITIONS AFTER COMPLETE MIXING/)
409  FORMAT(12H  P (PSIA) ,11HU (FT/SEC) ,10HPT (PSIA) ,9HT TOT (R),
111HRO(LB/FT3) ,10HK H2O LIQ ,9HK H2O VAP,3X6HK H2  ,2X8HMACH NO.)
439  FORMAT (18X41HINLET MACH NUMBER IMPOSSIBLE IF THE FLOWS/
120X37HCOMPLETELY MIX WITHIN THE MIXING DUCT)
C   SENSE SWITCH 2      STATEMENT NUMBER 403
C   COMPUTATION OF CONDITIONS AFTER COMPLETE MIXING
      MIX=0
      CDP=.25
      EMDOT=EMJT&EMHI
      T=(EMJT*TTJ&EMHI*TTH)/EMDOT*1.8
      PX=P2/14.696
      ITM=0
      DP=0.
400  ITM=ITM&1
      IF (ITM-30) 425,425,445
425  T=T/1.8
C   CALCULATION OF FINAL MOMENTUM FLUX
      PX=PX&DP
      AMIX=A1*D2/D1*D2/D1
      FOFX=(EMJT *UJ&EMHI *UH)/((AMIX*32.174*14.696)&P2/14.696
426  ROU2=FOFX-PX
C   FIX FOR NEGATIVE MOMENTUM
      IF (ROU2) 416,416,417
416  PX=(PX-DP&FOFX)/2.
      GO TO 426
C   FINAL MASS , MOMENTUM , AND ENTHALPY FLUXES
417  ROUK=EMJT /AMIX
      ROU2=ROU2*14.696
      ROUHT=ROUK*(HTJ-HTH)
      P=PX
      CALL STATE(ROU2,ROUHT,ROUK,HTH,U,P,T,RHO,VKK,VM,VPF)

```

```

ERRU=RHO*U/144.-EMDOT/AMIX
IF (MIX) 401,401,402
401 ERRUS=ERRU
DP=.01
MIX=1
DERP=0.
DERPS=0.
GO TO 403
402 DERP=(ERRU-ERRUS)/DP
IF (ERRU) 437,437,441
C TEST FOR CHOKE CONDITION
437 IF (DERPS*DERP) 438,441,441
438 WRITE(3,439)
GO TO 445
441 ERRUS=ERRU
DERPS=DERP
DP=-ERRU/DERP
DLNP=DP/PX
IF (ABS(DLNP)-CDP) 411,411,412
412 IF (DLNP-CDP) 413,413,414
413 DLNP=-CDP
DP =DLNP*PX
GO TO 411
414 DLNP=CDP
DP =DLNP*PX
411 IF (ABS(ERRU)-.0001*EMDOT/AMIX) 404,404,403
403 CALL SSWTCH(2,KI)
IF(KI-2) 405,400,400
405 WRITE(3,407)ITM,PX,DERP,DP,ERRU,VM
GO TO 400
404 PX=PX*14.696
C OUTPUT FOR COMPLETE MIXING CONDITIONS
WRITE(3,408)
WRITE(3,409)
WRITE(3,21) PX,U,P,T,RHO,VKK(1),VKK(2),VKK(3),VM
445 RETURN
END

```

```

SUBROUTINE SUMCL
C SUBROUTINE FOR AEROTHERM WET DIFFUSER MIXING PROGRAM
C THIS SUBROUTINE PERFORMS REICHARDT SUMMATIONS FOR A SINGLE JET ON
C THE DUCT CENTERLINE, AND ANALYTICALLY CORRECTS FOR THE CONFINED
C DUCT FLOW NOT CONSIDERED IN THE THEORY OF REICHARDT
DIMENSION S(3,11)
COMMON EMJT,EMHI,TTJ,TTH,P2,D2,D1,UJ,UH,HTJ,HTH,PX,VPF,CMK,CMKSQ,
1NN,KK,MM,INJ,ZB,BRATO,TSH,ROUH2,DROU2,DROUK,DROUH,A1,
2EMJC,DJC,RJC,DJCSQ,RD
COMMON RO(11),XO(8),DSY(11,8,2),DKSY(11,8,2),A(8,4),BUSQ(8),
1VKK(3),RJ(4),J(4),NJ(4)
DO 229 N=1,NN
C CALCULATION OF INCIDENT AND REFLECTED DISTANCES
S(1,N)=RO(N)
S(2,N)=D2-RO(N)
S(3,N)=D2&RO(N)

```

```

C 229 CONTINUE
CALCULATION OF FLUXES DUE TO CENTERLINE JETS
DO 235 M=1,MM
D2SQ=D2*D2
WSQ=D2SQ/BUSQ(M)*.25
W=SQRT(WSQ)
WSQ=WSQ*9.
IF(WSQ-200.) 2502,2502,2501
2501 YW=0.
GO TO 2503
2502 YW1=2.*(EXP(-WSQ/9.)-EXP(-4./9.*WSQ))
YW2=EXP(-WSQ)
YW3=4.*W*(ERF(W)&ERF(3.*W)-2.*ERF(2.*W))
YW=YW1&YW2&YW3
2503 SYW=DJCSQ/D2SQ*YW
IF(CMK-1.) 2504,2505,2504
2504 YWK1=-2.*EXP(-4./9.*WSQ*CMKSQ) &2.*EXP(-WSQ/9.*CMKSQ)
YWK2=&EXP(-WSQ*CMKSQ)
WK=W*CMK
YWK3= 4.*WK*(ERF(WK)&ERF(3.*WK)-2.*ERF(2.*WK))
YWK=YWK1&YWK2&YWK3
SYWK=DJCSQ/D2SQ*YWK
GO TO 2506
2505 SYWK=SYW
2506 DO 235 N=1,NN
DO 234 I=1,3
X=S(I,N)*S(I,N)/BUSQ(M)
IF(X-200.) 2342,2342,2341
2341 Y=0.
GO TO 2343
2342 Y=EXP(-X)
2343 AMC=DJCSQ/BUSQ(M)*.25
SY=Y*AMC
DSY(N,M,1)=DSY(N,M,1)&SY
IF(CMK-1.) 2345,2346,2345
2345 X=X*CMKSQ
IF(X-200.) 302,302,301
301 Y=0.
GO TO 303
302 Y=EXP(-X)
303 DKSY(N,M,1)=DKSY(N,M,1)&Y*AMC*CMKSQ
GO TO 234
2346 DKSY(N,M,1)=DSY(N,M,1)
234 CONTINUE
DSY(N,M,1)=DSY(N,M,1) &SYW
DSY(N,M,2)=DSY(N,M,1)
DKSY(N,M,1)=DKSY(N,M,1)&SYWK
DKSY(N,M,2)=DKSY(N,M,1)
235 CONTINUE
RETURN
END

```

SUBROUTINE OUTCL

```

C   SUBROUTINE FOR AEROTHERM WET DIFFUSER MIXING PROGRAM
C   THIS SUBROUTINE CALLS THE STATE AND MINT SUBROUTINES FOR SOLUTION
C   OF ALL STATE PROPERTIES IN THE MIXING DUCT, AND IS USED IF THERE
C   IS ONLY ONE JET AND IT IS ON THE CENTERLINE, OR IF ALL JETS PEN-
C   ETRATE THE CENTERLINE. IT ALSO OUTPUTS THE FINAL RESULTS FOR
C   THESE CASES
    DIMENSION US(11,2),PTS(11,2),TTS(11,2),RHOS(11,2),CON1(11,2),
1  CON2(11,2),CON3(11,2),VMS(11,2)
    DIMENSION DUM(11),RUK3(11),ROUK3(11,2)
    COMMON EMJT,EMHI,TTJ,TTH,P2,D2,D1,UJ,UH,HTJ,HTH,PX,VPF,CMK,CMKSQ,
1  INN,KK,MM,INJ,ZB,BRAT0,TSH,ROUH2,DROU2,DROUK,DROUH,A1,
2  ZEMJC,DJC,RJC,DJCSQ,RD
    COMMON RO(11),XO(8),DSY(11,8,2),DKSY(11,8,2),A(8,4),BUSQ(8),
1  VKK(3),RJ(4),J(4),NJ(4)
40  FORMAT(/9X,59HCONVERGENCE ON PRESSURE NOT OBTAINED FOR THE FOLLOWI
    NG DATA)
26  FORMAT(2X,10H R (IN.),10HU (FT/SEC),10H PT (PSIA),10H T TOT (R),
    110HRO(LB/FT3),10H K H2O LIQ,10H K H2O VAP,10H K H2 ,
    21X8HMACH NO.)
27  FORMAT(/25X31HLOCAL HYDROGEN MASS FLOW RATE =,1XE10.3,8H LBS/SEC/)
21  FORMAT(2X,9E10.3)
407 FORMAT(1X,I10,5E10.3)
19  FORMAT(10X,2HX=,F10.3,2X,6HINCHES10X2HP=,F10.3,2X4HPSIA)
C   SENSE SWITCH 3 STATEMENT NUMBER 2558
    PS=P2
    II=1
    DO 2381 M=1,MM
    MIX=0
    PI=PS
    DP=0.
2550 PI=PI&DP
    DO 238 N=1,NN
    B=DSY(N,M,1)
    BK=DKSY(N,M,1)
    BRAT=B/ZB
    ARG=BRAT/BRAT0
    IF (ARG-1.) 2543,2543,2541
2543 T=TSH
    GO TO 2542
2541 EX=ALOG (ARG)*.4343
    TTIL=1.-1./(1.&EX*(1.3&4.*EX))
    T=TSH-(TSH-TTJ)*TTIL
2542 ROU2=ROUH2&P2-PI&DROU2*B
    IF(ROU2) 2551,2551,2552
2551 PZ=P2&ROUH2&DROU2*B
    DP=(PZ-PI-DP)/2.
    PI=PI&DP
    DO 8000 K=1,NN
    B=DSY(K,M,II)
    ROU2=ROUH2&P2-PI&DROU2*B
    IF(ROU2) 2551,2551,8000
8000 CONTINUE
    PI=PI-DP
    GO TO 2550
2552 PZ=PI-PX
    ROUK=DROUK*BK
    ROUHT=DROUH*BK
    P=PI/14.696

```

```

CALL STATE(ROU2,ROUHT,ROUK,HTH,U,P,T,RHO,VKK,VM,VPF)
ROUK3(N,1)=RHO*U*VKK(3)
US (N,II)=U
PTS (N,II)=P
TTS (N,II)=T
RHOS(N,II)=RHO
CON1(N,II)=VKK(1)
CON2(N,II)=VKK(2)
CON3(N,II)=VKK(3)
VMS (N,II)=VM
238 CONTINUE
C INTEGRATION OF HYDROGEN FLOW
EMHC =ROUK3(1,1)
DO 2382 N=1,NN
RUK3(N)=ROUK3(N,1)
DUM(N)=RUK3(N)*RO(N)
2382 CONTINUE
CALL MINT (NN,RO ,DUM ,EMHC)
EMHC =EMHC *3.1416/144. *2.
ERMH=EMHC-EMHI
IF(ABS(ERMH)-.001*EMHI) 2561,2561,2553
2553 IF(MIX) 2554,2554,2555
2554 DP=(PX-PI)*.1
ERMHS=ERMH
MIX=1
ITM=1
DERHP=0.
GO TO 2556
2555 DERHP=(ERMH-ERMHS)/DP
DP=-ERMH/DERHP
ERMHS=ERMH
ITM=ITM&1
2556 IF(ITM-20) 2558,2558,2557
2558 CALL SSWTCH(3,KI)
IF(KI-2) 2559,2550,2550
2559 WRITE(3,407)ITM,PI,DERHP,DP,ERMH,PZ
GO TO 2550
2557 WRITE(3,40)
WRITE(3,27)EMHC
2561 PS=PI
WRITE(3,19) XO(M),PS
WRITE(3,26)
DO 2381 N=1,NN
WRITE(3,21)RO(N),US(N,II),PTS(N,II),TTS(N,II),RHOS(N,II),
1CON1(N,II),CON2(N,II),CON3(N,II),VMS(N,II)
2381 CONTINUE
RETURN
END

```

```

SUBROUTINE SUMR1
C SUBROUTINE FOR AEROTHERM WET DIFFUSER MIXING PROGRAM

```

```

C     THIS SUBROUTINE PERFORMS REICHARDT SUMMATIONS FOR EVEN NUMBERS OF
C     JETS IN ALL ROWS THAT ARE NOT AT THE CENTERLINE.  THESE RESULTS
C     ARE SUPERIMPOSED ON CENTERLINE JET CONTRIBUTIONS, IF ANY.
      DIMENSION S(300,11)
      COMMON EMJT,EMHI,TTJ,TTH,P2,D2,D1,UJ,UH,HTJ,HTH,PX,VPF,CMK,CMKSQ
      1NN,KK,MM,INJ,ZB,BRAT0,TSH,ROUH2,DROU2,DROUK,DROUH,A1,
      2EMJC,DJC,RJC,DJCSQ,RD
      COMMON RO(11),XO(8),DSY(11,8,2),DKSY(11,8,2),A(8,4),BUSQ(8),
      1VKK(3),RJ(4),J(4),NJ(4)
      PI=3.1416
205  DO 220 K=1,KK
      IF(RJ(K)) 220,220,206
206  ENJ=NJ(K)
      INJK=NJ(K)/INJ
C     IF INJK IS EVEN,CALCULATIONS NEED ONLY BE PERFORMED AT ONE ANGLE
      VINJ=INJK
      VINJ=VINJ/2.
      FINJ=INJK/2
      IF((VINJ-FINJ)-.2) 2061,2061,2062
2061 INJK=0
      GO TO 2063
2062 INJK=1
2063 DO 213 N=1,MN
      I=0
      IF(INJK) 320,320,321
320  IF(J(K)) 321,321,210
C     CALCULATION OF INCIDENT AND REFLECTED DISTANCES, EVEN JETS, PHI=0
321  S(1,N)=RO(N)-RJ(K)
      S(2,N)=RJ(K)&D2&RO(N)
      S(3,N)=D2-RJ(K)-RO(N)
      S(4,N)=RO(N)&RJ(K)
      S(5,N)=D2-RJ(K)&RO(N)
      S(6,N)=D2&RJ(K)-RO(N)
      I=6
      TH=2.*PI/ENJ
208  IF(TH-.998*PI) 209,209,2064
209  CALL CIRFC (RD,RJ(K),RO(N),TH,S(I&1,N),S(I&2,N),S(I&3,N))
      TH=TH&2.*PI/ENJ
      I=I&3
      GO TO 208
2064 IF(INJK) 213,213,210
C     CALCULATION ALONG RADIAL LINE BETWEEN JETS
210  PHI1=PI/ENJ
      TH=PHI1
211  IF(TH-1.002*(PI-PI/ENJ)) 212,212,213
212  CALL CIRFC (RD,RJ(K),RO(N),TH,S(I&1,N),S(I&2,N),S(I&3,N))
      TH=TH&PI/ENJ*2.
      I=I&3
      GO TO 211
213  CONTINUE
      IF(INJK) 214,214,217
214  IF(J(K))215,215,216
215  IM2=3*NJ(K)/2&3
      GO TO 218
216  IM2=3*NJ(K)/2
      GO TO 218
217  IM0=3*NJ(K)/2&4
      IM2=3*NJ(K)&3

```

```

218 DO 305 N=1,NN
DO 305 I=1,IM2
S(I,N)=S(I,N)*S(I,N)
305 CONTINUE
C SUPERPOSITION OF FLUXES
DO 219 M=1,MM
DO 219 N=1,NN
II=1
DO 219 I=1,IM2
X=S(I,N)/BUSQ(M)
IF(X-200.) 2132,2132,2131
2131 Y=0.
YS=0.
GO TO 2066
2132 Y=EXP(-X)
YS=Y
2066 IF(INJK) 2067,2067,2133
2067 IF(J(K)) 2068,2068,2069
2068 FAC=1.
IF(I-7) 2138,2069,2069
2069 FAC=2.
GO TO 2138
2133 IF(I-7) 2134,2135,2135
2134 II=1&J(K)
FAC=1.
GO TO 2138
2135 IF(I-IM0) 2136,2137,2137
2136 FAC=2.
GO TO 2138
2137 FAC=2.
II=2-J(K)
2138 DSY(N,M,II)=DSY(N,M,II)&FAC*Y*A(M,K)
IF(CMK-1.) 2139,2140,2139
2139 X=X*CMKSQ
IF(X-200.) 302,302,301
301 Y=0.
GO TO 303
302 Y=EXP(-X)
303 DKSY(N,M,II)=DKSY(N,M,II)&FAC*Y*A(M,K)*CMKSQ
GO TO 2141
2140 DKSY(N,M,II)=DSY(N,M,II)
2141 IF(INJK) 2142,2142,219
2142 DSY(N,M,2)=DSY(N,M,2)&FAC *YS*A(M,K)
DKSY(N,M,2)=DKSY(N,M,2)&FAC *Y*A(M,K)*CMKSQ
219 CONTINUE
220 CONTINUE
RETURN
END

```

```

C SUBROUTINE SUMR2
SUBROUTINE FOR AEROTHERM WET DIFFUSER MIXING PROGRAM

```

```

C THIS SUBROUTINE CORRECTS THE FLUXES OF SUMR1 FOR THE CONFINED DUCT
C FLOW NOT CONSIDERED IN THE THEORY OF REICHARDT
  DIMENSION FLUX(11),DUM(11)
  COMMON EMJT,EMHI,TTJ,TTH,P2,D2,D1,UJ,UH,HTJ,HTH,PX,VPF,CMK,CMKSQ,
  1NN,KK,MM,INJ,ZB,BRATO,TSH,ROUH2,DROU2,DROUK,DROUH,A1,
  2EMJC,DJC,RJC,DJCSQ,RD
  COMMON RO(11),XO(8),DSY(11,8,2),DKSY(11,8,2),A(8,4),BUSQ(8),
  1VKK(3),RJ(4),J(4),NJ(4)
C FLUX CORRECTIONS DUE TO CONFINED DUCT FLOW
  RDSQ=RD*RD
  AMIX=3.1416*RDSQ
  AJT=EMJT/UJ*144./62.4
300 DO 309 M=1,MM
  IF((BUSQ(M)/RDSQ)-.16) 301,302,302
301 DLTM=0.
  GO TO 304
302 DO 303 N=1,NN
  FLUX(N)=DSY(N,M,1)&DSY(N,M,2)
  DUM(N)=FLUX(N)*RO(N)
303 CONTINUE
  VINT=FLUX(1)*2.
  CALL MINT (NN,RO,DUM,VINT)
  DLTM=AJT/AMIX-VINT/RDSQ
  DLK=DLTM
  IF(CMK-1.) 304,307,304
304 IF((BUSQ(M)/(RDSQ*CMKSQ))- .16) 3041,305,305
3041 DLK=0.
  GO TO 307
305 DO 306 N=1,NN
  FLUX(N)=DKSY(N,M,1)&DKSY(N,M,2)
  DUM(N)=FLUX(N)*RO(N)
306 CONTINUE
  VINT=FLUX(1)*2.
  CALL MINT (NN,RO,DUM,VINT)
  DLK =AJT/AMIX-VINT/RDSQ
307 DO 309 N=1,NN
  DSY(N,M,1)=DSY(N,M,1)&DLTM
  DSY(N,M,2)=DSY(N,M,2)&DLTM
  DKSY(N,M,1)=DKSY(N,M,1)&DLK
  DKSY(N,M,2)=DKSY(N,M,2)&DLK
309 CONTINUE
  RETURN
  END

```

```

SUBROUTINE OUTR
C SUBROUTINE FOR AEROTHERM WET DIFFUSER MIXING PROGRAM
C THIS SUBROUTINE CALLS THE MINT AND STATE SUBROUTINES FOR SOL-
C UTION OF ALL STATE PROPERTIES IN THE MIXING DUCT. THIS SUBROUTINE
C CONSIDERS CONTRIBUTIONS OF ALL JETS IF ANY ONE OR MORE OF THEM ARE
C NOT ON THE CENTERLINE
  DIMENSION US(11,2),PTS(11,2),TTS(11,2),RHOS(11,2),CON1(11,2),
  1CON2(11,2),CON3(11,2),VMS(11,2)
  DIMENSION DUM(11), ROUK3(11,2),RUK3(11)
  COMMON EMJT,EMHI,TTJ,TTH,P2,D2,D1,UJ,UH,HTJ,HTH,PX,VPF,CMK,CMKSQ,
  1NN,KK,MM,INJ,ZB,BRATO,TSH,ROUH2,DROU2,DROUK,DROUH,A1,

```



```

2EMJC,DJC,RJC,DJCSQ,RD
COMMON RO(11),XO(8),DSY(11,8,2),DKSY(11,8,2),A(8,4),BUSQ(8),
1VKK(3),RJ(4),J(4),NJ(4)
19 FORMAT(10X,2HX=,F10.3,2X,6HINCHES10X2HP=,F10.3,2X4HPSIA)
20 FORMAT(10X,5HPHI=0,3X,7HDEGREES)
21 FORMAT(2X,9E10.3)
22 FORMAT(10X,4HPHI=,F7.2,1X,7HDEGREES)
23 FORMAT(///)
26 FORMAT(2X,10H R (IN.),10HU (FT/SEC),10H PT (PSIA),10H T TOT (R),
110HRO(LB/FT3),10H K H2O LIQ,10H K H2O VAP,10H K H2 ,
21X8HMACH NO.)
27 FORMAT(/25X31HLOCAL HYDROGEN MASS FLOW RATE =,1XE10.3,8H LBS/SEC/)
40 FORMAT(/9X,59HCONVERGENCE ON PRESSURE NOT OBTAINED FOR THE FOLLOWI
ING DATA)
407 FORMAT(1X,I10,5E10.3)
C SENSE SWITCH 3 STATEMENT NUMBER 7558
CT=.9
PS=P2
DO 223 M=1,MM
ITM=0
PI=PS
DP=0.
7550 PI=PI&DP
II=1
220 DO 221 N=1,NN
B=DSY(N,M,II)
BK=DKSY(N,M,II)
BRAT=B/ZB
ARG=BRAT/BRATO
IF (ARG-1.) 140,140,141
140 T=TSH
GO TO 2202
141 EX=ALOG(ARG)*.4343
TTIL=1.-1./(1.&EX*(1.3&4.*EX))
T=TSH-(TSH-TTJ)*TTIL
2202 ROU2=ROUH2&P2-PI&DROU2*B
IF(ROU2) 7551,7551,7552
7551 PZ=P2&ROUH2&DROU2*B
DP=(PZ-PI-DP)/2.
PI=PI&DP
DO 8000 II=1,2
DO 8000 K=1,NN
B=DSY(K,M,II)
ROU2=ROUH2&P2-PI&DROU2*B
IF(ROU2) 7551,7551,8000
8000 CONTINUE
PI=PI-DP
GO TO 7550
7552 PZ=PI-PX
ROUK=DROUK*BK
ROUHT=DROUH*BK
P=PI/14.696
CALL STATE(ROU2,ROUHT,ROUK,HTH,U,P,T,RHO,VKK,VM,VPF)
ROUK3(N,II)=RHO*U*VKK(3)
US (N,II)=U
PTS (N,II)=P
TTS (N,II)=T

```

```

RHOS(N,II)=RHO
CON1(N,II)=VKK(1)
CON2(N,II)=VKK(2)
CON3(N,II)=VKK(3)
VMS (N,II)=VM
221 CONTINUE
IF (II-1)222,222,2221
222 II=2
GO TO 220
C INTEGRATION OF HYDROGEN FLOW
2221 EMHC =ROUK3(1,1) *2.
DO 2222 N=1,NN
RUK3(N)=ROUK3(N,1)&ROUK3(N,2)
DUM(N)=RUK3(N)*RO(N)
2222 CONTINUE
CALL MINT (NN,RO ,DUM ,EMHC)
EMHC=EMHC*3.1416/144.
ERMH=EMHC-EMHI
IF (ABS(ERMH)-.001*EMHI) 7561,7561,7553
7553 IF (ITM) 7554,7554,7555
7554 DP=(PX-PI)*.1
PIS=PI
ERMHS=ERMH
ITM=1
DERHP=0.
GO TO 7556
7555 DERHP=(ERMH-ERMHS)/(PI-PIS)
DP=-ERMH/DERHP
329 IF (ABS(DP/PIS)-.5) 328,328,330
330 DP=CT*DP
CT=CT/2.
GO TO 329
328 PIS=PI
ERMHS=ERMH
ITM=ITM&1
7556 IF (ITM-20) 7558,7558,7557
7558 CALL SSWTCH(3,KI)
IF (KI-2) 7559,7550,7550
7559 WRITE(3,407)ITM,PI,DERHP,DP,ERMH,PZ
GO TO 7550
7557 WRITE(3,40)
WRITE(3,27)EMHC
7561 PS=PI
WRITE(3,19) XO(M),PS
WRITE(3,20)
WRITE(3,26)
II=1
7564 DO 7562 N=1,NN
WRITE(3,21)RO(N),US(N,II),PTS(N,II),TTS(N,II),RHOS(N,II),
1CON1(N,II),CON2(N,II),CON3(N,II),VMS(N,II)
7562 CONTINUE
IF (II-1) 7563,7563,223
7563 II=2
VINJ=INJ
PHI1=3.1416/VINJ*57.296
WRITE(3,22)PHI1
GO TO 7564

```

```

223 CONTINUE
    WRITE(3,23)
    RETURN
    END

```

```

SUBROUTINE STATE(RUU,RUHT,RUK, HTH,U,P,T, RHO,VKK,VM,VPF)
C SUBROUTINE FOR AEROTHERM WET DIFFUSER MIXING PROGRAM
C THIS SUBROUTINE SOLVES THE MASS, MOMENTUM, AND ENTHALPY FLUXES SI-
C MULTANEOUSLY TO DETERMINE LOCAL STAGNATION PRESSURE, STAGNATION
C TEMPERATURE, DENSITY, MASS CONCENTRATIONS OF LIQUID WATER, VAPOR
C WATER, AND HYDROGEN, AND LOCAL MACH NUMBER (FOR TWO PHASE FLOW
C WHERE APPROPRIATE). THESE RESULTS ARE OBTAINED FOR AN ASSUMED
C PRESSURE WHICH IS MODIFIED AS NECESSARY IN EITHER OUTCL OR OUTR
C TO SATISFY HYDROGEN CONTINUITY
    DIMENSION VKK(3),H(3),CP(3),S(3)
    COMMON BIZ(458)
    COMMON RB(3,2),RC(3,2),RD(3,2),RE(3,2),RF(3,2),WW,WH,A9,RHOL
    2 FORMAT (2X,6E10.3)
8900 FORMAT(4H ITS2X1HT9X3HDLT7X5HERROR5X6HDERLNT4X3HRHO7X3HPM17X3HPM27
1X3HP2A7X3HP2E)
8901 FORMAT(I3,10E10.3)
C SENSE SWITCH 4 STATEMENT NUMBER 13,410,25
    LM=0
    TS=T
    CT=.25
    13 CALL SSWTCH(4,KI)
    IF(KI-2) 121,131,131
121 WRITE(3,2)RUU,RUHT,RUK,HTH,P,VPF
131 ITS=0
    CSQ=RUK/RUU*RUK*4.4757
    R=1.3146
    A4=CSQ*R
    A3=CSQ/RHOL
    A2=A4*P*WH
    A1=A4/2.*A9
    14 ITS=ITS&1
    PM2=T*(A1&SQRT(A1*A1&A2/T))
    P2A=PM2/WW
    VA=ALOG(T/3000.)
    VB=T-3000.
    VC=(T&3000.)/2.
    VD=3000.*T
    VE=VC/(VD*VD)
    RT=1.9869*T
    DO 17 I=1,3
    J=1
    IF(T-1000. ) 16,16,15
    15 J=2
    16 CP(I)=RC(I,J)&T*RD(I,J)&RE(I,J)/(T*T)
    H(I)=RB(I,J)&VB*(RC(I,J)&RD(I,J)*VC&RE(I,J)/VD)
    17 S(I)=RF(I,J)&RC(I,J)*VA&VB*(RD(I,J)&RE(I,J)*VE)
    P2E=VPF*EXP((H(1)-H(2))/RT&(S(2)-S(1))/1.9869)
    IF(P2A-P2E) 18,18,19
    18 P2=P2A

```

```

P1=0.
PM1=0.
P3=P-P2
PM3=P3*WH
GO TO 20
19 P2=P2E
PM2=P2*WW
P3=P-P2
PM3=P3*WH
A5=((2.-A3)*PM2-A4*T-A3*PM3)/2.
A6=PM2*PM2-A4*T*(PM2&PM3)
PM1=(-A5&SQRT(A5*A5-A6*(1.-A3)))/(1.-A3)
P1=PM1/WW
20 PM=PM1&PM2&PM3
RHO=PM/(R*T&PM1/RHOL)
VK=(PM1&PM2)/PM
A17=RUU/RHO*.10283
IF (A17) 221,221,222
221 U=0.
GO TO 25
222 U=SQRT(A17)
RHOU=RHO*U
HS=(P1*H(1)&P2*H(2)&P3*H(3))/PM
A19=HS&A17/2.-HTH
ERROR=RHOU*A19-RUHT*.6784
IF(LM-1) 400,403,403
400 ERRS=ERROR
DLT=.05
DERLT=0.
LM=1
GO TO 410
403 DERLT=(ERROR-ERRS)/DLT
IF(ERRS*ERROR) 497,497,498
497 CT=CT/2.
498 ERRS=ERROR
DLT=-ERROR/DERLT
IF (DLT) 500,500,502
500 IF(DLT&CT) 501,501,410
501 DLT=-CT
GO TO 410
502 IF(DLT-CT) 410,503,503
503 DLT=CT
410 CALL SSWTCH(4,KI)
IF(KI-2) 9001,9002,9002
9001 IF(ICZ-777) 9003,9004,9003
9003 WRITE(3,8900)
ICZ=777
9004 WRITE(3,8901)ITS,T,DLT,ERROR,DERLT ,RHO,PM1,PM2,
1P2A,P2E
9002 CONTINUE
T=T*EXP(DLT)
IF(ITS-30) 33,33,25
25 CALL SSWTCH(4,KI)
IF(KI-2) 24,26,26
26 P=0.
T=TS
VKK(1)=RUU
VKK(2)=RUHT

```

```

VKK(3)=RUK
GO TO 32
33 IF (PM1) 31,30,31
30 IF (ABS(DLT)-.0005) 24,24,14
31 IF(ABS(DLT)-.0001) 24,24,14
24 VKK(1)=PM1/PM
VKK(2)=PM2/PM
VKK(3)=PM3/PM
41 VK2M =VKK(2)/WW
VK3M=VKK(3)/WH
CPB=VK2M*CP(2)&VK3M*CP(3)
R=1.9869*(VK2M&VK3M)
GAM=1./(1.-R/CPB)
EN =VKK(1)/CPB
GAM = (GAM*(EN&1.))/(GAM* EN&1.)
ASQ=GAM*R*T
VMSQ=A17/ASQ
VM =SQRT(VMSQ)
TTOT=1.&(GAM-1.)*VMSQ/2.
T=T*TTOT*1.8
GAMX=GAM/(GAM-1.)
P=14.696*P*TTOT**GAMX
32 U=U*212.27
RETURN
END

```

```

SUBROUTINE CIRFC (R,R1,R2,TH,S1,S2,S3)
C SUBROUTINE FOR AEROTHERM WET DIFFUSER MIXING PROGRAM
C THIS SUBROUTINE CALCULATES ONE INCIDENT AND TWO REFLECTED RADIAL
C DISTANCES BETWEEN A SOURCE JET AND AN OUTPUT POINT, TO BE USED FOR
C DETERMINATION OF JET FLUX CONTRIBUTIONS
11 FORMAT(2X,I10,4(2X,E10.3))
15 FORMAT(2X,3HRD=,F10.3,3HRJ=,F10.3,2HR=,F10.3,3HTH=,E10.3,4HRAD.,23
1HREFLECTED DIST. INVALID)
C SENSE SWITCH 1 STATEMENT NUMBER 63
IF(R2) 31,31,32
31 S2=2.*R-R1
S3=2.*R&R1
GO TO 9
32 RR=R1/R2
IF(ABS(RR-1.)-.005) 70,70,71
70 R2=R1
RR=1.
71 ALP=0.
IT=0
A=SIN(TH)
B=COS(TH)
IF(R2-R1) 3,1,2
1 ALP=TH/2.
C=SIN(ALP)
D=COS(ALP)
GO TO 7
2 ALP=TH
3 ALPA=ATAN(R2*A/(R1&R2*B))

```

```

IF(ALPA) 21,21,4
21 ALPA=ALPA&3.141592
4 C=SIN(ALP)
D=COS(ALP)
F=1.-2.*C**2
G=C*D
H=2.*G*B-F*A
O=C*B-D*A
P=F*B&2.*G*A
Q=D*B&C*A
RZ=R1*H/(O&RR*C)
IF(ABS(RZ/R-1.)-.005) 7,7,5
5 DADR=R1/RZ*H/(2.*R1*P-RZ*Q-RZ*RR*D)
ALPP=DADR*(R-RZ)&ALP
IF((ALPP-ALPA)/(ALP-ALPA)-.25) 6,61,61
6 ALPP=.25*ALP&.75*ALPA
61 IT=IT&1
IF(IT-20) 63,63,64
63 CALL SSWTCH(1,KI)
IF(KI-2) 10,62,62
64 WRITE(3,15) R,R1,R2,TH
S2=2.*R
S3=S2
GO TO 9
10 WRITE(3,11) IT,ALP,ALPP,DADR,RZ
62 ALP=ALPP
GO TO 4
7 S3=SQRT((R*D-R1)**2&(R*C)**2)&SQRT((R*D-R2*B)**2&(R*C-R2*A)**2)
IT=0
IF(R) 9,9,8
8 R=-R
S2=S3
ALP=ALPA/2.&TH/4.
IF (R2-R1) 4,1,4
9 S1=SQRT((R2*B-R1)**2&(R2*A)**2)
R=ABS(R)
RETURN
END

```

```

SUBROUTINE MINT(N,X,Y,Z)
C SUBROUTINE FOR AEROTHERM WET DIFFUSER MIXING PROGRAM
C THIS SUBROUTINE PERFORMS INTEGRATIONS ACROSS THE FLOW FIELD WHEN
C REQUIRED IN SUMR2, AND WHEN REQUIRED IN EITHER OUTCL OR OUTR.
C IT IS AN ADAPTATION OF R.M.KENDALL'S SLOPQ
DIMENSION X(1),Y(1),S(11)
C SENSE SWITCH 5 STATEMENT NUMBER 10
S(2)=(Y(2)-Y(1))/(X(2)-X(1))
S(1)=S(2)
QC=S(2)
DO 7 I=1,N
IF(I&1-N)2,1,6
1 QB=QC
IF(I-2)7,6,5
2 XOT=X(I)-X(I&1)

```

CMIX

```
C AEROTHERM WET DIFFUSER MIXING PROGRAM----T.J.DAHM, 1967
COMMON EMJT,EMHI,TTJ,TTH,P2,D2,D1,UJ,UH,HTJ,HTH,PX,VPF,CMK,CMKSQ,
INN,KK,MM,INJ,ZB,BRATO,TSH,ROUH2,DROU2,DROUK,DROUH,A1,
2EMJC,DJC,RJC,DJCSQ,RD
COMMON RO(11),XO(8),DSY(11,8,2),DKSY(11,8,2),A(8,4),BUSQ(8),
1VKK(3),RJ(4),J(4),NJ(4)
COMMON RB(3,2),RC(3,2),RG(3,2),RE(3,2),RF(3,2),WW,WH,A9,RHOL
COMMON EZ(8),EW(8),Y2(8),SP(8),TP(8),YP(8)
CALL DEFIO(0,2,8)
CALL DEFIO(0,3,5)
C AEROTHERM WET DIFFUSER PROGRAM
CALL KEMD
100 CALL PREL
CALL FINAL
IF(EMJC) 205,205,2343
C CALCULATION FOR SINGLE JET ON CENTERLINE
2343 CALL SUMCL
IF (KK-1) 2344,2344,205
C OUTPUT FOR SINGLE JET ON CENTERLINE
2344 CALL OUTCL
GO TO 100
C EVEN JET CALCULATIONS , INCLUDING SUPERPOSITION OF CENTERLINE
205 CALL SUMR1
CALL SUMR2
C CALCULATION OF OUTPUT, EVEN JETS
CALL OUTR
GO TO 100
END
```

SUBROUTINE KEMD

```
C SUBROUTINE FOR AEROTHERM WET DIFFUSER MIXING PROGRAM
C THIS SUBROUTINE CONTAINS THERMOCHEMICAL CURVE FIT AND OTHER DATA
C AND PERFORMS CURVE FITS FOR STREAMLINE AND JET PENETRATION RESULTS
C FOR VARIABLE INLET PROFILE
DIMENSION Y1(8),XT(8)
COMMON EMJT,EMHI,TTJ,TTH,P2,D2,D1,UJ,UH,HTJ,HTH,PX,VPF,CMK,CMKSQ,
INN,KK,MM,INJ,ZB,BRATO,TSH,ROUH2,DROU2,DROUK,DROUH,A1,
2EMJC,DJC,RJC,DJCSQ,RD
COMMON RO(11),XO(8),DSY(11,8,2),DKSY(11,8,2),A(8,4),BUSQ(8),
1VKK(3),RJ(4),J(4),NJ(4)
COMMON RB(3,2),RC(3,2),RG(3,2),RE(3,2),RF(3,2),WW,WH,A9,RHOL
COMMON EZ(8),EW(8),Y2(8),SP(8),TP(8),YT(8)
11 RHOL=62.4
WH=2.016
WW=18.016
A9=1.0-WH/WW
RB(1,1)=-1.9698E&4
RB(1,2)=-1.9698E&4
RB(2,1)=-2.7089E&4
RB(2,2)=-2.7597E&4
RB(3,1)=2.0228E&4
RB(3,2)=2.121E&4
RC(1,1)=1.8016E&1
RC(1,2)=1.8016E&1
```

```

XTT=X(I&1)-X(I&2)
XTO=X(I&2)-X(I)
AA=Y(I)/(XOT*XTO)
XOTT=XOT*XTT
AB=Y(I&1)/XOTT
AC=Y(I&2)/(XTT*XTO)
AAA=AA*XTT
ABB=AB*XTO
ACC=AC*XOT
QA=QC
QB=S(I)
QC=S(I&1)
S(I)=AA*(XTO-XOT)&ABB-ACC
S(I&1)=AB*(XOT-XTT)&ACC-AAA
S(I&2)=AC*(XTT-XTO)&AAA-ABB
3 IF(I-2) 9,5,4
9 S(1)=Z
Z=0.
GO TO 10
4 S(I)=(S(I)&QA)/2.
5 S(I)=(S(I)&QB)/2.
6 XD=X(I)-X(I-1)
YS=Y(I)&Y(I-1)
SD=S(I)-S(I-1)
Z=Z&XD/2.*(YS-XD/6.*SD)
10 CALL SSWTCH(5,KI)
IF(KI-2) 11,7,7
11 WRITE(3,12) I,X(I),Y(I),Z,S(I)
12 FORMAT(2X,I2,4(1XE10.3))
7 CONTINUE
RETURN
END

```

FUNCTION ERF(X)

```

C THIS IS AN ANALYTICAL REPRESENTATION OF THE ERROR FUNCTION FROM
C NBS-AMS-55-ABSOLUTE ERROR LESS THAN .000025 - USED IN SUMCL
C OF THE AEROTHERM WET DIFFUSER MIXING PROGRAM
P=.47047
A1=.3480242
A2=-.0958798
A3=.7478556
T=1./(1.&P*X)
XSQ=X*X
ERF=1.-T*(A1&T*(A2&T*A3))*EXP(-XSQ)
RETURN
END

```


APPENDIX G

COMPUTED RESULTS FOR "REFERENCE CASE" OF FULL-SCALE
E/STS 2-3 PERFORMANCE PREDICTION ANALYSIS

MIXING INPUT FOR CASE NUMBER 2

D1 (IN.)	D2 (IN.)	XJ (IN.)	ALFM (DEG)	CW	INJ				
0.128+003	0.384+003	0.	0.880+002	0.136+001	0				
MDOT W	MDOT J	PT1 (PSIA)	PTJ (PSIA)	TTH (R)	TTJ (R)	M1	M2		
0.230+003	0.274+004	0.120+002	0.136+003	0.450+004	0.530+003	0.338+000	0.487+001		
P1 (PSIA)	PT2 (PSIA)	PR (PSIA)	WJ (FT/SEC)	WJH (FT/SEC)	MIX-CM	MIX-CMK	VAP PRES		
0.111+002	0.113+002	0.113+002	0.136+003	0.807+003	0.750+001	0.100+001	0.100+001		

WATER PENETRATES CENTERLINE

JET DATA

NJ	MDOTJ (LB/SEC)	JET DIAM (IN)	JET RAD. (IN)	AZIMUTH (DEG)
96	0.279+003	0.250+000	0.150+003	0.
72	0.836+003	0.500+000	0.119+003	0.
6	0.218+003	0.884+000	0.351+002	0.
1	0.141+003	0.551+001	0.	0.

CONDITIONS AFTER COMPLETE MIXING

P (PSIA)	U (FT/SEC)	PT (PSIA)	T TOT (R)	RO (LB/FT3)	K H2O LIQ	K H2O VAP	K H2	MACH NO.
0.112+002	0.262+003	0.113+002	0.829+003	0.141+001	0.	0.923+000	0.774+001	0.118+000
X= 50.000 INCHES		PHI=0 DEGREES		P= 11.270 PSIA				

R (IN.)	U (FT/SEC)	PT (PSIA)	T TOT (R)	RO (LB/FT3)	K H2O LIQ	K H2O VAP	K H2	MACH NO.
0.	0.136+003	0.524+007	0.555+003	0.337+002	0.100+001	0.299+004	0.488+004	0.511+001
0.192+002	0.646+003	0.113+002	0.449+004	0.471+003	0.	0.611+005	0.100+001	0.538+001
0.384+002	0.139+003	0.121+002	0.615+003	0.394+000	0.969+000	0.255+001	0.584+002	0.538+000
0.576+002	0.646+003	0.113+002	0.449+004	0.471+003	0.	0.901+013	0.100+001	0.538+001
0.768+002	0.646+003	0.113+002	0.449+004	0.471+003	0.	0.824+051	0.100+001	0.538+001
0.960+002	0.646+003	0.113+002	0.449+004	0.471+003	0.	0.197+013	0.100+001	0.538+001
0.115+003	0.146+003	0.113+002	0.633+003	0.114+000	0.853+000	0.132+000	0.144+001	0.213+000
0.134+003	0.646+003	0.113+002	0.449+004	0.471+003	0.	0.321+005	0.100+001	0.538+001
0.154+003	0.175+003	0.113+002	0.641+003	0.246+001	0.231+000	0.714+000	0.544+001	0.109+000
0.173+003	0.646+003	0.113+002	0.449+004	0.471+003	0.	0.448+014	0.100+001	0.538+001
0.192+003	0.646+003	0.113+002	0.449+004	0.471+003	0.	0.512+052	0.100+001	0.538+001
PHI= 30.00 DEGREES								
0.	0.136+003	0.524+007	0.555+003	0.337+002	0.100+001	0.299+004	0.488+004	0.511+001
0.192+002	0.646+003	0.113+002	0.449+004	0.471+003	0.	0.623+007	0.100+001	0.538+001
0.384+002	0.646+003	0.113+002	0.449+004	0.471+003	0.	0.251+008	0.100+001	0.538+001
0.576+002	0.646+003	0.113+002	0.449+004	0.471+003	0.	0.335+029	0.100+001	0.538+001
0.768+002	0.646+003	0.113+002	0.449+004	0.471+003	0.	0.123+051	0.100+001	0.538+001
0.960+002	0.646+003	0.113+002	0.449+004	0.471+003	0.	0.197+013	0.100+001	0.538+001
0.115+003	0.146+003	0.113+002	0.633+003	0.114+000	0.853+000	0.132+000	0.144+001	0.213+000
0.134+003	0.646+003	0.113+002	0.449+004	0.471+003	0.	0.321+005	0.100+001	0.538+001
0.154+003	0.175+003	0.113+002	0.641+003	0.246+001	0.231+000	0.714+000	0.544+001	0.109+000
0.173+003	0.646+003	0.113+002	0.449+004	0.471+003	0.	0.448+014	0.100+001	0.538+001
0.192+003	0.646+003	0.113+002	0.449+004	0.471+003	0.	0.512+052	0.100+001	0.538+001
PHI= 30.00 DEGREES								
X= 100.000 INCHES		P= 11.264 PSIA						

R (IN.)	U (FT/SEC)	PT (PSIA)	T TOT (R)	RO (LB/FT3)	K H2O LIQ	K H2O VAP	K H2	MACH NO.
0.	0.137+003	0.640+002	0.559+003	0.842+001	0.999+000	0.255+003	0.360+003	0.186+001
0.192+002	0.227+003	0.113+002	0.114+004	0.955+002	0.	0.907+000	0.930+001	0.842+001
0.384+002	0.144+003	0.117+002	0.629+003	0.121+000	0.908+000	0.810+001	0.106+001	0.258+000
0.576+002	0.687+003	0.113+002	0.448+004	0.477+003	0.	0.111+001	0.989+000	0.576+001
0.768+002	0.691+003	0.113+002	0.449+004	0.471+003	0.	0.487+011	0.100+001	0.575+001
0.960+002	0.689+003	0.113+002	0.449+004	0.473+003	0.	0.466+002	0.999+000	0.575+001
0.115+003	0.155+003	0.113+002	0.637+003	0.667+001	0.732+000	0.246+000	0.223+001	0.171+000
0.134+003	0.552+003	0.113+002	0.401+004	0.818+003	0.	0.399+000	0.601+000	0.606+001
0.154+003	0.206+003	0.113+002	0.857+003	0.136+001	0.	0.921+000	0.787+001	0.907+001
0.173+003	0.690+003	0.113+002	0.449+004	0.472+003	0.	0.102+002	0.999+000	0.575+001
0.192+003	0.691+003	0.113+002	0.449+004	0.471+003	0.	0.535+012	0.100+001	0.575+001
PHI= 30.00 DEGREES								
0.	0.137+003	0.640+002	0.559+003	0.842+001	0.999+000	0.255+003	0.360+003	0.186+001
0.192+002	0.243+003	0.113+002	0.135+004	0.765+002	0.	0.895+000	0.103+000	0.808+001
0.384+002	0.623+003	0.113+002	0.429+004	0.606+003	0.	0.210+000	0.790+000	0.589+001
0.576+002	0.691+003	0.113+002	0.449+004	0.471+003	0.	0.147+005	0.100+001	0.575+001
0.768+002	0.691+003	0.113+002	0.449+004	0.471+003	0.	0.146+011	0.100+001	0.575+001
0.960+002	0.689+003	0.113+002	0.449+004	0.473+003	0.	0.466+002	0.999+000	0.575+001
0.115+003	0.155+003	0.113+002	0.637+003	0.667+001	0.732+000	0.246+000	0.223+001	0.171+000
0.134+003	0.552+003	0.113+002	0.401+004	0.818+003	0.	0.399+000	0.601+000	0.606+001
0.154+003	0.206+003	0.113+002	0.857+003	0.136+001	0.	0.921+000	0.787+001	0.907+001
0.173+003	0.690+003	0.113+002	0.449+004	0.472+003	0.	0.102+002	0.999+000	0.575+001
0.192+003	0.691+003	0.113+002	0.449+004	0.471+003	0.	0.535+012	0.100+001	0.575+001

X= 200.000 INCHES

PR 11.244 PSIA

PHI=0 DEGREES

R (IN.)	U (FT/SEC)	PT (PSIA)	T TOT (R)	RO (LB/FT ³)	K H2O LIQ	K H2O VAP	K H2	MACH NO.
0.	0.137+003	0.166+002	0.575+003	0.210+001	0.977+000	0.175+002	0.150+002	0.885+000
0.192+002	0.141+003	0.122+002	0.613+003	0.417+000	0.971+000	0.234+001	0.560+002	0.399+000
0.384+002	0.173+003	0.114+002	0.639+003	0.446+001	0.987+000	0.381+000	0.316+001	0.154+000
0.576+002	0.419+003	0.119+002	0.271+004	0.243+002	0.	0.769+000	0.232+000	0.794+001
0.768+002	0.819+003	0.113+002	0.448+004	0.479+003	0.	0.164+001	0.984+000	0.688+001
0.960+002	0.441+003	0.113+002	0.288+004	0.214+002	0.	0.739+000	0.261+000	0.783+001
0.115+003	0.183+003	0.114+002	0.640+003	0.334+001	0.441+000	0.519+000	0.410+001	0.138+000
0.134+003	0.244+003	0.113+002	0.102+004	0.110+001	0.	0.913+000	0.866+001	0.969+001
0.154+003	0.303+003	0.113+002	0.165+004	0.574+002	0.	0.875+000	0.125+000	0.876+001
0.173+003	0.696+003	0.113+002	0.415+004	0.704+003	0.	0.312+000	0.688+000	0.709+001
0.192+003	0.824+003	0.113+002	0.449+004	0.472+003	0.	0.303+002	0.997+000	0.687+001

PHI= 30.00 DEGREES

0.	0.137+003	0.166+002	0.575+003	0.210+001	0.977+000	0.175+002	0.150+002	0.885+000
0.192+002	0.141+003	0.122+002	0.613+003	0.413+000	0.971+000	0.237+001	0.563+002	0.397+000
0.384+002	0.218+003	0.113+002	0.744+003	0.160+001	0.	0.926+000	0.736+001	0.104+000
0.576+002	0.705+003	0.119+002	0.419+004	0.682+003	0.	0.292+000	0.708+000	0.707+001
0.768+002	0.822+003	0.113+002	0.449+004	0.475+003	0.	0.863+002	0.951+000	0.687+001
0.960+002	0.441+003	0.113+002	0.288+004	0.214+002	0.	0.739+000	0.261+000	0.783+001
0.115+003	0.183+003	0.114+002	0.640+003	0.334+001	0.441+000	0.519+000	0.410+001	0.138+000
0.134+003	0.244+003	0.113+002	0.102+004	0.110+001	0.	0.913+000	0.866+001	0.969+001
0.154+003	0.303+003	0.113+002	0.165+004	0.574+002	0.	0.875+000	0.125+000	0.876+001
0.173+003	0.696+003	0.113+002	0.415+004	0.704+003	0.	0.312+000	0.688+000	0.709+001
0.192+003	0.824+003	0.113+002	0.449+004	0.472+003	0.	0.303+002	0.997+000	0.687+001

X= 300.000 INCHES

PR 11.236 PSIA

PHI=0 DEGREES

R (IN.)	U (FT/SEC)	PT (PSIA)	T TOT (R)	RO (LB/FT ³)	K H2O LIQ	K H2O VAP	K H2	MACH NO.
0.	0.139+003	0.134+002	0.593+003	0.934+000	0.991+000	0.636+002	0.304+002	0.592+000
0.192+002	0.142+003	0.123+002	0.611+003	0.460+000	0.975+000	0.201+001	0.521+002	0.421+000
0.384+002	0.169+003	0.114+002	0.637+003	0.644+001	0.723+000	0.254+000	0.229+001	0.182+000
0.576+002	0.346+003	0.113+002	0.185+004	0.484+002	0.	0.860+000	0.140+000	0.920+001
0.768+002	0.689+003	0.113+002	0.393+004	0.882+003	0.	0.440+000	0.590+000	0.787+001
0.960+002	0.323+003	0.113+002	0.163+004	0.583+002	0.	0.876+000	0.124+000	0.940+001
0.115+003	0.214+003	0.113+002	0.641+003	0.206+001	0.795+001	0.856+000	0.641+001	0.118+000
0.134+003	0.242+003	0.113+002	0.858+003	0.135+001	0.	0.921+000	0.788+001	0.107+000
0.154+003	0.357+003	0.113+002	0.195+004	0.443+002	0.	0.851+000	0.149+000	0.912+001
0.173+003	0.628+003	0.113+002	0.369+004	0.110+002	0.	0.539+000	0.461+000	0.801+001
0.192+003	0.847+003	0.113+002	0.438+004	0.545+003	0.	0.129+000	0.871+000	0.760+001

PHI= 30.00 DEGREES

0.	0.139+003	0.134+002	0.593+003	0.934+000	0.991+000	0.636+002	0.304+002	0.592+000
0.192+002	0.142+003	0.123+002	0.611+003	0.460+000	0.975+000	0.201+001	0.522+002	0.421+000
0.384+002	0.170+003	0.114+002	0.637+003	0.610+001	0.706+000	0.270+000	0.240+001	0.179+000
0.576+002	0.413+003	0.113+002	0.242+004	0.506+002	0.	0.804+000	0.196+000	0.877+001
0.768+002	0.726+003	0.113+002	0.405+004	0.779+003	0.	0.374+000	0.626+000	0.780+001
0.960+002	0.323+003	0.113+002	0.164+004	0.582+002	0.	0.876+000	0.124+000	0.940+001
0.115+003	0.214+003	0.113+002	0.641+003	0.206+001	0.795+001	0.856+000	0.641+001	0.118+000
0.134+003	0.242+003	0.113+002	0.858+003	0.135+001	0.	0.921+000	0.788+001	0.107+000
0.154+003	0.357+003	0.113+002	0.195+004	0.443+002	0.	0.851+000	0.149+000	0.912+001
0.173+003	0.628+003	0.113+002	0.369+004	0.110+002	0.	0.539+000	0.461+000	0.801+001
0.192+003	0.847+003	0.113+002	0.438+004	0.545+003	0.	0.129+000	0.871+000	0.760+001

X# 400.000 INCHES
PHI#0 DEGREES

P# 11.219 PSIA

R (IN.)	U (FT/SEC)	PT (PSIA)	T TOT (K) (R) (LB/FT3)	K H2O LIQ	K H2O VAP	K H2	MACH NO.	
0.	0.142+003	0.124+002	0.607+003	0.529+000	0.979+000	0.161+001	0.470+002	0.493+000
0.192+002	0.144+003	0.120+002	0.617+003	0.354+000	0.964+000	0.298+001	0.627+002	0.376+000
0.364+002	0.161+003	0.113+002	0.634+003	0.105+000	0.939+000	0.146+000	0.153+001	0.223+000
0.576+002	0.258+003	0.113+002	0.874+003	0.132+001	0.	0.921+000	0.794+001	0.113+000
0.768+002	0.478+003	0.113+002	0.263+004	0.255+002	0.	0.774+000	0.226+000	0.929+001
0.960+002	0.324+003	0.113+002	0.143+004	0.693+002	0.	0.889+000	0.111+000	0.103+000
0.115+003	0.253+003	0.113+002	0.829+003	0.141+001	0.	0.923+000	0.773+001	0.114+000
0.134+003	0.272+003	0.113+002	0.995+003	0.113+001	0.	0.915+000	0.854+001	0.110+000
0.154+003	0.380+003	0.113+002	0.193+004	0.453+002	0.	0.854+000	0.146+000	0.980+001
0.173+003	0.618+003	0.113+002	0.343+004	0.138+002	0.	0.623+000	0.377+000	0.863+001
0.192+003	0.800+003	0.113+002	0.409+004	0.754+003	0.	0.359+000	0.645+000	0.846+001

PHI# 30.00 DEGREES

0.	0.142+003	0.124+002	0.607+003	0.529+000	0.979+000	0.161+001	0.470+002	0.493+000
0.192+002	0.144+003	0.120+002	0.617+003	0.354+000	0.964+000	0.298+001	0.627+002	0.376+000
0.364+002	0.161+003	0.113+002	0.634+003	0.105+000	0.938+000	0.146+000	0.154+001	0.223+000
0.576+002	0.262+003	0.113+002	0.907+003	0.127+001	0.	0.919+000	0.811+001	0.112+000
0.768+002	0.492+003	0.113+002	0.274+004	0.238+002	0.	0.791+000	0.259+000	0.924+001
0.960+002	0.324+003	0.113+002	0.143+004	0.688+002	0.	0.889+000	0.111+000	0.103+000
0.115+003	0.253+003	0.113+002	0.829+003	0.141+001	0.	0.923+000	0.773+001	0.114+000
0.134+003	0.272+003	0.113+002	0.995+003	0.113+001	0.	0.915+000	0.854+001	0.110+000
0.154+003	0.380+003	0.113+002	0.193+004	0.453+002	0.	0.854+000	0.146+000	0.980+001
0.173+003	0.618+003	0.113+002	0.343+004	0.138+002	0.	0.623+000	0.377+000	0.863+001
0.192+003	0.800+003	0.113+002	0.409+004	0.754+003	0.	0.359+000	0.645+000	0.846+001

X# 600.000 INCHES

P# 11.192 PSIA

PHI#0 DEGREES

R (IN.)	U (FT/SEC)	PT (PSIA)	T TOT (K) (R) (LB/FT3)	K H2O LIQ	K H2O VAP	K H2	MACH NO.	
0.	0.151+003	0.118+002	0.624+003	0.232+000	0.937+000	0.541+001	0.845+002	0.317+000
0.192+002	0.154+003	0.117+002	0.627+003	0.192+000	0.921+000	0.694+001	0.969+002	0.293+000
0.364+002	0.165+003	0.115+002	0.633+003	0.108+000	0.944+000	0.141+000	0.150+001	0.234+000
0.576+002	0.199+003	0.114+002	0.639+003	0.410+001	0.952+000	0.414+000	0.339+001	0.168+000
0.768+002	0.273+003	0.113+002	0.853+003	0.136+001	0.	0.921+000	0.786+001	0.120+000
0.960+002	0.323+003	0.113+002	0.125+004	0.840+002	0.	0.901+000	0.992+001	0.113+000
0.115+003	0.320+003	0.113+002	0.123+004	0.861+002	0.	0.902+000	0.979+001	0.113+000
0.134+003	0.341+003	0.113+002	0.140+004	0.727+002	0.	0.892+000	0.108+000	0.111+000
0.154+003	0.418+003	0.113+002	0.198+004	0.432+002	0.	0.849+000	0.151+000	0.109+000
0.173+003	0.558+003	0.113+002	0.288+004	0.213+002	0.	0.739+000	0.261+000	0.993+001
0.192+003	0.652+003	0.113+002	0.334+004	0.148+002	0.	0.646+000	0.354+000	0.967+001

PHI# 30.00 DEGREES

0.	0.151+003	0.118+002	0.624+003	0.232+000	0.937+000	0.541+001	0.845+002	0.317+000
0.192+002	0.154+003	0.117+002	0.627+003	0.192+000	0.921+000	0.694+001	0.969+002	0.293+000
0.364+002	0.165+003	0.115+002	0.633+003	0.108+000	0.944+000	0.141+000	0.150+001	0.234+000
0.576+002	0.199+003	0.114+002	0.639+003	0.410+001	0.952+000	0.414+000	0.339+001	0.168+000
0.768+002	0.273+003	0.113+002	0.857+003	0.135+001	0.	0.921+000	0.787+001	0.120+000
0.960+002	0.324+003	0.113+002	0.126+004	0.838+002	0.	0.901+000	0.994+001	0.113+000
0.115+003	0.321+003	0.113+002	0.123+004	0.860+002	0.	0.902+000	0.980+001	0.113+000
0.134+003	0.341+003	0.113+002	0.140+004	0.727+002	0.	0.892+000	0.108+000	0.111+000
0.154+003	0.418+003	0.113+002	0.198+004	0.431+002	0.	0.849+000	0.151+000	0.109+000
0.173+003	0.558+003	0.113+002	0.288+004	0.213+002	0.	0.739+000	0.261+000	0.993+001
0.192+003	0.652+003	0.113+002	0.334+004	0.148+002	0.	0.646+000	0.354+000	0.967+001

X= 800.000 INCHES

Pr 11.190 PMA

PHI=0 DEGREES

R (IN.)	U (FT/SEC)	PT (PMA)	T TOT (R)	NO(LB/FT3)	K H2O LIQ	K H2O VAP	K H2	MACH NO.
0.	0.162+003	0.115+002	0.632+003	0.126+000	0.869+000	0.117+000	0.133+001	0.290+000
0.192+002	0.165+003	0.115+002	0.633+003	0.113+000	0.852+000	0.134+000	0.149+001	0.290+000
0.364+002	0.174+003	0.115+002	0.636+003	0.816+001	0.767+000	0.195+000	0.188+001	0.214+000
0.576+002	0.193+003	0.114+002	0.638+003	0.483+001	0.623+000	0.347+000	0.294+001	0.179+000
0.768+002	0.228+003	0.113+002	0.641+003	0.252+001	0.554+000	0.663+000	0.530+001	0.149+000
0.960+002	0.278+003	0.113+002	0.664+003	0.134+001	0.	0.921+000	0.790+001	0.122+000
0.115+003	0.329+003	0.113+002	0.125+004	0.840+002	0.	0.901+000	0.992+001	0.115+000
0.134+003	0.376+003	0.113+002	0.161+004	0.591+002	0.	0.878+000	0.122+000	0.110+000
0.154+003	0.435+003	0.113+002	0.205+004	0.407+002	0.	0.842+000	0.158+000	0.107+000
0.173+003	0.507+003	0.113+002	0.252+004	0.281+002	0.	0.792+000	0.208+000	0.104+000
0.192+003	0.545+003	0.113+002	0.274+004	0.237+002	0.	0.761+000	0.239+000	0.102+000

PHI= 30.00 DEGREES

0.	0.162+003	0.115+002	0.632+003	0.126+000	0.869+000	0.117+000	0.133+001	0.290+000
0.192+002	0.165+003	0.115+002	0.633+003	0.113+000	0.852+000	0.134+000	0.149+001	0.290+000
0.364+002	0.174+003	0.115+002	0.636+003	0.816+001	0.767+000	0.195+000	0.188+001	0.214+000
0.576+002	0.193+003	0.114+002	0.638+003	0.483+001	0.623+000	0.347+000	0.294+001	0.179+000
0.768+002	0.228+003	0.113+002	0.641+003	0.252+001	0.554+000	0.663+000	0.530+001	0.149+000
0.960+002	0.278+003	0.113+002	0.664+003	0.134+001	0.	0.921+000	0.790+001	0.122+000
0.115+003	0.329+003	0.113+002	0.125+004	0.840+002	0.	0.901+000	0.992+001	0.115+000
0.134+003	0.376+003	0.113+002	0.162+004	0.591+002	0.	0.878+000	0.122+000	0.110+000
0.154+003	0.435+003	0.113+002	0.205+004	0.407+002	0.	0.842+000	0.158+000	0.107+000
0.173+003	0.507+003	0.113+002	0.252+004	0.281+002	0.	0.792+000	0.208+000	0.104+000
0.192+003	0.545+003	0.113+002	0.274+004	0.237+002	0.	0.761+000	0.239+000	0.102+000

X= 1000.000 INCHES

Pr 11.189 PMA

PHI=0 DEGREES

R (IN.)	U (FT/SEC)	PT (PMA)	T TOT (R)	NO(LB/FT3)	K H2O LIQ	K H2O VAP	K H2	MACH NO.
0.	0.175+003	0.115+002	0.636+003	0.786+001	0.778+000	0.203+000	0.194+001	0.211+000
0.192+002	0.178+003	0.114+002	0.636+003	0.734+001	0.761+000	0.219+000	0.205+001	0.206+000
0.364+002	0.185+003	0.114+002	0.637+003	0.601+001	0.702+000	0.274+000	0.243+001	0.193+000
0.576+002	0.199+003	0.114+002	0.639+003	0.435+001	0.679+000	0.389+000	0.323+001	0.174+000
0.768+002	0.221+003	0.113+002	0.640+003	0.284+001	0.643+000	0.610+000	0.473+001	0.151+000
0.960+002	0.255+003	0.113+002	0.666+003	0.176+001	0.	0.929+000	0.710+001	0.128+000
0.115+003	0.304+003	0.113+002	0.105+004	0.105+001	0.	0.912+000	0.884+001	0.118+000
0.134+003	0.362+003	0.113+002	0.150+004	0.659+002	0.	0.886+000	0.114+000	0.112+000
0.154+003	0.421+003	0.113+002	0.194+004	0.448+002	0.	0.853+000	0.147+000	0.108+000
0.173+003	0.471+003	0.113+002	0.228+004	0.340+002	0.	0.820+000	0.180+000	0.106+000
0.192+003	0.492+003	0.113+002	0.241+004	0.306+002	0.	0.805+000	0.199+000	0.105+000

PHI= 30.00 DEGREES

0.	0.175+003	0.115+002	0.636+003	0.786+001	0.778+000	0.203+000	0.194+001	0.211+000
0.192+002	0.178+003	0.114+002	0.636+003	0.734+001	0.761+000	0.219+000	0.205+001	0.206+000
0.364+002	0.185+003	0.114+002	0.637+003	0.601+001	0.702+000	0.274+000	0.243+001	0.193+000
0.576+002	0.199+003	0.114+002	0.639+003	0.435+001	0.679+000	0.389+000	0.323+001	0.174+000
0.768+002	0.221+003	0.113+002	0.640+003	0.284+001	0.643+000	0.610+000	0.473+001	0.151+000
0.960+002	0.255+003	0.113+002	0.666+003	0.176+001	0.	0.929+000	0.710+001	0.128+000
0.115+003	0.304+003	0.113+002	0.105+004	0.105+001	0.	0.912+000	0.884+001	0.118+000
0.134+003	0.362+003	0.113+002	0.150+004	0.659+002	0.	0.886+000	0.114+000	0.112+000
0.154+003	0.421+003	0.113+002	0.194+004	0.448+002	0.	0.853+000	0.147+000	0.108+000
0.173+003	0.471+003	0.113+002	0.228+004	0.340+002	0.	0.820+000	0.180+000	0.106+000
0.192+003	0.492+003	0.113+002	0.241+004	0.306+002	0.	0.805+000	0.199+000	0.105+000

APPENDIX H

COMPUTED RESULTS FOR "MODIFIED DESIGN"
CASE OF FULL-SCALE E/STS 2-3
PERFORMANCE PREDICTION ANALYSIS

MIXING INPUT FOR CASE NUMBER 5									
D1 (IN.)	D2 (IN.)	XJ (IN.)	ALFM (DEG)	CM	LNJ				
0.126+003	0.384+003	0.	0.890+002	0.049+000	4				
MDOT H	MDOT J	PT1 (PSIA)	PTJ (PSIA)	TIM (R)	TIJ (R)	M1	M2		
0.230+003	0.274+004	0.151+002	0.359+002	0.450+004	0.230+003	0.081+000	0.477+001		
P1 (PSIA)	PT2 (PSIA)	P2 (PSIA)	UJ (FT/SEC)	UH (FT/SEC)	MIX-CM	MIX-CMK	VAP PRES		
0.111+002	0.115+002	0.115+002	0.688+002	0.294+003	0.720+001	0.100+001	0.100+001		

JET DATA

NJ	MDOTJ (LB/SEC)	JET DIAM (IN)	JET MAD. (IN)	ALMUTH (DEG)
264	0.136+004	0.829+000	0.161+003	0.
60	0.698+003	0.750+000	0.149+003	0.
4	0.681+003	0.287+001	0.020+002	0.

CONDITIONS AFTER COMPLETE MIXING									
P (PSIA)	U (FT/SEC)	PT (PSIA)	T TOT (R)	HO (LB/FT3)	K H2O LIO	K H2O VAP	K H2	MACH NO.	
0.114+002	0.258+003	0.115+002	0.830+003	0.143+001	0.	0.923+000	0.774+001	0.118+000	
X = 50.000 INCHES		P = 11.518 PSIA							
PHI = 0 DEGREES									

R (IN.)	U (FT/SEC)	PT (PSIA)	T TOT (R)	HO (LB/FT3)	K H2O LIO	K H2O VAP	K H2	MACH NO.
0.	0.655+003	0.115+002	0.449+004	0.482+003	0.	0.	0.100+001	0.545+001
0.192+002	0.655+003	0.115+002	0.449+004	0.482+003	0.	0.471+033	0.100+001	0.545+001
0.384+002	0.655+003	0.115+002	0.449+004	0.482+003	0.	0.111+013	0.100+001	0.545+001
0.576+002	0.621+002	0.125+002	0.574+003	0.226+001	0.997+000	0.139+000	0.844+000	0.464+000
0.768+002	0.655+003	0.115+002	0.449+004	0.482+003	0.	0.382+003	0.100+001	0.545+001
0.960+002	0.655+003	0.115+002	0.449+004	0.482+003	0.	0.331+032	0.100+001	0.545+001
0.115+003	0.655+003	0.115+002	0.449+004	0.482+003	0.	0.628+033	0.100+001	0.545+001
0.134+003	0.655+003	0.115+002	0.449+004	0.482+003	0.	0.319+004	0.100+001	0.545+001
0.154+003	0.816+002	0.116+002	0.634+003	0.116+000	0.853+000	0.133+000	0.144+001	0.119+000
0.173+003	0.652+003	0.115+002	0.449+004	0.485+003	0.	0.732+002	0.993+000	0.545+001
0.192+003	0.655+003	0.115+002	0.449+004	0.482+003	0.	0.613+027	0.100+001	0.545+001

PHI = 45.00 DEGREES									
R (IN.)	U (FT/SEC)	PT (PSIA)	T TOT (R)	HO (LB/FT3)	K H2O LIO	K H2O VAP	K H2	MACH NO.	
0.	0.655+003	0.115+002	0.449+004	0.482+003	0.	0.	0.100+001	0.545+001	
0.192+002	0.655+003	0.115+002	0.449+004	0.482+003	0.	0.274+074	0.100+001	0.545+001	
0.384+002	0.655+003	0.115+002	0.449+004	0.482+003	0.	0.188+056	0.100+001	0.545+001	
0.576+002	0.655+003	0.115+002	0.449+004	0.482+003	0.	0.220+061	0.100+001	0.545+001	
0.768+002	0.655+003	0.115+002	0.449+004	0.482+003	0.	0.	0.100+001	0.545+001	
0.960+002	0.655+003	0.115+002	0.449+004	0.482+003	0.	0.	0.100+001	0.545+001	
0.115+003	0.655+003	0.115+002	0.449+004	0.482+003	0.	0.443+034	0.100+001	0.545+001	
0.134+003	0.655+003	0.115+002	0.449+004	0.482+003	0.	0.127+005	0.100+001	0.545+001	
0.154+003	0.213+003	0.115+002	0.161+004	0.610+002	0.	0.878+000	0.122+000	0.625+001	
0.173+003	0.652+003	0.115+002	0.449+004	0.485+003	0.	0.732+002	0.993+000	0.545+001	
0.192+003	0.655+003	0.115+002	0.449+004	0.482+003	0.	0.613+027	0.100+001	0.545+001	

PHI = 0 DEGREES									
R (IN.)	U (FT/SEC)	PT (PSIA)	T TOT (R)	HO (LB/FT3)	K H2O LIO	K H2O VAP	K H2	MACH NO.	
0.	0.801+003	0.115+002	0.449+004	0.481+003	0.	0.382+020	0.100+001	0.667+001	
0.192+002	0.801+003	0.115+002	0.449+004	0.481+003	0.	0.239+011	0.100+001	0.667+001	
0.384+002	0.793+003	0.115+002	0.448+004	0.490+003	0.	0.179+001	0.982+000	0.667+001	
0.576+002	0.637+002	0.122+002	0.581+003	0.155+001	0.995+000	0.287+002	0.202+002	0.347+000	
0.768+002	0.158+003	0.115+002	0.648+003	0.192+001	0.	0.931+000	0.694+001	0.817+001	
0.960+002	0.801+003	0.115+002	0.449+004	0.481+003	0.	0.428+000	0.100+001	0.667+001	
0.115+003	0.801+003	0.115+002	0.449+004	0.481+003	0.	0.339+007	0.100+001	0.667+001	
0.134+003	0.608+003	0.115+002	0.397+004	0.871+003	0.	0.421+000	0.579+000	0.682+001	
0.154+003	0.846+002	0.116+002	0.631+003	0.148+000	0.889+000	0.991+001	0.120+001	0.139+000	
0.173+003	0.273+003	0.115+002	0.181+004	0.213+002	0.	0.863+000	0.137+000	0.738+001	
0.192+003	0.801+003	0.115+002	0.449+004	0.481+003	0.	0.272+003	0.100+001	0.667+001	

PHI = 45.00 DEGREES									
R (IN.)	U (FT/SEC)	PT (PSIA)	T TOT (R)	HO (LB/FT3)	K H2O LIO	K H2O VAP	K H2	MACH NO.	
0.	0.801+003	0.115+002	0.449+004	0.481+003	0.	0.382+020	0.100+001	0.667+001	
0.192+002	0.801+003	0.115+002	0.449+004	0.481+003	0.	0.214+010	0.100+001	0.667+001	
0.384+002	0.801+003	0.115+002	0.449+004	0.481+003	0.	0.617+012	0.100+001	0.667+001	
0.576+002	0.801+003	0.115+002	0.449+004	0.481+003	0.	0.361+013	0.100+001	0.667+001	
0.768+002	0.801+003	0.115+002	0.449+004	0.481+003	0.	0.428+020	0.100+001	0.667+001	
0.960+002	0.801+003	0.115+002	0.449+004	0.481+003	0.	0.503+020	0.100+001	0.667+001	
0.115+003	0.801+003	0.115+002	0.449+004	0.481+003	0.	0.323+007	0.100+001	0.667+001	
0.134+003	0.654+003	0.115+002	0.412+004	0.744+003	0.	0.332+000	0.668+000	0.678+001	
0.154+003	0.903+002	0.116+002	0.634+003	0.112+000	0.847+000	0.139+000	0.148+001	0.129+000	
0.173+003	0.273+003	0.115+002	0.181+004	0.213+002	0.	0.863+000	0.137+000	0.738+001	
0.192+003	0.801+003	0.115+002	0.449+004	0.481+003	0.	0.272+003	0.100+001	0.667+001	

X= 200.000 INCHES P= 11.475 PSIA

PHI=0 DEGREES

R (IN.)	U (FT/SEC)	PT (PSIA)	T TOT (K)	MO (LB/FT3)	K M2U LIQ	K M2U VAP	K M2	MACH NO.
0.	0.928+003	0.115+002	0.449+004	0.480+003	0.	0.117+004	0.100+001	0.773+001
0.192+002	0.918+003	0.115+002	0.448+004	0.492+003	0.	0.224+001	0.978+000	0.774+001
0.384+002	0.186+003	0.115+002	0.728+003	0.168+001	0.	0.927+000	0.729+001	0.909+001
0.576+002	0.733+002	0.117+002	0.613+003	0.437+000	0.772+000	0.229+001	0.530+002	0.210+000
0.768+002	0.922+002	0.115+002	0.631+003	0.148+000	0.887+000	0.181+000	0.121+001	0.149+000
0.960+002	0.743+003	0.115+002	0.489+004	0.771+003	0.	0.389+000	0.849+000	0.785+001
0.115+003	0.898+003	0.115+002	0.444+004	0.215+003	0.	0.639+001	0.936+000	0.775+001
0.134+003	0.242+003	0.115+002	0.120+004	0.210+002	0.	0.904+000	0.962+001	0.870+001
0.154+003	0.103+003	0.116+002	0.635+003	0.941+001	0.815+000	0.170+000	0.170+001	0.134+000
0.173+003	0.154+003	0.115+002	0.641+003	0.280+001	0.316+000	0.635+000	0.490+001	0.103+000
0.192+003	0.755+003	0.115+002	0.412+004	0.746+003	0.	0.335+000	0.665+000	0.784+001

PHI= 49.00 DEGREES

0.	0.928+003	0.115+002	0.449+004	0.480+003	0.	0.117+004	0.100+001	0.773+001
0.192+002	0.927+003	0.115+002	0.449+004	0.481+003	0.	0.204+002	0.998+000	0.773+001
0.384+002	0.916+003	0.115+002	0.447+004	0.494+003	0.	0.262+001	0.974+000	0.774+001
0.576+002	0.922+003	0.115+002	0.448+004	0.487+003	0.	0.130+001	0.987+000	0.774+001
0.768+002	0.928+003	0.115+002	0.449+004	0.480+003	0.	0.243+003	0.100+001	0.773+001
0.960+002	0.928+003	0.115+002	0.449+004	0.480+003	0.	0.431+004	0.100+001	0.773+001
0.115+003	0.898+003	0.115+002	0.444+004	0.215+003	0.	0.630+001	0.936+000	0.775+001
0.134+003	0.242+003	0.115+002	0.120+004	0.210+002	0.	0.904+000	0.962+001	0.870+001
0.154+003	0.103+003	0.116+002	0.635+003	0.940+001	0.813+000	0.170+000	0.170+001	0.134+000
0.173+003	0.154+003	0.115+002	0.641+003	0.280+001	0.316+000	0.635+000	0.490+001	0.103+000
0.192+003	0.755+003	0.115+002	0.412+004	0.746+003	0.	0.335+000	0.665+000	0.784+001

X= 300.000 INCHES P= 11.439 PSIA

PHI=0 DEGREES

R (IN.)	U (FT/SEC)	PT (PSIA)	T TOT (K)	MO (LB/FT3)	K M2U LIQ	K M2U VAP	K M2	MACH NO.
0.	0.106+004	0.115+002	0.445+004	0.210+003	0.	0.575+001	0.945+000	0.914+001
0.192+002	0.747+003	0.115+002	0.373+004	0.108+002	0.	0.524+000	0.476+000	0.934+001
0.384+002	0.165+003	0.115+002	0.641+003	0.324+001	0.115+000	0.542+000	0.428+001	0.121+000
0.576+002	0.983+002	0.116+002	0.631+003	0.153+000	0.994+000	0.947+001	0.117+001	0.165+000
0.768+002	0.116+003	0.116+002	0.636+003	0.878+001	0.799+000	0.183+000	0.180+001	0.146+000
0.960+002	0.365+003	0.115+002	0.182+004	0.205+002	0.	0.862+000	0.138+000	0.981+001
0.115+003	0.717+003	0.115+002	0.364+004	0.117+002	0.	0.559+000	0.441+000	0.936+001
0.134+003	0.223+003	0.115+002	0.781+003	0.154+001	0.	0.925+000	0.792+001	0.104+000
0.154+003	0.139+003	0.115+002	0.639+003	0.221+001	0.645+000	0.327+000	0.280+001	0.132+000
0.173+003	0.181+003	0.115+002	0.641+003	0.258+001	0.258+000	0.689+000	0.528+001	0.115+000
0.192+003	0.386+003	0.115+002	0.197+004	0.245+002	0.	0.820+000	0.130+000	0.978+001

PHI= 45.00 DEGREES

0.	0.106+004	0.115+002	0.445+004	0.210+003	0.	0.575+001	0.945+000	0.914+001
0.192+002	0.900+003	0.115+002	0.414+004	0.726+003	0.	0.320+000	0.680+000	0.923+001
0.384+002	0.622+003	0.115+002	0.328+004	0.159+002	0.	0.661+000	0.339+000	0.945+001
0.576+002	0.713+003	0.115+002	0.362+004	0.119+002	0.	0.563+000	0.437+000	0.936+001
0.768+002	0.101+004	0.115+002	0.436+004	0.264+003	0.	0.142+000	0.858+000	0.917+001
0.960+002	0.108+004	0.115+002	0.447+004	0.496+003	0.	0.335+001	0.967+000	0.914+001
0.115+003	0.752+003	0.115+002	0.375+004	0.106+002	0.	0.517+000	0.483+000	0.933+001
0.134+003	0.223+003	0.115+002	0.782+003	0.154+001	0.	0.925+000	0.792+001	0.104+000
0.154+003	0.139+003	0.115+002	0.639+003	0.221+001	0.645+000	0.327+000	0.280+001	0.132+000
0.173+003	0.181+003	0.115+002	0.641+003	0.258+001	0.258+000	0.689+000	0.528+001	0.115+000
0.192+003	0.386+003	0.115+002	0.197+004	0.245+002	0.	0.820+000	0.130+000	0.978+001

X= 400.000 INCHES P= 11.414 PSIA

PHI=0 DEGREES

R (IN.)	U (FT/SEC)	PT (PSIA)	T TOT (K)	MO (LB/FT3)	K M2U LIQ	K M2U VAP	K M2	MACH NO.
0.	0.801+003	0.115+002	0.369+004	0.112+002	0.	0.540+000	0.480+000	0.102+000
0.192+002	0.481+003	0.115+002	0.233+004	0.332+002	0.	0.814+000	0.186+000	0.106+000
0.384+002	0.196+003	0.115+002	0.641+003	0.255+001	0.249+000	0.898+000	0.333+001	0.123+000
0.576+002	0.138+003	0.115+002	0.638+003	0.829+001	0.711+000	0.286+000	0.237+001	0.147+000
0.768+002	0.157+003	0.115+002	0.639+003	0.249+001	0.285+000	0.383+000	0.318+001	0.138+000
0.960+002	0.299+003	0.115+002	0.116+004	0.243+002	0.	0.900+000	0.942+001	0.110+000
0.115+003	0.449+003	0.115+002	0.215+004	0.385+002	0.	0.834+000	0.186+000	0.106+000
0.134+003	0.237+003	0.115+002	0.752+003	0.161+001	0.	0.926+000	0.739+001	0.113+000
0.154+003	0.178+003	0.115+002	0.641+003	0.222+001	0.910+000	0.547+000	0.430+001	0.130+000
0.173+003	0.209+003	0.115+002	0.642+003	0.217+001	0.112+000	0.826+000	0.626+001	0.118+000
0.192+003	0.283+003	0.115+002	0.106+004	0.107+001	0.	0.912+000	0.885+001	0.110+000

PHI= 45.00 DEGREES

0.	0.801+003	0.115+002	0.369+004	0.112+002	0.	0.540+000	0.480+000	0.102+000
0.192+002	0.544+003	0.115+002	0.267+004	0.255+002	0.	0.771+000	0.229+000	0.105+000
0.384+002	0.359+003	0.115+002	0.157+004	0.628+002	0.	0.881+000	0.119+000	0.108+000
0.576+002	0.407+003	0.115+002	0.189+004	0.476+002	0.	0.857+000	0.143+000	0.107+000
0.768+002	0.723+003	0.115+002	0.343+004	0.139+002	0.	0.620+000	0.380+000	0.103+000
0.960+002	0.964+003	0.115+002	0.410+004	0.759+003	0.	0.348+000	0.652+000	0.101+000
0.115+003	0.542+003	0.115+002	0.266+004	0.257+002	0.	0.772+000	0.228+000	0.105+000
0.134+003	0.238+003	0.115+002	0.759+003	0.159+001	0.	0.926+000	0.742+001	0.113+000
0.154+003	0.178+003	0.115+002	0.641+003	0.222+001	0.910+000	0.547+000	0.430+001	0.130+000
0.173+003	0.209+003	0.115+002	0.642+003	0.217+001	0.112+000	0.826+000	0.626+001	0.118+000
0.192+003	0.283+003	0.115+002	0.106+004	0.107+001	0.	0.912+000	0.885+001	0.110+000

X= 600.000 INCHES P= 11.409 PSIA

PHI=0 DEGREES

R (IN.)	U (FT/SEC)	PT (PSIA)	T TOT (K)	MO(LB/FT3)	K H2O LIQ	K H2O VAP	K H2	MACH NO.
0.	0.331+003	0.115+002	0.134+004	0.781-002	0.	0.895+000	0.105+000	0.110+000
0.192+002	0.297+003	0.115+002	0.112+004	0.790-002	0.	0.908+000	0.919-001	0.111+000
0.384+002	0.243+003	0.115+002	0.770+003	0.156-001	0.	0.925+000	0.747-001	0.114+000
0.576+002	0.219+003	0.115+002	0.642+003	0.201-001	0.411-001	0.892+000	0.686-001	0.117+000
0.768+002	0.232+003	0.115+002	0.698+003	0.175-001	0.	0.929+000	0.715-001	0.115+000
0.960+002	0.273+003	0.115+002	0.959+003	0.120-001	0.	0.918+000	0.836-001	0.113+000
0.115+003	0.282+003	0.115+002	0.102+004	0.111-001	0.	0.913+000	0.867-001	0.112+000
0.134+003	0.244+003	0.115+002	0.771+003	0.156-001	0.	0.925+000	0.748-001	0.114+000
0.154+003	0.220+003	0.115+002	0.642+003	0.198-001	0.280-001	0.904+000	0.674-001	0.117+000
0.173+003	0.224+003	0.115+002	0.649+003	0.191-001	0.	0.931+000	0.695-001	0.116+000
0.192+003	0.233+003	0.115+002	0.707+003	0.173-001	0.	0.928+000	0.714-001	0.115+000

PHI= 45.00 DEGREES

0.	0.331+003	0.115+002	0.134+004	0.781-002	0.	0.895+000	0.105+000	0.110+000
0.192+002	0.301+003	0.115+002	0.114+004	0.765-002	0.	0.907+000	0.931-001	0.111+000
0.384+002	0.270+003	0.115+002	0.938+003	0.124-001	0.	0.917+000	0.820-001	0.113+000
0.576+002	0.288+003	0.115+002	0.106+004	0.106-001	0.	0.911+000	0.885-001	0.112+000
0.768+002	0.367+003	0.115+002	0.159+004	0.919-002	0.	0.880+000	0.120+000	0.109+000
0.960+002	0.430+003	0.115+002	0.199+004	0.538-002	0.	0.840+000	0.152+000	0.108+000
0.115+003	0.348+003	0.115+002	0.146+004	0.098-002	0.	0.888+000	0.112+000	0.110+000
0.134+003	0.256+003	0.115+002	0.851+003	0.139-001	0.	0.922+000	0.784-001	0.113+000
0.154+003	0.222+003	0.115+002	0.642+003	0.194-001	0.810-002	0.923+000	0.687-001	0.116+000
0.173+003	0.224+003	0.115+002	0.651+003	0.190-001	0.	0.930+000	0.695-001	0.116+000
0.192+003	0.233+003	0.115+002	0.708+003	0.173-001	0.	0.928+000	0.726-001	0.115+000

X= 800.000 INCHES P= 11.400 PSIA

PHI=0 DEGREES

R (IN.)	U (FT/SEC)	PT (PSIA)	T TOT (K)	MO(LB/FT3)	K H2O LIQ	K H2O VAP	K H2	MACH NO.
0.	0.284+003	0.115+002	0.988+003	0.116-001	0.	0.915+000	0.850-001	0.115+000
0.192+002	0.282+003	0.115+002	0.973+003	0.118-001	0.	0.910+000	0.843-001	0.115+000
0.384+002	0.278+003	0.115+002	0.947+003	0.122-001	0.	0.917+000	0.830-001	0.115+000
0.576+002	0.277+003	0.115+002	0.944+003	0.123-001	0.	0.917+000	0.820-001	0.115+000
0.768+002	0.281+003	0.115+002	0.967+003	0.119-001	0.	0.910+000	0.840-001	0.115+000
0.960+002	0.282+003	0.115+002	0.974+003	0.118-001	0.	0.916+000	0.845-001	0.115+000
0.115+003	0.273+003	0.115+002	0.916+003	0.127-001	0.	0.919+000	0.815-001	0.116+000
0.134+003	0.258+003	0.115+002	0.822+003	0.145-001	0.	0.925+000	0.771-001	0.116+000
0.154+003	0.247+003	0.115+002	0.756+003	0.160-001	0.	0.928+000	0.745-001	0.117+000
0.173+003	0.244+003	0.115+002	0.739+003	0.164-001	0.	0.927+000	0.733-001	0.117+000
0.192+003	0.245+003	0.115+002	0.746+003	0.162-001	0.	0.928+000	0.736-001	0.117+000

PHI= 45.00 DEGREES

0.	0.284+003	0.115+002	0.988+003	0.116-001	0.	0.915+000	0.850-001	0.115+000
0.192+002	0.282+003	0.115+002	0.975+003	0.118-001	0.	0.910+000	0.844-001	0.115+000
0.384+002	0.282+003	0.115+002	0.976+003	0.118-001	0.	0.910+000	0.844-001	0.115+000
0.576+002	0.293+003	0.115+002	0.105+004	0.108-001	0.	0.912+000	0.880-001	0.115+000
0.768+002	0.313+003	0.115+002	0.117+004	0.735-002	0.	0.903+000	0.947-001	0.114+000
0.960+002	0.320+003	0.115+002	0.122+004	0.887-002	0.	0.903+000	0.974-001	0.114+000
0.115+003	0.301+003	0.115+002	0.110+004	0.101-001	0.	0.909+000	0.907-001	0.114+000
0.134+003	0.273+003	0.115+002	0.915+003	0.127-001	0.	0.919+000	0.814-001	0.116+000
0.154+003	0.253+003	0.115+002	0.794+003	0.151-001	0.	0.924+000	0.758-001	0.117+000
0.173+003	0.247+003	0.115+002	0.754+003	0.160-001	0.	0.926+000	0.740-001	0.117+000
0.192+003	0.247+003	0.115+002	0.754+003	0.160-001	0.	0.926+000	0.740-001	0.117+000

X= 1000.000 INCHES P= 11.396 PSIA

PHI=0 DEGREES

R (IN.)	U (FT/SEC)	PT (PSIA)	T TOT (K)	MO(LB/FT3)	K H2O LIQ	K H2O VAP	K H2	MACH NO.
0.	0.288+003	0.115+002	0.995+003	0.115-001	0.	0.915+000	0.854-001	0.116+000
0.192+002	0.289+003	0.115+002	0.999+003	0.114-001	0.	0.914+000	0.850-001	0.116+000
0.384+002	0.290+003	0.115+002	0.101+004	0.113-001	0.	0.914+000	0.881-001	0.116+000
0.576+002	0.291+003	0.115+002	0.101+004	0.112-001	0.	0.914+000	0.884-001	0.116+000
0.768+002	0.290+003	0.115+002	0.100+004	0.113-001	0.	0.914+000	0.854-001	0.116+000
0.960+002	0.284+003	0.115+002	0.970+003	0.118-001	0.	0.910+000	0.842-001	0.116+000
0.115+003	0.276+003	0.115+002	0.918+003	0.127-001	0.	0.918+000	0.816-001	0.117+000
0.134+003	0.267+003	0.115+002	0.866+003	0.136-001	0.	0.921+000	0.791-001	0.117+000
0.154+003	0.262+003	0.115+002	0.833+003	0.143-001	0.	0.923+000	0.775-001	0.118+000
0.173+003	0.261+003	0.115+002	0.825+003	0.144-001	0.	0.923+000	0.771-001	0.118+000
0.192+003	0.261+003	0.115+002	0.828+003	0.143-001	0.	0.923+000	0.773-001	0.118+000

PHI= 45.00 DEGREES

0.	0.288+003	0.115+002	0.995+003	0.115-001	0.	0.915+000	0.854-001	0.116+000
0.192+002	0.289+003	0.115+002	0.100+004	0.114-001	0.	0.914+000	0.850-001	0.116+000
0.384+002	0.291+003	0.115+002	0.101+004	0.112-001	0.	0.914+000	0.864-001	0.116+000
0.576+002	0.295+003	0.115+002	0.104+004	0.109-001	0.	0.913+000	0.874-001	0.116+000
0.768+002	0.297+003	0.115+002	0.105+004	0.107-001	0.	0.912+000	0.881-001	0.116+000
0.960+002	0.294+003	0.115+002	0.103+004	0.110-001	0.	0.913+000	0.873-001	0.116+000
0.115+003	0.286+003	0.115+002	0.983+003	0.117-001	0.	0.913+000	0.848-001	0.116+000
0.134+003	0.276+003	0.115+002	0.919+003	0.127-001	0.	0.918+000	0.816-001	0.117+000
0.154+003	0.268+003	0.115+002	0.869+003	0.135-001	0.	0.921+000	0.792-001	0.117+000
0.173+003	0.265+003	0.115+002	0.850+003	0.139-001	0.	0.922+000	0.783-001	0.117+000
0.192+003	0.265+003	0.115+002	0.849+003	0.139-001	0.	0.922+000	0.783-001	0.117+000